Intrinsic and extrinsic forces that guide growth cone motility

by

Robert Henry Nichol IV

A dissertation submitted in partial fulfillment of

the requirements for the degree of

Doctor of Philosophy

(Neuroscience)

at the

UNIVERSITY OF WISCONSIN - MADISON

2017

Date of final oral examination: 1/20/2017

This dissertation is approved by the following members of the Final Oral Committee:

Timothy M. Gomez, Professor, Neuroscience
Erik W. Dent, Associate Professor, Neuroscience
Mary C. Halloran, Professor, Zoology
David M. Gamm, Associate Professor, Ophthalmology and Visual Sciences
Anita Bhattacharyya, Senior Scientist, Waisman Center
Avtar Roopra, Associate Professor, Neuroscience

Acknowledgments

First, I would like to thank my PhD advisor Timothy Gomez. Not only have you been a dedicated scientific mentor but you have also been a mentor and friend in life. Your depth of knowledge and dedication to biomedical research is a model to how I will approach scientific research in the future. I would also like to thank Erik Dent, who has been like a second PhD advisor to me. Your door was always been open and you have always able to provided a fresh perspective for Tim and I. You provided me with an example of a different mentoring style. I hope to one day integrate both Tim and Erik's mentoring styles when I have my own lab. I would also like to acknowledge my committee members, Mary C. Halloran, David M. Gamm, Anita Bhattacharyya, and Avtar Roopra, who contributed a lot of ideas and critiques for my projects. I am really appreciative to the Neuroscience Training Program administrative staff Mallory Musolf, Jenny Dahlberg, Tera Holtz, and Jessica Karis.

I would like to thank the members of the Gomez lab, in particular Miguel Santiago-Medina, Pat Kerstein, and Timothy Catlett who have been like family over the last six years. Miguel and Pat were great graduate students and one of the reasons for my joining the Gomez lab. You showed me how to be a successful graduate while also providing entertainment and support. Tim Catlett supplied me with years of engrossing conversations on everything from science to sports to philosophy. Other members of the Gomez lab, Caitlin Warlick-Short, Ed Suarez-Zayas, Sarah Rempel, Sean O'Toole, and Emma Svenson, have been good friends and incredible colleagues. I have also had the pleasure to mentor two amazing and productive undergraduate students, Drew Hollender and Kate Hagen.

I have had a wonderful six years in Madison largely due to my friends who made me feel at home from the beginning. I would like to thank all the people who have made the last six years fun. First I would like to express my gratitude to my NTP classmates, specifically Kendra Taylor, Trina Basu, David Ruhl, Rikki Hullinger, and Alex Rodriguez for the years of

encouragement and fun. We came in as novices and will leave here as accomplished scientists. I would also like to specifically thank my friends Tom Fothergill and Valerie Joers, who helped me through the stresses of graduate school and life in general. Finally, I would like to thank my best friend and his wife, Dan and Nikki Plaag, for being my refuge from the pressures of graduate school.

My family is one of the two most important things in my life and I would be nothing without the love and support of my parents and sister. To my dad, thank you for supporting me and allowing me to find my passion. You have shown me what it is to be an adult and how to carry myself with dignity and respect others. You showed me the importance of hard work and perseverance. To my mother, thank you for the emotional support through the challenges of adulthood and graduate school. You have always been there for me through the good and bad times. Thank you for your patience and unconditionally love. I appreciate both of you for supporting my academic endeavors throughout the years. To my sister Amy, thank you for the years of support and encouragement. You showed me the importance of helping others above financial gain. To my brother in law Josh, thank you for the years of brotherhood and fun.

Finally, I would like to thank my partner, Kourtney Franck, for the amazing life we have built together. Your humor, your compassion, and your silliness are the reasons I know I found the perfect person for me. Whether staying in and watching a movie during a blizzard or hiking with our dog, Allie, on a warm summer day, every day I have spent with you has been a blessing. Thank you for helping me through the stresses of graduate school and helping me celebrate my achievements. I love you and thank you.

Table of Contents

Chapter 1

Introduction

This chapter was published in part as the following journal article:

Kerstein, P. C., Nichol IV R. H., and Gomez, T. M. (2015) Mechanochemical regulation of growth cone motility. *Front. Cell. Neurosci.* 9, 244.

During development of the human nervous system axon tracts form in remarkably predictable ways. However, because of the spatial and temporal complexities of neural network formation, cognitive and sensory defects can arise from dysregulation of this tightly controlled process. We are now beginning to elucidate human disorders with specific axon guidance phenotypes. Importantly, aberrant axon guidance and tract formation, and the underlying genetic changes, have been discovered in a number of neurodevelopmental disorders, such as Fragile X Syndrome (*FMR1*), Tuberous Sclerosis (*TSC1, TSC2*), L1 Syndrome (*L1CAM*), Kallmann Syndrome (*KAL1*), Horizontal Gaze Palsy with Progressive Scoliosis (HGPPS) (*ROBO3*), Dyslexia (*ROBO1*), and X-linked mental retardation (*PAK3*) (Engle, 2010, Van Battum et al., 2015). Defects can vary and can include commissural guidance defects, e.g. failed commissural crossing, in disorders such as HGPPS and L1 Syndrome, as well as sensory processing defects in disorders such as Kallmann Syndrome and Fragile X Syndrome. While the genetic changes have been elucidated in these disorders, how these defects regulate molecular and cellular processes during development is still being extensively studied. To better understand and provide therapies for these disorders, a basic understanding of stereotypical axon tract formation is required, particularly for disorders with specific axon guidance defects. An important early step during neural network formation involves pioneering axonal navigation through a dense and complex matrix of extracellular molecules. Our lab has focused on understanding the intracellular signaling pathways that control transduction of extracellular signals into guided axonal growth. In Chapters 2 and 3, I provide key insights that further illuminate the complex cellular and environmental interactions that regulate axon development.

Classic studies investigating embryonic neural network assembly have sought to identified the chemical ligands and corresponding receptors that guide developing neurites to their proper synaptic partner (Kolodkin and Tessier-Lavigne, 2011). Several assays have been

developed to demonstrate that graded chemical ligands deposited in the environment of developing neurons serve as navigational cues that guide neuronal migration and morphogenesis. Nerve growth cones are sensory-motile structures that respond to soluble, cell surface, and substratum-associated extracellular cues to regulate neurite motility and directionality. Extracellular ligands interact with growth cone receptors to activate a web of biochemical signaling cascades that affect cytoskeletal dynamics, membrane trafficking directly, or new protein translation (Vitriol and Zheng, 2012, Shigeoka et al., 2013). Receptors on growth cones for growth factors, guidance cues and adhesive ligands activate signals that both promote and inhibit motility. How the nerve growth cone integrates multiple positive and negative signals *in vivo* concomitantly for a stereotyped response is still being intensely studied (Dudanova and Klein, 2013).

It is apparent chemical guidance cues clearly have significant influence on intracellular signaling, however, new studies have probed how intracellular force and the mechanical properties of the microenvironment also influence signaling and motility. Our laboratory and others have found that immobilized ligands on cell surfaces or secreted into the extracellular environment provide adhesive support for migrating cells (Moore et al., 2012, Nichol IV et al., 2016). On the intracellular side of adhesion receptors, molecular adaptor proteins link receptors to rigid cytoskeletal elements that generate opposing forces (Chen, 2008, Kerstein et al., 2015). These opposing forces underlie growth cone motility and are mediated by myosin generated contraction and polymerization of the cytoskeleton (Letourneau et al., 1987; Lamoureux et al., 1989; Heidemann et al., 1990). These forces are known to reciprocally influence cell signaling as a feedback homeostatic regulator of cell adhesion, shape and movements. These mechanical and biochemical signals likely undergo intricate crosstalk to coordinate specific morphological responses *in vivo*.

Mechanical force generation within neuronal growth cones

The cytomechanical forces that control growth cone motility have been intensely studied for the last 30 years, yet our understanding is still incomplete. Similar to non-neuronal cells, actin and microtubule polymerization play central roles as force-generating polymers in axonal growth cones. Complex mechanisms function within growth cones downstream of chemical and mechanical signals to tightly regulate the dynamic assembly and organization of the cytoskeleton (Lowery and Van Vactor, 2009, Dent et al., 2011). Leading edge protrusion is thought to be driven largely by filamentous actin (F-actin) polymerization. Actin polymerization at the leading edge produces tensile forces, which are distributed between plasma membrane protrusion and rearward movement of F-actin bundles (Figure 1) (Symons and Mitchison, 1991, Lin et al., 1996, Mogilner and Oster, 2003, Carlier and Pantaloni, 2007). Balance between membrane fluid dynamics and F-actin tensile strength may contribute to the extent of the balance between forward protrusion and rearward flow of F-actin (Figure 1) (Bornschlogl, 2013). Conversely, ADF-cofilin mediated depolymerization of F-actin minus ends relieves compressive actin network forces and replenishes G-actin pools needed for further F-actin polymerization at the leading edge (Bamburg, 1999, Marsick et al., 2010, Zhang et al., 2012). A second force that powers F-actin retrograde flow (RF) is myosin-II motor dimers, which centripetally contract antiparallel F-actin networks toward the growth cone central domain (Figure 1) (Turney and Bridgman, 2005, Medeiros et al., 2006, Yang et al., 2013, Shin et al., 2014). The contractile force of myosin-II, coupled with the rearward flow of F-actin due to leading edge polymerization, drives RF in growth cones (Forscher and Smith, 1988, Lin and Forscher, 1995, Brown and Bridgman, 2003). Other F-actin motor proteins, such as myosin I (Wang et al., 2003), V, VI (Suter et al., 2000, Kubota et al., 2010), and X (Berg and Cheney, 2002), also contribute to growth cone movements, morphology, and vesicle trafficking.

During neurite development and guidance, the equilibrium between actin polymerization and RF is a key regulator of growth cone protrusion and retraction. Increased leading edge protrusion could theoretically result from either increased actin polymerization or decreased myosin-II contraction. Conversely, leading edge retraction or collapse could result from reduced actin polymerization, increased depolymerization, or increased myosin-II contraction. Another key force that counteracts RF in growth cones, as in non-neuronal cells (Smilenov et al., 1999, Giannone et al., 2009, Thievessen et al., 2013), are clutching forces at cell-substratum adhesions, which physically link to the F-actin cytoskeleton through a complex web of adaptor and signaling proteins (Figure 2A) (Suter et al., 1998, Woo and Gomez, 2006, Bard et al., 2008, Shimada et al., 2008, Santiago-Medina et al., 2013, Toriyama et al., 2013, Nichol IV et al., 2016). The molecular ‘‘clutch’’ is thought to restrain myosin-II mediated contractile forces upon the F-actin network to redirect the force of actin polymerization toward membrane protrusion. Many signaling and adaptor proteins target to growth cone point contact adhesions to regulate clutching, which provide numerous possible sites for regulatory control of axon guidance downstream of soluble, immobilized, and mechanical cues (Bard et al., 2008, Santiago-Medina et al., 2013, Toriyama et al., 2013, Nichol IV et al., 2016).

Growth cone point contact adhesions are related to fibroblast focal adhesions, which are multi-functional, macromolecular protein complexes (Figure 2A-B) (Smilenov et al., 1999, Bard et al., 2008, Shimada et al., 2008, Geiger et al., 2009, Giannone et al., 2009, Toriyama et al., 2013). However, much less is understood about the molecular regulation and function of growth cone adhesions, and it is likely that these adhesions serve many functions that are unique to growth cones. Point contact adhesions typically assemble within growth cone filopodia that contain parallel bundled actin, have a short lifetime, then disassemble near the base of filopodia (Figure 2C). Point contact adhesions appear to require integrin engagement, as they are observed primarily in growth cones on extracellular matrix (ECM) proteins (Woo et

al., 2006, Myers et al., 2011). The ECM contains many ligands that modulate growth cone motility, such as laminin, tenascin, and fibronectin. Each type of ECM ligand activates specific integrin receptors, as we have recently reviewed (Myers et al., 2011). Activation of integrins leads to recruitment of scaffolding and signaling proteins, such as talin, focal adhesion kinase (FAK), paxillin, zyxin, and a-actinin (Figure 2B) (Gomez et al., 1996, Cluzel et al., 2005, Robles and Gomez, 2006, Myers and Gomez, 2011). In non-neuronal cells, scaffolding proteins link to actin filaments to clutch RF, which supports actin polymerization to drive protrusion of the leading edge (Smilenov et al., 1999, Giannone et al., 2009, Thievessen et al., 2013). Similar clutching of RF likely occurs at growth cone point contacts (Santiago-Medina et al., 2013) and higher density adhesions have been linked to slower RF (Koch et al., 2012). Importantly, since point contact adhesions are modulated by ECM and soluble guidance factors (Woo et al., 2006, Myers et al., 2012), it is plausible that growth cone guidance is controlled by local changes in RF. Indeed, early studies from Paul Forscher and colleagues suggested that local reduction in RF is correlated with increased growth cone motility (Lin et al., 1995, Lin et al., 1996). For example, reduced RF is correlated with translocation of the growth cone central domain toward areas of strong adhesion of Aplysia neurons in contact with ApCAM-coated beads (Lin et al., 1995, Suter et al., 1998). While the adapter proteins that link and clutch F-actin differ between cell adhesion molecules, such as ApCAM, L1 and N-cadherin, and integrin-ECM adhesions, they both function to restrain RF and promote axon outgrowth (Lin et al., 1995, Suter et al., 1998, Bard et al., 2008, Toriyama et al., 2013).

The inverse relationship between RF and growth cone motility is well established, however there are exceptions to this model. For example, actin RF and motility both increase in Aplysia growth cones stimulated with 5-HT (5-hydroxytryptamine, serotonin) (Zhang et al., 2012). This difference may be stimulus dependent, as 5-HT may increase actin polymerization without modulating adhesion dynamics leading to increase actin drag on existing adhesions.

This has been described as the viscous slip clutch model (Giannone et al., 2009, Zhang et al., 2012). Conversely, guidance cues such as brain-derived neurotrophic factor (BDNF) and Semaphorin 3A regulate traction forces and actin RF speeds by changing adhesion dynamics (Woo et al., 2006, Myers et al., 2011, Nichol IV et al., 2016). However, it is still unclear whether these two mechanisms operate within individual cells, but work in epithelial cells suggests RF rates may slow at focal adhesions through clutching and increases at the leading edge through increased actin polymerization (Gardel et al., 2008). It remains unclear how clutching mechanisms in growth cones depend upon the adhesive environment, soluble guidance cues and cell type.

Increased protrusive forces at the leading edge membrane generated by molecular clutching of F-actin RF, are balanced by adhesive (traction) forces with the cell substratum at adhesion sites (Figure 3). Traction forces with the cell substratum have been measured in migrating cells and growth cones using deformable substrata containing fluorescent tracer beads as fiducial marks (Hyland et al., 2014). Early work showed that cells migrate in the direction of the strongest substratum forces (Lo et al., 2000), which occur at focal adhesions (Plotnikov et al., 2012). In growth cones, these traction forces on the substratum are distributed within the actin-rich peripheral domain, where point contact adhesions are formed (Figure 1) (Hyland et al., 2014). In response to guidance cues, localized assembly of adhesion complexes likely yield a redistribution of the traction forces on the substratum. This differential increase in traction forces on one side of the growth cone results in preferential growth in that direction. Moreover, the strength of traction forces generated by cells and growth cones increases on more rigid substrata, suggesting homeostatic regulation of force production (Chan and Odde, 2008, Koch et al., 2012). Substratum elasticity regulates integrin activity, internalization and adhesion site assembly (Du et al., 1993, Friedland et al., 2009), which likely accounts for increased traction forces at higher rigidity. Interestingly, growth cones from

different neuronal types have been shown to generate different levels of substratum traction stress. For example, CNS hippocampal neurons exhibit rapid RF rates, due to decreased clutching, and can only generate modest peak traction stress. Conversely, dorsal root ganglion (DRG) neurons, which form more point contact adhesions that slow RF, can generate larger traction forces (Koch et al., 2012). These differences in traction stress may be related to the types of elastic environments CNS vs. PNS neurons encounter.

Mechanically sensitive proteins within neuronal growth cones

Motile cells can sense the mechanical properties of their environment by expressing proteins that undergo conformational changes in response to mechanical force or tension (Table 1). Depending on the type of mechanosensitive protein, conformational changes may lead to modulation of enzymatic activity, accessibility of binding sites for protein-protein interactions, or regulation of ion channel gating (Paszek et al., 2005, Sawada et al., 2006, Ciobanasu et al., 2014, Zhang et al., 2014). One site where cell mechanosensors are likely concentrated is at integrin receptor and adhesion protein complexes, which function at the interface between the cytoskeleton and ECM. Adhesion complexes are spatially and temporally regulated by mechanical strain and substrate elasticity (Pelham and Wang, 1997, Schedin and Keely, 2011), suggesting they provide homeostatic feedback, termed tensional homeostasis.

Several signaling molecules within adhesion complexes are mechanosensitive. For example, mechanical forces applied to cells change both the localization and activity of FAK, a key non-receptor tyrosine kinase (Bae et al., 2014, Zhang et al., 2014). Importantly, FAK signaling is necessary for cell behavioral responses to locally applied forces and changes in substratum rigidity (Wang et al., 2001). In growth cones, FAK is essential for point contact adhesion dynamics (assembly/disassembly) and axon guidance (Robles et al., 2006, Woo et

al., 2009, Myers et al., 2011, Moore et al., 2012) and it is likely that mechanical properties of the environment influence FAK function. For example, FAK activation through deleted in colorectal cancer (DCC) requires both the immobilization of Netrin and acto-myosin contractility, suggesting that the kinase activity of FAK is mechanically dependent (Moore et al., 2012). Furthermore, inhibition of FAK during Netrin stimulation disrupts recruitment of adhesion complexes and traction force generation in growth cones. A second signaling kinase, receptor-like protein tyrosine phosphatase alpha (RPTP-α), is important for both sensing substratum stiffness and regulating axon extension (Kostic et al., 2007). RPTP-α co-localizes with αvβ6 integrins where it regulates adhesion signaling by activating Src tyrosine kinases (Kostic et al., 2007). Specifically on a rigid fibronectin substratum, RPTP-α promotes Src and p130Cas function and clustering to reinforce adhesion complexes and decrease axon outgrowth of hippocampal neurons (Kostic et al., 2007). However, whether RPTP-α senses substratum stiffness through a direct or indirect mechanism remains unclear.

Scaffolding proteins within adhesion complexes, such as p130Cas, talin, and filamin, also likely act as mechanosensors (Schiller and Fassler, 2013). Stretching of p130Cas exposes cryptic tyrosine residues that are phosphorylated by Src and FAK and initiate several signaling cascades (Sawada et al., 2006, Zhang et al., 2014). Loss of p130Cas function in developing neurons leads to aberrant axon pathfinding and dendrite patterning in vivo (Huang et al., 2007, Riccomagno et al., 2014). Recent evidence suggest that p130Cas may also be regulated by mechanically-dependent Netrin-DCC signaling during axon guidance (Moore et al., 2012). Similarly, stretching of talin leads to increased binding of the adapter vinculin to reinforce integrin-actin linkages (del Rio et al., 2009, Margadant et al., 2011, Ciobanasu et al., 2014). Talin has bifunctional roles in growth cones where it is important for the assembly of adhesions and as an integral scaffold within point contact adhesions (Sydor et al., 1996, Kerstein et al., 2013). Disruption of talin function leads to changes in filopodial dynamics and

reduced growth cone motility (Sydor et al., 1996, Kerstein et al., 2013). In a similar fashion, filamins are scaffolding proteins that are stretched when bound between integrins and F-actin. Tension along filamin unveils cryptic binding sites for many signaling molecules such as RhoA, Rho-associated coiled-coil kinase (ROCK), p21-activated kinase (PAK), and PKC (Furuike et al., 2001, Razinia et al., 2012). In developing animals, mutations in filamins produce premature axon termination, ectopic branching, and aberrant pathfinding in vivo (Zheng et al., 2011, Nakamura et al., 2014).

A second set of mechanosensors expressed by growth cones are mechanosensitive ion channels, including the Transient Receptor Potential (TRP) family. How mechanical forces are transduced into mechanosensitive channel gating is uncertain, but may involve coupling with the cytoskeleton (Clark et al., 2007, Hayakawa et al., 2008), interactions with lipids (Anishkin et al., 2014), and second messenger signals (Vriens et al., 2004). One intriguing site where local mechanical forces may regulate the opening of mechanosensitive ion channels is at cell-cell contact sites or integrin adhesions with the ECM (Hayakawa et al., 2008, Kobayashi and Sokabe, 2010, Kazmierczak and Muller, 2012, Eisenhoffer and Rosenblatt, 2013). In support of this notion, both Ca2+ signals and TRP channels localize near integrin adhesion sites (Gomez et al., 2001, Matthews et al., 2010, Kerstein et al., 2013). In neurons, these Ca2+ signals may act as a feedback mechanism on adhesion assembly and disassembly controlling growth cone motility (Robles et al., 2003, Kerstein et al., 2013). Interestingly, mechanical gating of mechanosensitive channels likely depends on substratum rigidity and traction forces (Doyle et al., 2004, Munevar et al., 2004, Kerstein et al., 2013). This suggests that differences in the elastic environment of neurons may control their development in vivo through regulation of mechanosensitive ion channel expression and function. In addition, mechanosensitive ion channels may exert homeostatic regulation of the cytoskeleton and adhesion complexes through activation of downstream Ca2+ effectors. Previous studies have identified the Ca2+

effectors, calcineurin, CaMKII, and calpain as the main signaling pathways that regulate Ca2+ dependent growth cone motility and axon guidance (Robles et al., 2003, Wen et al., 2004). However the most intriguing example of mechanical feedback is the Ca2+-dependent protease calpain since it cleaves several adhesion and actin binding proteins to inhibit or modulate their function (Franco et al., 2004). Recent studies have shown that axon outgrowth and morphology are regulated through calpain specific cleavage of talin and cortactin, respectively (Mingorance-Le Meur and O'Connor, 2009, Kerstein et al., 2013). However, additional calpain targets in growth cones are likely to exist. For example, in non-neuronal cells calpain cleaves the adhesion proteins Src, FAK, and Paxillin and the actin binding proteins Filamin and a-actinin (reviewed in Franco and Huttenlocher, 2005; Chan et al., 2010; Cortesio et al., 2011). It is important to further elucidate the mechanism of feedback inhibition between mechanosensitive channels and adhesion/cytoskeleton structures particularly in neuronal growth cones.

An interesting area where mechanotransduction has not been studied in growth cones is membrane trafficking. Endocytosis and exocytosis play an important role in growth cone navigation. For example, endocytosis of membrane and surface integrin receptors is required for repulsive growth turning from myelin- associated glycoprotein and semaphorin 3A (Hines et al., 2010, Tojima et al., 2010). Conversely, exocytosis is important for attractive axon turning and increased axon branching (Tojima et al., 2014, Winkle et al., 2014). Endocytosis and exocytosis may also directly influence mechanical signals. Recent studies showed that during cell migration leading edge protrusions increase plasma membrane tension, which activates further exocytosis to relieve increased tension (Gauthier et al., 2011). However, the mechanism of sensing membrane tension remains unknown. One possibility is that membrane tension activates mechanosensitive ion channels. Consistent with this, hypotonic solutions induce cell swelling and increase membrane tension, which activates Ca2+ influx through

mechanosensitive ion channels in growth cones (Jacques-Fricke et al., 2006, Kerstein et al., 2013). Another possibility is that membrane tension is required for the localization of leading edge signaling proteins such as Rac1 GTPase and the SCAR/WAVE complex, as shown recently in neutrophils (Houk et al., 2012). Our understanding of the relationship membrane tension and trafficking is largely limited in neuronal growth cones and more investigation is required to completely understand the mechanisms.

Mechanical properties of the environment regulate neurite growth

Pioneering studies on the mechanisms of growth cone guidance performed both in vitro and in vivo focused on the role of cell adhesion as a principal determinant of pathfinding (Gomez et al., 1996, Woo et al., 2006, Bard et al., 2008, Bechara et al., 2008, Myers et al., 2011). Using patterned substrata of differential adhesivity, investigators showed that growth cones could be directed in vitro simply by differences in adhesion (Hammarback et al., 1985, Gomez and Letourneau, 1994). These early experiments implied that axons may be targeted in vivo by adhesive interactions with extracellular ligands. A number of different cell recognition molecules on the surface of growth cones are known to have adhesive properties (Rutishauser, 1985, Lagenaur and Lemmon, 1987, Schmidt et al., 1995), which function to stabilize leading edge protrusions. While it is still uncertain the relative contributions of adhesion versus biochemical signaling in the control of axon pathfinding in vivo, it is likely that differential cell adhesion has some influence (Caudy and Bentley, 1986, O'Connor et al., 1990).

In addition to the classical ECM components, axon guidance cues are immobilized in the extracellular environment to some extent. While this includes large ECM proteins and cell surface adhesion molecules, small secreted growth factors and chemokines are also likely immobilized. Growing evidence suggests that growth factors bind with high specificity to

fibronectin type III repeats and heparin sulfate glycosaminoglycans contained within many ECM proteins such as fibronectin, tenascin, and laminin (Hynes, 2002, Hynes, 2009). Growth factor binding to the ECM likely serves to localize or concentrate soluble factors [e.g., fibroblast growth factor (FGF), Wnt, bone morphogenic proteins (BMPs)] near the cell binding sites and help establish stable gradients necessary for pattern formation in vivo. In some cases, growth factor receptors may cooperate with cell adhesion receptors (e.g., integrin) for cell binding, as has been demonstrated for a5ß1 and vascular endothelial growth factor (VEGF) receptor (Rahman et al., 2005). Secreted axon guidance cues have also been demonstrated to bind ECM proteins suggesting that immobilized guidance factors serve as adhesive ligands or provide mechanical support in association with ECM. For example, the repellant Slit must bind collagen for proper lamination of the zebrafish optic tectum (Xiao et al., 2011). Other secreted axon guidance cues such as netrins, BMPs and Sema3s bind the ECM and induce mechanical signals (Hu, 2001, Manitt and Kennedy, 2002, De Wit et al., 2005, Moore et al., 2012). To provide an additional level of control, local proteolysis of ECM may serve to release growth factors in a spatially and temporally controlled manner. Growth cones have recently been shown to target matrix metalloproteases using invadosomes (Santiago-Medina et al., 2015). Therefore, while bath application or local gradients of soluble guidance cues has been the prevailing method for studying axon guidance behaviors in vitro, the role of mechanical signaling by immobilized ligands in three dimensional environments is an important and often overlooked consideration for our full understanding of the mechanisms of neural network formation.

Growth cones in vitro have been shown to generate tension on neighboring cells and the underlying matrix (Lamoureux et al., 1989, Balgude et al., 2001, Moore et al., 2010, Moore and Sheetz, 2011). Many axon guidance cues are immobilized in the extracellular environment to some extent (as described above), therefore mechanical tensile forces likely contribute to

many attractive and repulsive (release of adhesion) guidance behaviors. Recent evidence suggest that even under classic chemical gradient turning assays, mechanotransduction is necessary for chemoattraction. For example, chemical gradients of netrin-1 generated in vitro only promote growth cone turning when netrin can bind to the substratum (Moore et al., 2009). Here growth cones utilize netrin as an adhesive ligand that supports traction forces that exceed 60 pN (Moore et al., 2009). Inhibition of netrin substrata adsorption, via co-treatment with heparin, inhibited axon outgrowth (Moore et al., 2012). Interestingly, commissural interneurons in vivo will turn towards ectopically secreted full length netrin, but are not guided towards truncated netrin lacking the domains required for substratum adsorption (Moore et al., 2012). Further, guidance toward Netrin depends upon FAK activity, a MS kinase, and myosin-II motor-induced traction forces. Other ‘‘soluble’’ axon guidance cues may require immobilization to elicit their guidance effects on extending axons. For example, ephrinA5 appears to produce repulsive turning or collapse in both border turning assays or as a soluble ligand, but the ability of ‘‘soluble’’ ephrinA5 to bind was not tested in this study (Weinl et al., 2003). EphrinA repellants may disrupt growth cone adhesion to the ECM or to neighboring cells by preventing point contact formation (Woo et al., 2009), or by activating metalloprotease-mediated cleavage of cell surface ephrinA ligands (Hattori et al., 2000), respectively.

While immobilized ligands clearly support traction forces generated by cells and growth cones, many recent studies show that substratum elasticity, or stiffness, also influences the development of neurons (Table 2) (Tyler, 2012, Franze, 2013). Cells and neurons have a remarkable ability to adapt to their mechanical environment. While most cells minimally require anchorage to a solid substratum and do not fully differentiate in liquid suspension, the elasticity of the supporting adhesive substratum can vary over a wide range. Elasticity of a material, such as tissue, is defined as the resistance to deformation in response to a mechanical stress. Elasticity is quantified as the elastic modulus or Young’s modulus (E) of a material. Young’s

modulus is the relationship of tensile stress to extensional strain. Tensile stress is determined by pulling or lengthening of the material and is quantified in terms of pressure or force per unit area. The extensional strain of a material is defined as the deformation of a solid due to stress, and is quantified as the change in length upon stress relative to the initial length. Extensional strain is unit-less. Therefore, Young's modulus has units of pressure, which is quantified in pascals (N/m2). Importantly, elasticity can vary greatly among different tissues during development. Neurons are particularly adaptable cells, as they will morphologically differentiate on extremely soft substrata and tissues, such as brain [Young's modulus = 100–1000 Pascal (Pa)], as well as on extremely rigid environments, such as ECM-coated glass and bone (>10 gPa, 20 mPa, respectively), covering an impressive >10,000 fold range of elasticities (Kruse et al., 2008, Tyler, 2012). Importantly, the elastic modulus (rigidity) of the cell substratum can strongly influence cell differentiation, morphology, motility, and survival (Geiger et al., 2001, Geiger et al., 2009, Moore et al., 2011, Musah et al., 2014). Understanding the roles of substratum elasticity on neuronal development is critical since developing axons and dendrites will encounter widely varying elastic environments during pathfinding to their targets.

Numerous studies over the past decade have shown that growth cone motility depends on the compliance of the cell substratum (Tyler, 2012, Franze, 2013). This is a cell migration process known as durotaxis. Previous studies used a variety of materials to generate variable elastic cell culture conditions to study neuronal durotaxis, including polyacrylamide (Flanagan et al., 2002, Georges et al., 2006, Kostic et al., 2007, Jiang et al., 2008, Koch et al., 2012) and polydimethylsiloxane (PDMS) in 2D (von Philipsborn et al., 2006, Cheng et al., 2011, Kerstein et al., 2013), as well as collagen I gels (Willits and Skornia, 2004, Sundararaghavan et al., 2009) and agarose hydrogels for 3D conditions (Hammarback and Letourneau, 1986, Balgude et al., 2001, Mai et al., 2009). Here we compare results across these conditions (Table 2), but it is important to note that many variables beyond substratum compliance may contribute to

observed differences. For example, non-biological materials typically must be conditioned with a biological ligand to support axon extension. A range of ECM proteins at varying concentrations or serum have been used to promote axon outgrowth. In addition to the variable biological conditions tested, the methods used to measure the elastic moduli of the cell substrata also varies. Therefore, Young's modulus values determined by atomic force microscopy (AFM) may differ from those measured by sheer stress rheometry or micro-position displacement devices. These caveats should be considered whenever comparing between different studies.

One of the first studies to examine neurite outgrowth under different elastic conditions cultured dorsal root ganglia (DRG) neurons within varying concentrations of agarose gels in the presence of 10% fetal bovine serum (FBS). This study found that axons extend more rapidly within softer gels (<20 Pa) and that the rate of outgrowth plateaus above 60 Pa (Balgude et al., 2001). More recently, polyacrylamide gels were used to test the effects of substratum elasticity on DRG axon outgrowth. By examining neurite lengths from fixed DRG neurons plated on polyacrylamide coated with laminin, Urbach and colleagues found that axon outgrowth peaks on 1000 Pa gels and decreases on polyacrylamide gels below and above this optimal elasticity (Koch et al., 2012). Interestingly, under the same conditions, this group found that hippocampal neurons exhibit no preference for soft substrata, suggesting this behavior may be selective for peripheral neurons. However, this result is contradictory to a previous report that found that hippocampal axons preferred soft conditions (500 Pa) over more rigid (4 kPa) (Kostic et al., 2007). It is important to note that the latter study differed from the former as they used polyacrylamide gels coated with fibronectin rather than laminin. Other studies using different types of neurons and culture conditions, including within collagen gels, have found preferential outgrowth on softer substrata (Table 2) (Balgude et al., 2001, Flanagan et al., 2002, Willits et al., 2004, Georges et al., 2006, Jiang et al., 2008, Kerstein et al., 2013), but it

will be important to standardize experimental conditions and elastic modulus measurements to make general statements regarding the effects of the mechanical environment on outgrowth. In addition to effects on axon outgrowth, other studies have shown that softer substrata promote neurite branching of several neuronal types (Wang et al., 2001, Flanagan et al., 2002, Georges et al., 2006, von Philipsborn et al., 2006).

Figure 1. Force generation in neuronal growth cones. Super resolution structure illumination microscopy image of a neuronal growth cone is labeled for filamentous actin (red) and ßI-II tubulin (green) using immunocytochemistry to illustrate correlation between forces and leading edge morphology (Santiago-Medina et al., 2015). Myosin (blue) binds to the actin network in the central domain to produce a rearward force (blue arrows) causing leading edge retraction. Adhesion complexes (yellow) antagonize this rearward force allowing actin polymerization to expand the leading edge membrane (yellow arrows) causing forward motility. This figure was modified from (Kerstein et al., 2015).

Figure 1.

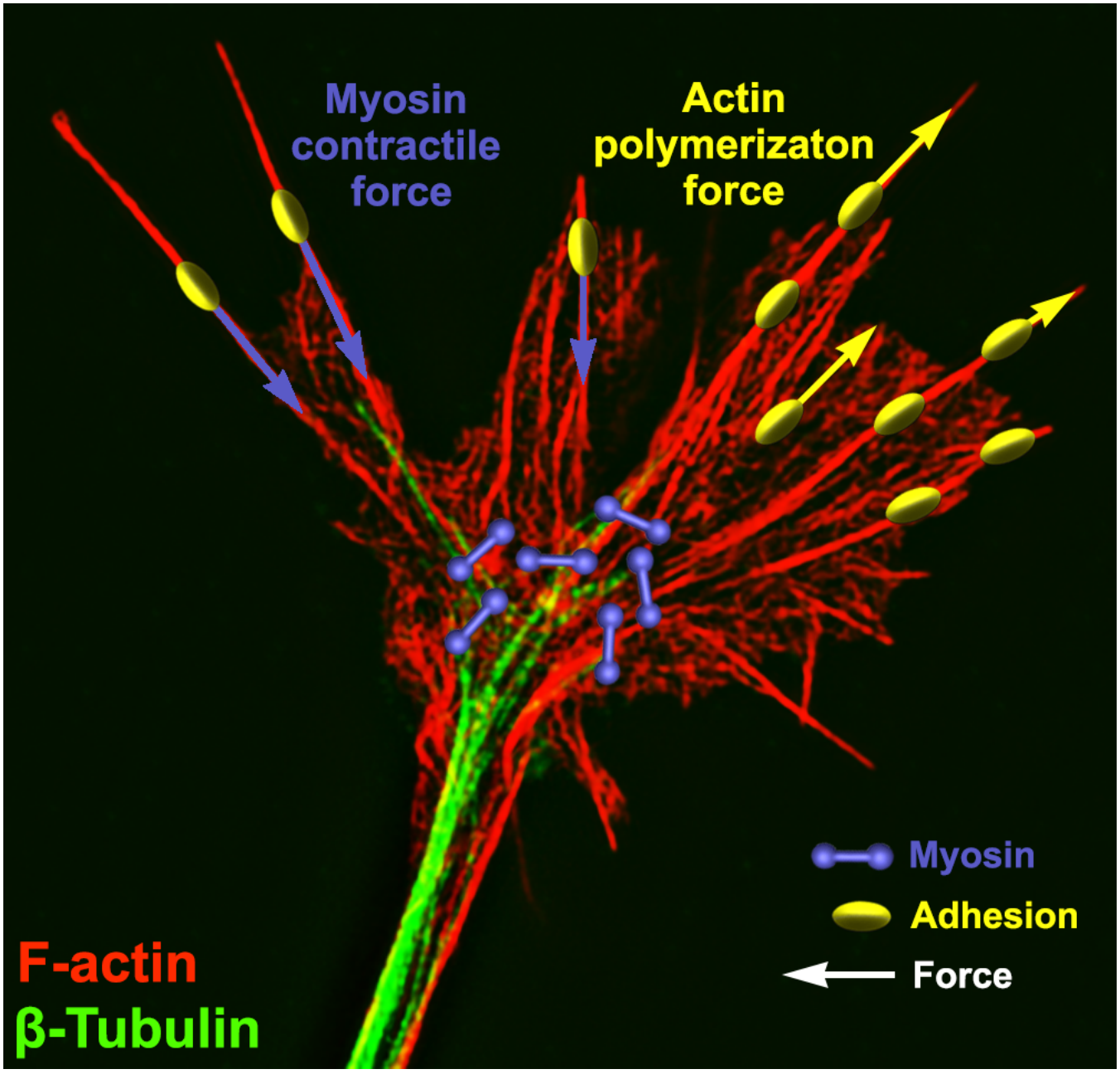
Myosin
contractile
force
Actin
polymerizaton
force
Myosin
Adhesion
Force
F-actin
β-Tubulin

Figure 2. Complexities of adhesion dynamics in motile cells. (A) Schematic showing the complexity of integrin based adhesion complex signaling. Over 160 different signaling molecules have been identified to play a role in adhesion dynamics, with intrinsic components and associated components. This figure was modified from (Geiger et al., 2009) **(B)** Our laboratory has identified a number of adhesion signaling molecules in neuronal growth cone including signaling molecules, FAK and Src, and actin and adhesion modulators, such as Rac1 and RhoA. This figure was modified from (Myers et al., 2011). **(C)** Inverted contrast images of a Xenopus growth cone expressing Paxillin-GFP captured every 1 min over a 4 min period using TIRF microscopy. The arrows denote stable adhesions spatially correlated with local protrusion of the growth cone leading edge. This figure was created with an original time-lapse captured for demonstration purposes in this manuscript using techniques previously described (Nichol IV et al., 2016). Scale bar, 5 μm for all panels.

Figure 2.

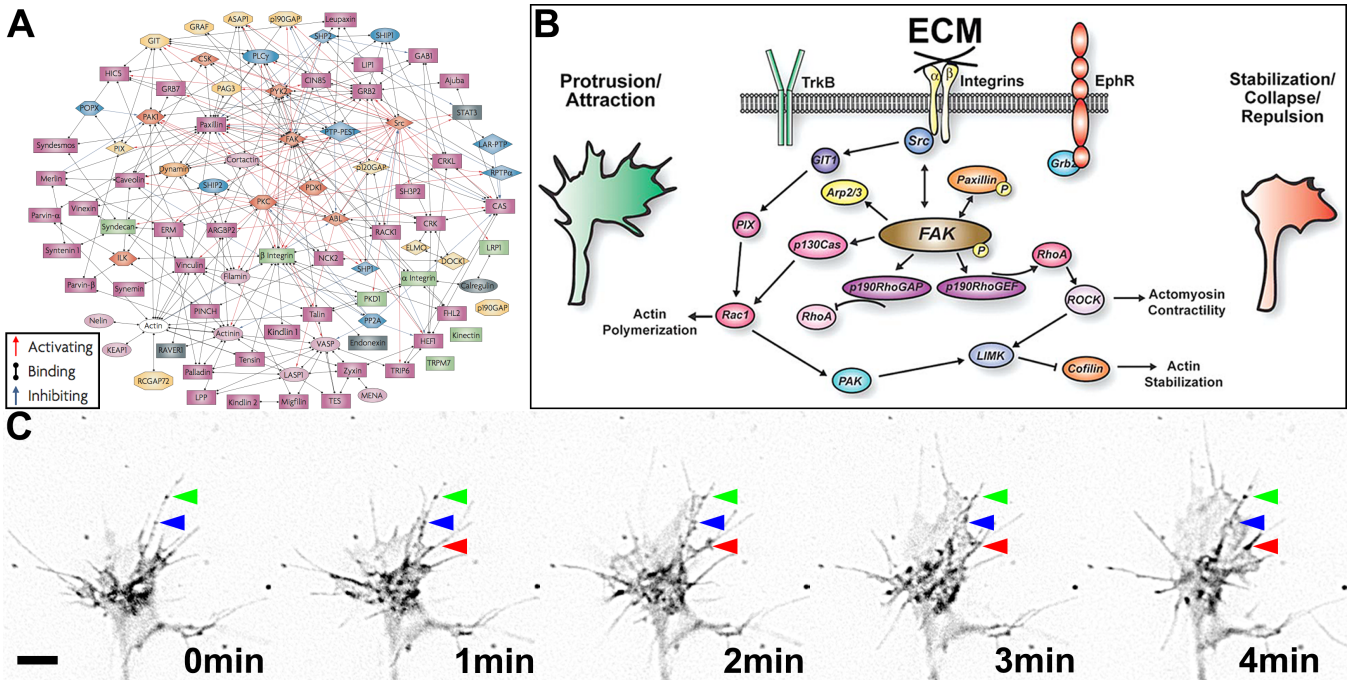
A
Activating
Binding
Inhibiting
B
ECM
Protrusion/
Attraction
TrkB
Integrins
EphR
Stabilization/
Collapse/
Repulsion
Src
SIT1
Arp2/3
Paxillin
P
PIX
p130Cas
FAK
P
RhoA
p190RhoGAP
p190RhoGEF
ROCK
Actomyosin
Contractility
Actin
Polymerization
Rac1
RhoA
LIMK
Cofilin
Actin
Stabilization
PAK
C
0min
1min
2min
3min
4min

Figure 3. Model of growth cone traction forces on varying compliant substrata. Distal to the leading edge, active myosin-II generates contractile forces (F_{myosin}) that pulls F-actin rearward. In addition, actin polymerization at the leading edge pushes against the plasma membrane to propel F-actin rearward ($F_{polymerization}$). These forces integrate to drive constitutive retrograde flow (RF) of F-actin filaments at the leading edge. **Stage 1 (ligand unbound)**: The molecular clutch is disengaged in the absence of integrin activation and clustering leading to rapid RF due to unrestrained F_{myosin} and $F_{polymerization}$. **Stage 2 (ligand bound)**: Upon contact with extracellular matrix (ECM) proteins, integrin receptors become activated, cluster and begin recruiting adhesome-related adaptor and signaling proteins. **Stage 3 (clutching)**: Mature point contact adhesions link with actin filaments ($F_{adhesion}$) to restrict RF and generate traction forces ($F_{traction}$) on the substratum. Therefore, forces generated by clutching of RF are distributed between traction forces with the ECM, adhesive forces on point contacts, and protrusive forces at the leading edge. Conditions that maintain clutching of RF produce robust protrusion. **Stage 3a (low substratum stiffness)**: On soft substrata, $F_{traction}$ forces are directed onto the elastic substrata at adhesions sites inducing substratum displacement. However, due to pliability of the elastic substrata there is little activation of mechanosensitive proteins, leading to decreased growth cone motility. **Stage 3b (optimal stiffness)**: On optimal substrata, $F_{traction}$ forces are distributed to the elastic substrata at point contact adhesions through substratum displacement, which reduces $F_{adhesion}$ at point contact adhesions. Lower $F_{adhesion}$ at point contacts prevents clutch slippage (breaking), while simultaneously activating mechanosensitive signaling and stretch gated proteins, leading to increased protrusion and growth cone translocation. **Stage 3c (high stiffness)**: Little displacement of the ECM occurs on rigid substrata. Subsequently, most force of RF is transferred to $F_{adhesion}$ at point contacts during clutching. The increased force on adhesions results in breaking or disassembly of point contacts via molecular stretching or activation of cellular signals. Fewer, short lived adhesions

on rigid ECM disrupt clutching forces necessary for membrane protrusion and rapid outgrowth. This figure was modified from (Kerstein et al., 2015)

Figure 3.

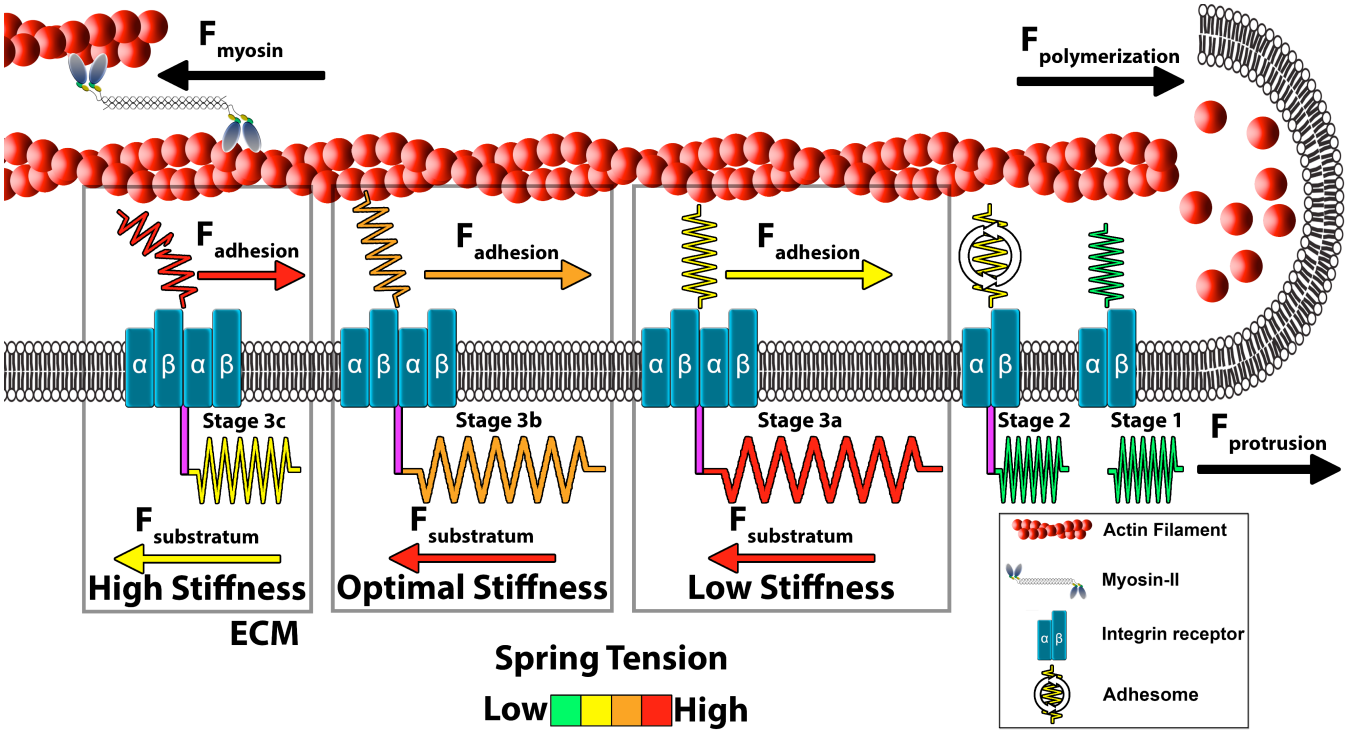
F myosin
F polymerization
F adhesion
F adhesion
F adhesion
α β α β
Stage 3c
Stage 3b
Stage 3a
Stage 2
Stage 1
F protrusion
F substratum
F substratum
F substratum
High Stiffness
ECM
Optimal Stiffness
Low Stiffness
Spring Tension
Low
High
Actin Filament
Myosin-II
Integrin receptor
Adhesome

Table 1. Mechanosensitive adhesion proteins in growth cones. A number of force activated adhesion proteins have been identified in neuronal growth cones. Mechanical gating can cause a variety of different forms of activation leading to increased adhesion dynamics. It has been discovered that activation of these signaling pathways can regulate growth cone motility and neurite guidance. This table was created in this manuscript (Kerstein et al., 2015).

Table 1.

Gene name	Mechanical activation	Downstream signaling	Growth cone mechanism	Key References (Bold - Mechano. *Italics - Growth cone)*
Adhesion proteins				
FAK	Increased kinase activity	• Tyrosine phosphorylation • Regulation of adhesion dynamics	• Required for attractive axon turning • Promotes axon outgrowth	*Robles et al. 2006* *Myers et al. 2011* ***Moore et al. 2012***
RPTP-α	Increased phosphatase activity	• Fyn recruitment to integrins • p130Cas phosphorylation	• Phosphatase activity inhibits axon outgrowth.	***Kostic et al. 2006***
p130Cas	Increased availability of tyrosine residues	• Phosphorylated by Src and Abl kinases	• Required for *in vivo* and *in vitro* axon pathfinding and dendritic patterning.	**Sawada et al. 2008** *Huang et al. 2007* *Riccomagno et al. 2014*
Talin	Increased availability of vinculin binding sites	• Vinculin binding • Reinforcement of integrin-actin linkages	• Required for filopodia and growth cone motility.	**del Rio et al. 2009** **Margadant et al. 2011** ***Kerstein et al. 2013*** *Sydor et al. 1996*
Filamin	Increased availability of protein binding sites.	• Recruitment of Rho, ROCK, PAK, and PKC to actin cytoskeleton and adhesions.	• Required for *in vivo* axon pathfinding.	**Furuike et al. 2001** **Razinia et al. 2012** *Zheng et al. 2011* *Nakamura et al. 2014*

Table 2. The effects of substrate rigidity on neurite outgrowth and morphology. Multiple studies, using a number of different neuronal models, have investigated the effect of substrata rigidity on neurite development. Results differ dependent upon neuron type, substrata, and elastic range. This table was created in this manuscript (Kerstein et al., 2015).

Table 2.

Neuron Type	Substrate (ECM)	Elasticity Range (Modulus)	Neurite Phenotype	References
E9 Chick DRG	3D Agarose (None)	0.003-0.130 kPa* (Shear)	Increased length on soft substrates	Balgude et al. 2000
E9 Chick DRG	3D Collagen I Gel (varied collegan conc.)	0.002-0.017 kPa (Shear)	Increased length on soft substrates	Willits et al. 2004
E8 Chick DRG	3D Collagen I Gel (varied genipin crosslinking)	0.05-0.80 kPa (Shear)	Increased length on soft substrates	Sundararaghavan et al. 2009
E13.5 Mouse Spinal Cord	PAA (Matrigel)	0.050-0.550 kPa* (Shear)	Increased branching on soft substrates	Flanagan et al. 2002
P0 Mouse Hippocampal	PAA (Fibronectin or Laminin)	0.5-7.5 kPa (Young's)	Increased length on soft substrates	Kostic et al. 2007
P0 Rat DRG	PAA (Laminin)	0.150-5.0 kPa (Young's)	Maximum length on 1.0 kPa substratum.	Koch et al. 2012
E18 Rat Hippocampal	PAA (Laminin)	0.150-5.0 kPa (Young's)	No affect on length	Koch et al. 2012
E16 Rat Spinal Cord	PAA (PDL or Collagen I) (DNA oligonucleotide pairs used to vary crosslinking)	6.6-30 kPa (Young's)	Increased length on soft substrates.	Jiang et al. 2008
Adult Mouse DRG	PDMS (Poly-L-Lysine)	18-1882 kPa (Young's)	Maximum length on 88 kPa substratum	Cheng et al. 2011
Stage 22 Xenopus spinal cord	PDMS (Fibronectin)	950-1800 kPa (Young's)	Increased outgrowth on soft substrates	Kerstein et al. 2013
E8-9 Chick DRG	Silk Fibroin Hydrogel (Fibronectin or Laminin)	4-33 kPa (Young's)	Maximum length on 7-22 kPa substrates	Hopkins et al. 2013

Bibliography

Alessandri-Haber, N., Dina, O. A., Joseph, E. K., Reichling, D. B., and Levine, J. D. (2008). Interaction of transient receptor potential vanilloid 4, integrin and SRC tyrosine kinase in mechanical hyperalgesia. *J. Neurosci.* 28, 1046–1057.

Anishkin, A., Loukin, S. H., Teng, J., and Kung, C. (2014). Feeling the hidden mechanical forces in lipid bilayer is an original sense. *Proc. Natl. Acad. Sci. U S A* 111, 7898–7905.

Balgude, A. P., Yu, X., Szymanski, A., and Bellamkonda, R. V. (2001). Agarose gel stiffness determines rate of DRG neurite extension in 3D cultures. *Biomaterials* 22, 1077–1084.

Bamburg, J. R. (1999). Proteins of the ADF/cofilin family: essential regulators of actin dynamics. *Annu. Rev. Cell Dev. Biol.* 15, 185–230.

Bard, L., Boscher, C., Lambert, M., Mège, R. M., Choquet, D., and Thoumine, O. (2008). A molecular clutch between the actin flow and N-cadherin adhesions drives growth cone migration. *J. Neurosci.* 28, 5879–5890.

Bechara, A., Nawabi, H., Moret, F., Yaron, A., Weaver, E., Bozon, M., et al. (2008). FAK-MAPK-dependent adhesion disassembly downstream of L1 contributes to semaphorin3A-induced collapse. *EMBO J.* 27, 1549–1562.

Berg, J. S., and Cheney, R. E. (2002). Myosin-X is an unconventional myosin that undergoes intrafilopodial motility. *Nat. Cell Biol.* 4, 246–250.

Bonanomi, D., and Pfaff, S. L. (2010). Motor axon pathfinding. *Cold Spring Harb. Perspect. Biol.* 2:a001735.

Bornschlögl, T. (2013). How filopodia pull: what we know about the mechanics and dynamics of filopodia. *Cytoskeleton (Hoboken)* 70, 590–603.

Boyd, N. F., Lockwood, G. A., Byng, J. W., Tritchler, D. L., and Yaffe, M. J. (1998). Mammographic densities and breast cancer risk. *Cancer Epidemiol. Biomarkers Prev.* 7, 1133–1144.

Brown, M. E., and Bridgman, P. C. (2003). Retrograde flow rate is increased in growth cones from myosin IIB knockout mice. *J. Cell Sci.* 116, 1087–1094.

Carlier, M. F., and Pantaloni, D. (2007). Control of actin assembly dynamics in cell motility. *J. Biol. Chem.* 282, 23005–23009.

Caudy, M., and Bentley, D. (1986a). Pioneer growth cone morphologies reveal proximal increases in substrate affinity within leg segments of grasshopper embryos. *J. Neurosci.* 6, 364–379.

Caudy, M., and Bentley, D. (1986b). Pioneer growth cone steering along a series of neuronal and non-neuronal cues of different affinities. *J. Neurosci.* 6, 1781–1795.

Chan, K. T., Bennin, D. A., and Huttenlocher, A. (2010). Regulation of adhesion dynamics by calpain-mediated proteolysis of focal adhesion kinase (FAK). *J. Biol. Chem.* 285, 11418–11426.

Chan, C. E., and Odde, D. J. (2008). Traction dynamics of filopodia on compliant substrates. *Science* 322, 1687–1691.

Chèdotal, A., and Richards, L. J. (2010). Wiring the brain: the biology of neuronal guidance. *Cold Spring Harb. Perspect. Biol.* 2:a001917.

Cheng, C. M., LeDuc, P. R., and Lin, Y. W. (2011). Localized bimodal response of neurite extensions and structural proteins in dorsal-root ganglion neurons with controlled polydimethylsiloxane substrate stiffness. *J. Biomech.* 44, 856–862.

Christ, A. F., Franze, K., Gautier, H., Moshayedi, P., Fawcett, J., Franklin, R. J., et al. (2010). Mechanical difference between white and gray matter in the rat cerebellum measured by scanning force microscopy. *J. Biomech.* 43, 2986–2992.

Clark, K., Langeslag, M., Figdor, C. G., and van Leeuwen, F. N. (2007). Myosin II and mechanotransduction: a balancing act. *Trends Cell Biol.* 17, 178–186.

Cluzel, C., Saltel, F., Lussi, J., Paulhe, F., Imhof, B. A., and Wehrle-Haller, B. (2005). The mechanisms and dynamics of (alpha)v(beta)3 integrin clustering in living cells. *J. Cell Biol.* 171, 383–392.

Cortesio, C. L., Boateng, L. R., Piazza, T. M., Bennin, D. A., and Huttenlocher, A. (2011). Calpain-mediated proteolysis of paxillin negatively regulates focal adhesion dynamics and cell migration. *J. Biol. Chem.* 286, 9998–10006.

Coste, B., Mathur, J., Schmidt, M., Earley, T. J., Ranade, S., Petrus, M. J., et al. (2010). Piezo1 and Piezo2 are essential components of distinct mechanically activated cation channels. *Science* 330, 55–60.

Davare, M. A., Fortin, D. A., Saneyoshi, T., Nygaard, S., Kaech, S., Banker, G., et al. (2009). Transient receptor potential canonical 5 channels activate Ca2+/calmodulin kinase Igamma to promote axon formation in hippocampal neurons. *J. Neurosci.* 29, 9794–9808.

De Wit, J., De Winter, F., Klooster, J., and Verhaagen, J. (2005). Semaphorin 3A displays a punctate distribution on the surface of neuronal cells and interacts with proteoglycans in the extracellular matrix. *Mol. Cell. Neurosci.* 29, 40–55.

Dent, E. W., Gupton, S. L., and Gertler, F. B. (2011). The growth cone cytoskeleton in axon outgrowth and guidance. *Cold Spring Harb. Perspect. Biol.* 3:a001800.

del Rio, A., Perez-Jimenez, R., Liu, R., Roca-Cusachs, P., Fernandez, J. M., and Sheetz, M. P. (2009). Stretching single talin rod molecules activates vinculin binding. *Science* 323, 638–641.

Discher, D. E., Janmey, P., and Wang, Y. L. (2005). Tissue cells feel and respond to the stiffness of their substrate. *Science* 310, 1139–1143.

Discher, D. E., Mooney, D. J., and Zandstra, P. W. (2009). Growth factors, matrices and forces combine and control stem cells. *Science* 324, 1673–1677.

Doyle, A., Marganski, W., and Lee, J. (2004). Calcium transients induce spatially coordinated increases in traction force during the movement of fish keratocytes. *J. Cell Sci.* 117, 2203–2214.

Du, X., Gu, M., Weisel, J. W., Nagaswami, C., Bennett, J. S., Bowditch, R., et al. (1993). Long range propagation of conformational changes in integrin alpha IIb beta 3. *J. Biol. Chem.* 268, 23087–23092.

Dudanova, I., and Klein, R. (2013). Integration of guidance cues: parallel signaling and crosstalk. *Trends Neurosci.* 36, 295–304.

Eisenhoffer, G. T., and Rosenblatt, J. (2013). Bringing balance by force: live cell extrusion controls epithelial cell numbers. *Trends Cell Biol.* 23, 185–192.

Engler, A. J., Griffin, M. A., Sen, S., Bönnemann, C. G., Sweeney, H. L., and Discher, D. E. (2004). Myotubes differentiate optimally on substrates with tissue-like stiffness: pathological implications for soft or stiff microenvironments. *J. Cell Biol.* 166, 877–887.

Faucherre, A., Nargeot, J., Mangoni, M. E., and Jopling, C. (2013). piezo2b regulates vertebrate light touch response. *J. Neurosci.* 33, 17089–17094.

Flanagan, L. A., Ju, Y. E., Marg, B., Osterfield, M., and Janmey, P. A. (2002). Neurite branching on deformable substrates. *Neuroreport* 13, 2411–2415.

Forscher, P., and Smith, S. J. (1988). Actions of cytochalasins on the organization of actin filaments and microtubules in a neuronal growth cone. *J. Cell Biol.* 107, 1505–1516.

Franco, S. J., and Huttenlocher, A. (2005). Regulating cell migration: calpains make the cut. *J. Cell Sci.* 118, 3829–3838.

Franze, K. (2011). Atomic force microscopy and its contribution to understanding the development of the nervous system. *Curr. Opin. Genet. Dev.* 21, 530–537.

Franze, K. (2013). The mechanical control of nervous system development. *Development* 140, 3069–3077.

Franze, K., Gerdelmann, J., Weick, M., Betz, T., Pawlizak, S., Lakadamyali, M., et al. (2009). Neurite branch retraction is caused by a threshold-dependent mechanical impact. *Biophys. J.* 97, 1883–1890.

Friedland, J. C., Lee, M. H., and Boettiger, D. (2009). Mechanically activated integrin switch controls alpha5beta1 function. *Science* 323, 642–644.

Furuike, S., Ito, T., and Yamazaki, M. (2001). Mechanical unfolding of single filamin A (ABP-280) molecules detected by atomic force microscopy. *FEBS Lett.* 498, 72–75.

Gardel, M. L., Sabass, B., Ji, L., Danuser, G., Schwarz, U. S., and Waterman, C. M. (2008). Traction stress in focal adhesions correlates biphasically with actin retrograde flow speed. *J. Cell Biol.* 183, 999–1005.

Gauthier, N. C., Fardin, M. A., Roca-Cusachs, P., and Sheetz, M. P. (2011). Temporary increase in plasma membrane tension coordinates the activation of exocytosis and contraction during cell spreading. *Proc. Natl. Acad. Sci. U S A* 108, 14467–14472.

Geffeney, S. L., and Goodman, M. B. (2012). How we feel: ion channel partnerships that detect mechanical inputs and give rise to touch and pain perception. *Neuron* 74, 609–619.

Geiger, B., Bershadsky, A., Pankov, R., and Yamada, K. M. (2001). Transmembrane crosstalk between the extracellular matrix–cytoskeleton crosstalk. *Nat. Rev. Mol. Cell Biol.* 2, 793–805.

Geiger, B., Spatz, J. P., and Bershadsky, A. D. (2009). Environmental sensing through focal adhesions. *Nat. Rev. Mol. Cell Biol.* 10, 21–33.

Georges, P. C., Miller, W. J., Meaney, D. F., Sawyer, E. S., and Janmey, P. A. (2006). Matrices with compliance comparable to that of brain tissue select neuronal over glial growth in mixed cortical cultures. *Biophys. J.* 90, 3012–3018.

Giannone, G., Mège, R. M., and Thoumine, O. (2009). Multi-level molecular clutches in motile cell processes. *Trends Cell Biol.* 19, 475–486.

Gilmour, D., Knaut, H., Maischein, H. M., and Nusslein-Volhard, C. (2004). Towing of sensory axons by their migrating target cells in vivo. *Nat. Neurosci.* 7, 491–492.

Gomez, T. M., and Letourneau, P. C. (1994). Filopodia initiate choices made by sensory neuron growth cones at laminin/fibronectin borders in vitro. *J. Neurosci.* 14, 5959–5972.

Gomez, T. M., and Letourneau, P. C. (2014). Actin dynamics in growth cone motility and navigation. *J. Neurochem.* 129, 221–234.

Gomez, T. M., Robles, E., Poo, M., and Spitzer, N. C. (2001). Filopodial calcium transients promote substrate-dependent growth cone turning. *Science* 291, 1983–1987.

Gomez, T. M., Roche, F. K., and Letourneau, P. C. (1996). Chick sensory neuronal growth cones distinguish fibronectin from laminin by making substratum contacts that resemble focal contacts. *J. Neurobiol.* 29, 18–34.

Gomez, T. M., and Zheng, J. Q. (2006). The molecular basis for calcium-dependent axon pathfinding. *Nat. Rev. Neurosci.* 7, 115–125.

Gomis, A., Soriano, S., Belmonte, C., and Viana, F. (2008). Hypoosmotic- and pressure-induced membrane stretch activate TRPC5 channels. *J. Physiol.* 586, 5633–5649.

Goswami, C., Kuhn, J., Heppenstall, P. A., and Hucho, T. (2010). Importance of non-selective cation channel TRPV4 interaction with cytoskeleton and their reciprocal regulations in cultured cells. *PLoS One* 5:e11654.

Granato, M., van Eeden, F. J., Schach, U., Trowe, T., Brand, M., Furutani-Seiki, M., et al. (1996). Genes controlling and mediating locomotion behavior of the zebrafish embryo and larva. *Development* 123, 399–413.

Greka, A., Navarro, B., Oancea, E., Duggan, A., and Clapham, D. E. (2003). TRPC5 is a regulator of hippocampal neurite length and growth cone morphology. *Nat. Neurosci.* 6, 837–845.

Hammarback, J. A., and Letourneau, P. C. (1986). Neurite extension across regions of low cell-substratum adhesivity: implications for the guidepost hypothesis of axonal pathfinding. *Dev. Biol.* 117, 655–662.

Hammarback, J. A., Palm, S. L., Furcht, L. T., and Letourneau, P. C. (1985). Guidance of neurite outgrowth by pathways of substratum-adsorbed laminin. *J. Neurosci. Res.* 13, 213–220.

Hattori, M., Osterfield, M., and Flanagan, J. G. (2000). Regulated cleavage of a contact-mediated axon repellent. *Science* 289, 1360–1365.

Hayakawa, K., Tatsumi, H., and Sokabe, M. (2008). Actin stress fibers transmit and focus force to activate mechanosensitive channels. *J. Cell Sci.* 121, 496–503.

Heidemann, S. R., Lamoureux, P., and Buxbaum, R. E. (1990). Growth cone behavior and production of traction force. *J. Cell Biol.* 111, 1949–1957.

Hines, J. H., Abu-Rub, M., and Henley, J. R. (2010). Asymmetric endocytosis and remodeling of beta1-integrin adhesions during growth cone chemorepulsion by MAG. *Nat. Neurosci.* 13, 829–837.

Hopkins, A. M., De Laporte, L., Tortelli, F., Spedden, E., Staii, C., Atherton, T. J., et al. (2013). Silk hydrogels as soft substrates for neural tissue engineering. *Adv. Funct. Mater.* 23, 5140–5149.

Houk, A. R., Jilkine, A., Mejean, C. O., Boltyanskiy, R., Dufresne, E. R., Angenent, S. B., et al. (2012). Membrane tension maintains cell polarity by confining signals to the leading edge during neutrophil migration. *Cell* 148, 175–188.

Hu, H. (2001). Cell-surface heparan sulfate is involved in the repulsive guidance activities of Slit2 protein. *Nat. Neurosci.* 4, 695–701.

Huang, Z., Yazdani, U., Thompson-Peer, K. L., Kolodkin, A. L., and Terman, J. R. (2007). Crk-associated substrate (Cas) signaling protein functions with integrins to specify axon guidance during development. *Development* 134, 2337–2347.

Hui, H., McHugh, D., Hannan, M., Zeng, F., Xu, S. Z., Khan, S. U., et al. (2006). Calcium-sensing mechanism in TRPC5 channels contributing to retardation of neurite outgrowth. *J. Physiol.* 572, 165–172.

Humphries, J. D., Paul, N. R., Humphries, M. J., and Morgan, M. R. (2015). Emerging properties of adhesion complexes: what are they and what do they do? *Trends Cell Biol.*

Hyland, C., Mertz, A. F., Forscher, P., and Dufresne, E. (2014). Dynamic peripheral traction forces balance stable neurite tension in regenerating Aplysia bag cell neurons. *Sci. Rep.* 4:4961.

Hynes, R. O. (2002). Integrins: bidirectional, allosteric signaling machines. *Cell* 110, 673–687.

Hynes, R. O. (2009). The extracellular matrix: not just pretty fibrils. *Science* 326, 1216–1219.

Hynes, R. O., and Naba, A. (2012). Overview of the matrisome–an inventory of extracellular matrix constituents and functions. *Cold Spring Harb. Perspect. Biol.* 4:a004903.

Isacson, O., Deacon, T. W., Pakzaban, P., Galpern, W. R., Dinsmore, J., and Burns, L. H. (1995). Transplanted xenogeneic neural cells in neurodegenerative disease models exhibit remarkable axonal target specificity and distinct growth patterns of glial and axonal fibres. *Nat. Med.* 1, 1189–1194.

Iwashita, M., Kataoka, N., Toida, K., and Kosodo, Y. (2014). Systematic profiling of spatiotemporal tissue and cellular stiffness in the developing brain. *Development* 141, 3793–3798.

Jacques-Fricke, B. T., Seow, Y., Gottlieb, P. A., Sachs, F., and Gomez, T. M. (2006). Ca2+ influx through mechanosensitive channels inhibits neurite outgrowth in opposition to other influx pathways and release from intracellular stores. *J. Neurosci.* 26, 5656–5664.

Jiang, F. X., Yurke, B., Firestein, B. L., and Langrana, N. A. (2008). Neurite outgrowth on a DNA crosslinked hydrogel with tunable stiffnesses. *Ann. Biomed. Eng.* 36, 1565–1579.

Kang, H., and Lichtman, J. W. (2013). Motor axon regeneration and muscle reinnervation in young adult and aged animals. *J. Neurosci.* 33, 19480–19491.

Kazmierczak, P., and Müller, U. (2012). Sensing sound: molecules that orchestrate mechanotransduction by hair cells. *Trends Neurosci.* 35, 220–229.

Kerstein, P. C., Jacques-Fricke, B. T., Rengifo, J., Mogen, B. J., Williams, J. C., Gottlieb, P. A., et al. (2013). Mechanosensitive TRPC1 channels promote calpain proteolysis of talin to regulate spinal axon outgrowth. *J. Neurosci.* 33, 273–285.

Keynes, R. J., and Stern, C. D. (1984). Segmentation in the vertebrate nervous system. *Nature* 310, 786–789.

Kim, S. N., Jeibmann, A., Halama, K., Witte, H. T., Wälte, M., Matzat, T., et al. (2014). ECM stiffness regulates glial migration in Drosophila and mammalian glioma models. *Development* 141, 3233–3242.

Kim, T. J., Seong, J., Ouyang, M., Sun, J., Lu, S., Hong, J. P., et al. (2009). Substrate rigidity regulates Ca2+ oscillation via RhoA pathway in stem cells. *J. Cell Physiol.* 218, 285–293.

Kobayashi, T., and Sokabe, M. (2010). Sensing substrate rigidity by mechanosensitive ion channels with stress fibers and focal adhesions. *Curr. Opin. Cell Biol.* 22, 669–676.

Koch, D., Rosoff, W. J., Jiang, J., Geller, H. M., and Urbach, J. S. (2012). Strength in the periphery: growth cone biomechanics and substrate rigidity response in peripheral and central nervous system neurons. *Biophys. J.* 102, 452–460.

Kolodkin, A. L., and Tessier-Lavigne, M. (2011). Mechanisms and molecules of neuronal wiring: a primer. *Cold Spring Harb. Perspect. Biol.* 3:a001727.

Kostic, A., Sap, J., and Sheetz, M. P. (2007). RPTPalpha is required for rigidity- dependent inhibition of extension and differentiation of hippocampal neurons. *J. Cell Sci.* 120, 3895–3904.

Kruse, S. A., Rose, G. H., Glaser, K. J., Manduca, A., Felmlee, J. P., Jack, C. R. Jr., et al. (2008). Magnetic resonance elastography of the brain. *Neuroimage* 39, 231–237.

Kubota, H., Ishikawa, R., Ohki, T., Ishizuka, J., Mikhailenko, S. V., and Ishiwata, S. (2010). Modulation of the mechano-chemical properties of myosin V by drebrin-E. *Biochem. Biophys. Res. Commun.* 400, 643–648.

Kuo, J. C., Han, X., Yates, J. R., III, and Waterman, C. M. (2012). Isolation of focal adhesion proteins for biochemical and proteomic analysis. *Methods Mol. Biol.* 757, 297–323.

Lagenaur, C., and Lemmon, V. (1987). An L1-like molecule, the 8D9 antigen, is a potent substrate for neurite extension. *Proc. Natl. Acad. Sci. U S A* 84, 7753–7757.

Lamoureux, P., Buxbaum, R. E., and Heidemann, S. R. (1989). Direct evidence that growth cones pull. *Nature* 340, 159–162.

Lee, J., Ishihara, A., Oxford, G., Johnson, B., and Jacobson, K. (1999). Regulation of cell movement is mediated by stretch-activated calcium channels. *Nature* 400, 382–386.

Letourneau, P. C., Shattuck, T. A., and Ressler, A. H. (1987). ‘‘Pull’’ and ‘‘push’’ in neurite elongation: observations on the effects of different concentrations of cytochalasin B and taxol. *Cell Motil. Cytoskeleton* 8, 193–209.

Li, J., Gu, X., Ma, Y., Calicchio, M. L., Kong, D., Teng, Y. D., et al. (2010). Nna1 mediates Purkinje cell dendritic development via lysyl oxidase propeptide and NF-kappaB signaling. *Neuron* 68, 45–60.

Li, Y., Jia, Y. C., Cui, K., Li, N., Zheng, Z. Y., Wang, Y. Z., et al. (2005). Essential role of TRPC channels in the guidance of nerve growth cones by brain-derived neurotrophic factor. *Nature* 434, 894–898.

Lin, C. H., and Forscher, P. (1995). Growth cone advance is inversely proportional to retrograde F-actin flow. *Neuron* 14, 763–771.

Lin, C. H., Espreafico, E. M., Mooseker, M. S., and Forscher, P. (1996). Myosin drives retrograde F-actin flow in neuronal growth cones. *Neuron* 16, 769–782.

Liu, C., and Montell, C. (2015). Forcing open TRP channels: Mechanical gating as a unifying activation mechanism. *Biochem. Biophys. Res. Commun.* 460, 22–25.

Lo, C. M., Wang, H. B., Dembo, M., and Wang, Y. L. (2000). Cell movement is guided by the rigidity of the substrate. *Biophys. J.* 79, 144–152.

Lowery, L. A., and van Vactor, D. (2009). The trip of the tip: understanding the growth cone machinery. *Nat. Rev. Mol. Cell Biol.* 10, 332–343.

Lu, Y. B., Franze, K., Seifert, G., Steinhäuser, C., Kirchhoff, F., Wolburg, H., et al. (2006). Viscoelastic properties of individual glial cells and neurons in the CNS. *Proc. Natl. Acad. Sci. U S A* 103, 17759–17764.

Mai, J., Fok, L., Gao, H., Zhang, X., and Poo, M. M. (2009). Axon initiation and growth cone turning on bound protein gradients. *J. Neurosci.* 29, 7450–7458.

Manitt, C., and Kennedy, T. E. (2002). Where the rubber meets the road: netrin expression and function in developing and adult nervous systems. *Prog. Brain Res.* 137, 425–442.

Margadant, F., Chew, L. L., Hu, X., Yu, H., Bate, N., Zhang, X., et al. (2011). Mechanotransduction in vivo by repeated talin stretch-relaxation events depends upon vinculin. *PLoS Biol.* 9:e1001223.

Maroto, R., Raso, A., Wood, T. G., Kurosky, A., Martinac, B., and Hamill, O. P. (2005). TRPC1 forms the stretch-activated cation channel in vertebrate cells. *Nat. Cell Biol.* 7, 179–185.

Marsick, B. M., Flynn, K. C., Santiago-Medina, M., Bamburg, J. R., and Letourneau, P. C. (2010). Activation of ADF/cofilin mediates attractive growth cone turning toward nerve growth factor and netrin-1. *Dev. Neurobiol.* 70, 565–588.

Matthews, B. D., Thodeti, C. K., Tytell, J. D., Mammoto, A., Overby, D. R., and Ingber, D. E. (2010). Ultra-rapid activation of TRPV4 ion channels by mechanical forces applied to cell surface beta1 integrins. *Integr. Biol. (Camb)* 2, 435–442.

McHugh, B. J., Buttery, R., Lad, Y., Banks, S., Haslett, C., and Sethi, T. (2010). Integrin activation by Fam38A uses a novel mechanism of R-Ras targeting to the endoplasmic reticulum. *J. Cell Sci.* 123, 51–61.

McHugh, B. J., Murdoch, A., Haslett, C., and Sethi, T. (2012). Loss of the integrin- activating transmembrane protein Fam38A (Piezo1) promotes a switch to a reduced integrin-dependent mode of cell migration. *PLoS One* 7:e40346.

Medeiros, N. A., Burnette, D. T., and Forscher, P. (2006). Myosin II functions in actin-bundle turnover in neuronal growth cones. *Nat. Cell Biol.* 8, 215–226.

Mingorance-Le Meur, A., and O'connor, T. P. (2009). Neurite consolidation is an active process requiring constant repression of protrusive activity. *EMBO J.* 28, 248–260.

Mogilner, A., and Oster, G. (2003). Polymer motors: pushing out the front and pulling up the back. *Curr. Biol.* 13, R721–R733.

Moore, S. W., Biais, N., and Sheetz, M. P. (2009). Traction on immobilized netrin-1 is sufficient to reorient axons. *Science* 325:166.

Moore, S. W., Biais, N., and Sheetz, M. P. (2009). Traction on immobilized netrin-1 is sufficient to reorient axons. *Science* 325:166.

Moore, S. W., Roca-Cusachs, P., and Sheetz, M. P. (2010). Stretchy proteins on stretchy substrates: the important elements of integrin-mediated rigidity sensing. *Dev. Cell* 19, 194–206.

Moore, S. W., and Sheetz, M. P. (2011). Biophysics of substrate interaction: influence on neural motility, differentiation and repair. *Dev. Neurobiol.* 71, 1090–1101.

Moore, S. W., Zhang, X., Lynch, C. D., and Sheetz, M. P. (2012). Netrin-1 attracts axons through FAK-dependent mechanotransduction. *J. Neurosci.* 32, 11574–11585

Munevar, S., Wang, Y. L., and Dembo, M. (2004). Regulation of mechanical interactions between fibroblasts and the substratum by stretch-activated Ca2+ entry. *J. Cell Sci.* 117, 85–92.

Musah, S., Wrighton, P. J., Zaltsman, Y., Zhong, X., Zorn, S., Parlato, M. B., et al. (2014). Substratum-induced differentiation of human pluripotent stem cells reveals the coactivator YAP is a potent regulator of neuronal specification. *Proc. Natl. Acad. Sci. U S A* 111, 13805–13810.

Myers, J. P., and Gomez, T. M. (2011). Focal adhesion kinase promotes integrin adhesion dynamics necessary for chemotropic turning of nerve growth cones. *J. Neurosci.* 31, 13585–13595.

Myers, J. P., Robles, E., Ducharme-Smith, A., and Gomez, T. M. (2012). Focal adhesion kinase modulates Cdc42 activity downstream of positive and negative axon guidance cues. *J. Cell Sci.* 125(Pt. 12), 2918–2929.

Myers, J. P., Santiago-Medina, M., and Gomez, T. M. (2011). Regulation of axonal outgrowth and pathfinding by integrin-ECM interactions. *Dev. Neurobiol.* 71, 901–923.

Nakamura, F., Kumeta, K., Hida, T., Isono, T., Nakayama, Y., Kuramata- Matsuoka, E., et al. (2014). Amino- and carboxyl-terminal domains of Filamin- A interact with CRMP1 to mediate Sema3A signalling. *Nat. Commun.* 5:5325.

Nguyen, Q. T., Sanes, J. R., and Lichtman, J. W. (2002). Pre-existing pathways promote precise projection patterns. *Nat. Neurosci.* 5, 861–867.

O'Connor, T. P., Duerr, J. S., and Bentley, D. (1990). Pioneer growth cone steering decisions mediated by single filopodial contacts in situ. *J. Neurosci.* 10, 3935–3946.

Oancea, E., Wolfe, J. T., and Clapham, D. E. (2006). Functional TRPM7 channels accumulate at the plasma membrane in response to fluid flow. *Circ. Res.* 98, 245–253.

Paszek, M. J., Zahir, N., Johnson, K. R., Lakins, J. N., Rozenberg, G. I., Gefen, A., et al. (2005). Tensional homeostasis and the malignant phenotype. *Cancer Cell* 8, 241–254.

Paulus, J. D., Willer, G. B., Willer, J. R., Gregg, R. G., and Halloran, M. C. (2009). Muscle contractions guide rohon-beard peripheral sensory axons. *J. Neurosci.* 29, 13190–13201.

Pelham, R. J. Jr., and Wang, Y. I. (1997). Cell locomotion and focal adhesions are regulated by substrate flexibility. *Proc. Natl. Acad. Sci. U S A* 94, 13661–13665.

Plotnikov, S. V., Pasapera, A. M., Sabass, B., and Waterman, C. M. (2012). Force fluctuations within focal adhesions mediate ECM-rigidity sensing to guide directed cell migration. *Cell* 151, 1513–1527.

Provenzano, P. P., Inman, D. R., Eliceiri, K. W., and Keely, P. J. (2009). Matrix density-induced mechanoregulation of breast cell phenotype, signaling and gene expression through a FAK-ERK linkage. *Oncogene* 28, 4326–4343.

Rahman, S., Patel, Y., Murray, J., Patel, K. V., Sumathipala, R., Sobel, M., et al. (2005). Novel hepatocyte growth factor (HGF) binding domains on fibronectin and vitronectin coordinate a distinct and amplified Met-integrin induced signalling pathway in endothelial cells. *BMC Cell Biol.* 6:8.

Ranade, S. S., Woo, S. H., Dubin, A. E., Moshourab, R. A., Wetzel, C., Petrus, M., et al. (2014). Piezo2 is the major transducer of mechanical forces for touch sensation in mice. *Nature* 516, 121–125.

Razinia, Z., Mäkelä, T., Ylänne, J., and Calderwood, D. A. (2012). Filamins in mechanosensing and signaling. *Annu. Rev. Biophys.* 41, 227–246.

Riccio, A., Medhurst, A. D., Mattei, C., Kelsell, R. E., Calver, A. R., Randall, A. D., et al. (2002). mRNA distribution analysis of human TRPC family in CNS and peripheral tissues. *Brain Res. Mol. Brain Res.* 109, 95–104.

Riccomagno, M. M., Sun, L. O., Brady, C. M., Alexandropoulos, K., Seo, S., Kurokawa, M., et al. (2014). Cas adaptor proteins organize the retinal ganglion cell layer downstream of integrin signaling. *Neuron* 81, 779–786.

Robles, E., and Gomez, T. M. (2006). Focal adhesion kinase signaling at sites of integrin-mediated adhesion controls axon pathfinding. *Nat. Neurosci.* 9, 1274–1283.

Robles, E., Huttenlocher, A., and Gomez, T. M. (2003). Filopodial calcium transients regulate growth cone motility and guidance through local activation of calpain. *Neuron* 38, 597–609.

Rutishauser, U. (1985). Influences of the neural cell adhesion molecule on axon growth and guidance. *J. Neurosci. Res.* 13, 123–131.

Santiago-Medina, M., Gregus, K. A., and Gomez, T. M. (2013). PAK-PIX interactions regulate adhesion dynamics and membrane protrusion to control neurite outgrowth. *J. Cell Sci.* 126, 1122–1133.

Santiago-Medina, M., Gregus, K. A., Nichol, R. H., O'Toole, S. M., and Gomez, T. M. (2015). Regulation of ECM degradation and axon guidance by growth cone invadosomes. *Development* 142, 486–496.

Sawada, Y., Tamada, M., Dubin-Thaler, B. J., Cherniavskaya, O., Sakai, R., Tanaka, S., et al. (2006). Force sensing by mechanical extension of the Src family kinase substrate p130Cas. *Cell* 127, 1015–1026.

Schedin, P., and Keely, P. J. (2011). Mammary gland ECM remodeling, stiffness and mechanosignaling in normal development and tumor progression. *Cold Spring Harb. Perspect. Biol.* 3:a003228.

Schmidt, C. E., Dai, J., Lauffenburger, D. A., Sheetz, M. P., and Horwitz, A. F. (1995). Integrin-cytoskeletal interactions in neuronal growth cones. *J. Neurosci.* 15, 3400–3407.

Schneider, V. A., and Granato, M. (2006). The myotomal diwanka (lh3) glycosyltransferase and type XVIII collagen are critical for motor growth cone migration. *Neuron* 50, 683–695.

Shibasaki, K., Murayama, N., Ono, K., Ishizaki, Y., and Tominaga, M. (2010). TRPV2 enhances axon outgrowth through its activation by membrane stretch in developing sensory and motor neurons. *J. Neurosci.* 30, 4601–4612.

Shigeoka, T., Lu, B., and Holt, C. E. (2013). Cell biology in neuroscience: RNA- based mechanisms underlying axon guidance. *J. Cell Biol.* 202, 991–999.

Shim, S., Goh, E. L., Ge, S. Y., Sailor, K., Yuan, J. P., Roderick, H. L., et al. (2005). XTRPC1-dependent chemotropic guidance of neuronal growth cones. *Nat. Neurosci.* 8, 730–735.

Shimada, T., Toriyama, M., Uemura, K., Kamiguchi, H., Sugiura, T., Watanabe, N., et al. (2008). Shootin1 interacts with actin retrograde flow and L1-CAM to promote axon outgrowth. *J. Cell Biol.* 181, 817–829.

Shin, E. Y., Lee, C. S., Yun, C. Y., Won, S. Y., Kim, H. K., Lee, Y. H., et al. (2014). Non-muscle myosin II regulates neuronal actin dynamics by interacting with guanine nucleotide exchange factors. *PLoS One* 9:e95212.

Smilenov, L. B., Mikhailov, A., Pelham, R. J., Marcantonio, E. E., and Gundersen, G. G. (1999). Focal adhesion motility revealed in stationary fibroblasts. *Science* 286, 1172–1174.

Spassova, M. A., Hewavitharana, T., Xu, W., Soboloff, J., and Gill, D. L. (2006). A common mechanism underlies stretch activation and receptor activation of TRPC6 channels. *Proc. Natl. Acad. Sci. U S A* 103, 16586–16591.

Strübing, C., Krapivinsky, G., Krapivinsky, L., and Clapham, D. E. (2003). Formation of novel TRPC channels by complex subunit interactions in embryonic brain. *J. Biol. Chem.* 278, 39014–39019.

Sundararaghavan, H. G., Monteiro, G. A., Firestein, B. L., and Shreiber, D. I. (2009). Neurite growth in 3D collagen gels with gradients of mechanical properties. *Biotechnol. Bioeng.* 102, 632–643.

Suter, D. M., Errante, L. D., Belotserkovsky, V., and Forscher, P. (1998). The Ig superfamily cell adhesion molecule, apCAM, mediates growth cone steering by substrate-cytoskeletal coupling. *J. Cell Biol.* 141, 227–240.

Suter, D. M., Espindola, F. S., Lin, C. H., Forscher, P., and Mooseker, M. S. (2000). Localization of unconventional myosins V and VI in neuronal growth cones. *J. Neurobiol.* 42, 370–382.

Sydor, A. M., Su, A. L., Wang, F. S., Xu, A., and Jay, D. G. (1996). Talin and vinculin play distinct roles in filopodial motility in the neuronal growth cone. *J. Cell Biol.* 134, 1197–1207.

Symons, M. H., and Mitchison, T. J. (1991). Control of actin polymerization in live and permeabilized fibroblasts. *J. Cell Biol.* 114, 503–513.

Thievessen, I., Thompson, P. M., Berlemont, S., Plevock, K. M., Plotnikov, S. V., Zemljic-Harpf, A., et al. (2013). Vinculin-actin interaction couples actin retrograde flow to focal adhesions, but is dispensable for focal adhesion growth. *J. Cell Biol.* 202, 163–177.

Tojima, T., Akiyama, H., Itofusa, R., Li, Y., Katayama, H., Miyawaki, A., et al. (2007). Attractive axon guidance involves asymmetric membrane transport and exocytosis in the growth cone. *Nat. Neurosci.* 10, 58–66.

Tojima, T., Itofusa, R., and Kamiguchi, H. (2010). Asymmetric clathrin-mediated endocytosis drives repulsive growth cone guidance. *Neuron* 66, 370–377.

Tojima, T., Itofusa, R., and Kamiguchi, H. (2014). Steering neuronal growth cones by shifting the imbalance between exocytosis and endocytosis. *J. Neurosci.* 34, 7165–7178.

Toriyama, M., Kozawa, S., Sakumura, Y., and Inagaki, N. (2013). Conversion of a signal into forces for axon outgrowth through Pak1-mediated shootin1 phosphorylation. *Curr. Biol.* 23, 529–534.

Turlova, E., Bae, C. Y., Deurloo, M., Chen, W., Barszczyk, A., Horgen, F. D., et al. (2014). TRPM7 Regulates Axonal Outgrowth and Maturation of Primary Hippocampal Neurons. *Mol. Neurobiol.*

Turney, S. G., and Bridgman, P. C. (2005). Laminin stimulates and guides axonal outgrowth via growth cone myosin II activity. *Nat. Neurosci.* 8, 717–719.

Tyler, W. J. (2012). The mechanobiology of brain function. *Nat. Rev. Neurosci.* 13, 867–878.

Vitriol, E. A., and Zheng, J. Q. (2012). Growth cone travel in space and time: the cellular ensemble of cytoskeleton, adhesion and membrane. *Neuron* 73, 1068–1081.

Von Niederhäusern, V., Kastenhuber, E., Stäuble, A., Gesemann, M., and Neuhauss, S. C. (2013). Phylogeny and expression of canonical transient receptor potential (TRPC) genes in developing zebrafish. *Dev. Dyn.* 242, 1427–1441.

von Philipsborn, A. C., Lang, S., Bernard, A., Loeschinger, J., David, C., Lehnert, D., et al. (2006). Microcontact printing of axon guidance molecules for generation of graded patterns. *Nat. Protoc.* 1, 1322–1328.

Vriens, J., Watanabe, H., Janssens, A., Droogmans, G., Voets, T., and Nilius, B. (2004). Cell swelling, heat and chemical agonists use distinct pathways for the activation of the cation channel TRPV4. *Proc. Natl. Acad. Sci. U S A* 101, 396–401.

Wang, H. B., Dembo, M., Hanks, S. K., and Wang, Y. (2001). Focal adhesion kinase is involved in mechanosensing during fibroblast migration. *Proc. Natl. Acad. Sci. U S A* 98, 11295–11300.

Wang, F. S., Liu, C. W., Diefenbach, T. J., and Jay, D. G. (2003). Modeling the role of myosin 1c in neuronal growth cone turning. *Biophys. J.* 85, 3319–3328.

Wang, G. X., and Poo, M. M. (2005). Requirement of TRPC channels in netrin- 1-induced chemotropic turning of nerve growth cones. *Nature* 434, 898–904.

Wei, C., Wang, X., Chen, M., Ouyang, K., Song, L. S., and Cheng, H. (2009). Calcium flickers steer cell migration. *Nature* 457, 901–905.

Weinl, C., Drescher, U., Lang, S., Bonhoeffer, F., and Löschinger, J. (2003). On the turning of Xenopus retinal axons induced by ephrin-A5. *Development* 130, 1635–1643.

Wen, Z., Guirland, C., Ming, G. L., and Zheng, J. Q. (2004). A CaMKII/calcineurin switch controls the direction of Ca(2+)-dependent growth cone guidance. *Neuron* 43, 835–846.

Wen, Z., Han, L., Bamburg, J. R., Shim, S., Ming, G. L., and Zheng, J. Q. (2007). BMP gradients steer nerve growth cones by a balancing act of LIM kinase and Slingshot phosphatase on ADF/cofilin. *J. Cell Biol.* 178, 107–119.

Willits, R. K., and Skornia, S. L. (2004). Effect of collagen gel stiffness on neurite extension. *J. Biomater. Sci. Polym. Ed.* 15, 1521–1531.

Winkle, C. C., McClain, L. M., Valtschanoff, J. G., Park, C. S., Maglione, C., and Gupton, S. L. (2014). A novel Netrin-1-sensitive mechanism promotes local SNARE-mediated exocytosis during axon branching. *J. Cell Biol.* 205, 217–232.

Woo, S., and Gomez, T. M. (2006). Rac1 and RhoA promote neurite outgrowth through formation and stabilization of growth cone point contacts. *J. Neurosci.* 26, 1418–1428.

Woo, S., Rowan, D. J., and Gomez, T. M. (2009). Retinotopic mapping requires focal adhesion kinase-mediated regulation of growth cone adhesion. *J. Neurosci.* 29, 13981–13991.

Woo, S. H., Ranade, S., Weyer, A. D., Dubin, A. E., Baba, Y., Qiu, Z., et al. (2014). Piezo2 is required for Merkel-cell mechanotransduction. *Nature* 509, 622–626.

Wright, K. M., Lyon, K. A., Leung, H., Leahy, D. J., Ma, L., and Ginty, D. D. (2012). Dystroglycan organizes axon guidance cue localization and axonal pathfinding. *Neuron* 76, 931–944.

Wu, G., Lu, Z. H., Obukhov, A. G., Nowycky, M. C., and Ledeen, R. W. (2007). Induction of calcium influx through TRPC5 channels by cross- linking of GM1 ganglioside associated with alpha5beta1 integrin initiates neurite outgrowth. *J. Neurosci.* 27, 7447–7458.

Wu, L. J., Sweet, T. B., and Clapham, D. E. (2010). International union of basic and clinical pharmacology. LXXVI. Current progress in the mammalian TRP ion channel family. *Pharmacol. Rev.* 62, 381–404.

Xiao, T., Staub, W., Robles, E., Gosse, N. J., Cole, G. J., and Baier, H. (2011). Assembly of lamina-specific neuronal connections by slit bound to type IV collagen. *Cell* 146, 164–176.

Yamauchi, M., and Sricholpech, M. (2012). Lysine post-translational modifications of collagen. *Essays Biochem.* 52, 113–133.

Yang, Q., Zhang, X. F., Van Goor, D., Dunn, A. P., Hyland, C., Medeiros, N., et al. (2013). Protein kinase C activation decreases peripheral actin network density and increases central nonmuscle myosin II contractility in neuronal growth cones. *Mol. Biol. Cell* 24, 3097–3114.

Zeller, J., and Granato, M. (1999). The zebrafish diwanka gene controls an early step of motor growth cone migration. *Development* 126, 3461–3472.

Zhang, X. F., Hyland, C., Van Goor, D., and Forscher, P. (2012). Calcineurin- dependent cofilin activation and increased retrograde actin flow drive 5-HT- dependent neurite outgrowth in Aplysia bag cell neurons. *Mol. Biol. Cell* 23, 4833–4848.

Zheng, L., Michelson, Y., Freger, V., Avraham, Z., Venken, K. J., Bellen, H. J., et al. (2011). Drosophila Ten-m and filamin affect motor neuron growth cone guidance. *PLoS One* 6:e22956.

Chapter 2

Guidance of Axons by Local Coupling of Retrograde Flow to Point Contact Adhesions

This chapter was published as the following journal article:

Nichol, R. H., Hagen, K. M., Lumbard, D. C., Dent, E. W., and Gomez, T. M. Guidance of axons by local coupling of retrograde flow to point contact adhesions. 2016. *Journal of Neuroscience*. 36(7):2267-82

Abstract

Growth cones interact with the extracellular matrix (ECM) through integrin receptors at adhesion sites termed point contacts. Point contact adhesions link ECM proteins to the actin cytoskeleton through numerous adaptor and signaling proteins. One presumed function of growth cone point contacts is to restrain or “clutch” myosin-II-based F-actin retrograde flow (RF) to promote leading edge membrane protrusion. In motile non-neuronal cells, myosin-II binds and exerts force upon actin filaments at the leading edge where clutching forces occur. However, in growth cones it is unclear whether similar F-actin clutching forces affect axon outgrowth and guidance. Here we show in Xenopus spinal neurons that RF is reduced in rapidly migrating growth cones on laminin (LN) compared to non-integrin binding poly-d-lysine (PDL). Moreover, acute stimulation with LN accelerates axon outgrowth over a time course that correlates with point contact formation and reduced RF. These results suggest that RF is restricted by the assembly of point contacts, which we show occurs locally by two channel imaging of RF and paxillin. Further, using micro-patterns of PDL and LN, we demonstrate that individual growth cones have differential RF rates while interacting with two distinct substrata. Opposing effects on RF rates were also observed in growth cones treated with chemoattractive and chemorepulsive axon guidance cues that influence point contact adhesions. Finally, we show RF is significantly attenuated in vivo, suggesting RF is being restrained by molecular clutching forces within the spinal cord. Together our results suggest that local clutching of RF can control axon guidance on ECM proteins downstream of axon guidance cues.

Introduction

The proper function of the adult nervous system depends on accurate guidance of axons to their correct synaptic targets during early development. Inaccurate neural network wiring may be an underlying cause of a number of severe neurodevelopmental disorders, including Tuberous Sclerosis Complex, Fragile X Syndrome, and other autism spectrum disorders (Weitzdoerfer et al., 2001, Antar et al., 2006, Nie et al., 2010). Axon guidance involves stabilizing leading edge membrane protrusions of axonal growth cones to the extracellular matrix (ECM). Membrane protrusions are stabilized at growth cone adhesion sites, termed point contacts (Woo et al., 2006, Myers et al., 2011). Point contacts form after integrin receptors bind ECM ligands leading to receptor clustering and recruitment of adhesion proteins such as talin, paxillin, and vinculin (Woo et al., 2006, Myers and Gomez, 2011, Myers et al., 2011), which link integrins to the actin cytoskeleton. The formation and turnover of point contacts at the growth cone periphery is regulated by the cell substratum and soluble growth factors, and strongly correlates with growth cone advance (Woo et al., 2006, Myers et al., 2011). In non-neuronal cells, the formation and stabilization of adhesions provides traction forces necessary to oppose both rearward myosin motor-dependent actin filament contractility and actin filament polymerization, which drives leading edge protrusion (Choi et al., 2008, Gardel et al., 2008, Yamashiro and Watanabe, 2014). However, interactions between growth cone point contacts and the actin cytoskeleton during axon extension and guidance remain poorly understood.

Complex mechanisms regulate filamentous actin (F-actin) in the growth cone peripheral domain to influence growth cone morphology and movement. The F-actin network is governed by a balance between F-actin barbed-end polymerization and pointed-end depolymerization (Lowery et al., 2009, Dent et al., 2011). Leading edge actin polymerization pushes membranes forward with some resistance (Symons et al., 1991, Lin et al., 1996, Mogilner and Oster, 2003,

Carlier and Pantaloni, 2007). The resistive force of the membrane on F-actin polymerization, together with barbed-end directed myosin-II contractility, powers F-actin retrograde flow (RF) from the growth cone periphery to the central domain (Bamburg, 1999, Forscher and Smith, 1988, Lin and Forscher, 1995, Brown et al., 2003, Marsick et al., 2010, Flynn et al., 2012, Zhang et al., 2012). The balance between actin polymerization, myosin-II driven RF and ADF-cofilin depolymerization controls F-actin treadmilling in the growth cone peripheral domain (Mogilner et al., 2003, Turney and Bridgman, 2005, Zhang et al., 2012). In non-neuronal cells, focal adhesions slow actin treadmilling by linking rearward F-actin flow to adhesion receptors (Smilenov et al., 1999, Giannone et al., 2009, Thievessen et al., 2013). Slowing or “clutching” of RF at focal adhesions increases the ability of F-actin polymerization to generate membrane protrusion and forward cell translocation (Smilenov et al., 1999, Giannone et al., 2009, Thievessen et al., 2013). Clutching of RF is thought to regulate the rate of axon extension (Bard et al., 2008, Shimada et al., 2008, Toriyama et al., 2013), but it is not known whether local regulation of RF also directs axon guidance. Recent evidence from our laboratory and others has shown that the rate of RF has an inverse relationship with the rate of growth cone advance (Lin et al., 1995, Santiago-Medina et al., 2013, Shimada et al., 2008, Toriyama et al., 2013, Kubo et al., 2015). However, it is unclear how RF rate depends on cell substratum or whether local differences may be responsible for axon guidance behaviors.

Here we show that RF is reduced in rapidly migrating growth cones on laminin (LN) compared to less motile, non-integrin binding poly-d-lysine (PDL). Moreover, acute stimulation with LN leads to accelerated axon outgrowth over a time course that correlates with point contact formation and reduced RF. We confirm that integrin receptor-binding is both necessary and sufficient to slow RF through gain and loss-of-function manipulations. Moreover, we show that RF can be locally restrained within growth cones at integrin adhesions sites. We also suggest a role for RF in regulating axon guidance using a substratum stripe assay. Finally, we

show that soluble guidance cues that promote assembly or disassembly of point contacts regulate RF accordingly. These data suggest that regulation of clutching at point contacts is an important mechanism in axon guidance. Local differences in clutching forces at point contact adhesions may guide growth cone movements by locally slowing retrograde flow.

Materials and methods

Plasmid constructs and reagents. GFP-γ-actin (rat) was provided by Andrew Matus (Friedrich Miescher Institute, Basel, Switzerland). Paxillin–GFP (chicken) was provided by A. F. Horwitz (University of Virginia, Charlottesville). Yellow fluorescent protein-Src homology-2 domain (dSH2) was provided by Benjamin Geiger (Weizmann Institute, Rehovot, Israel) and converted to GFP-dSH2 (Robles et al., 2005). Td-Tomato F-tractin was provided by Erik Dent (University of Wisconsin, Madison). Most expression constructs were sub-cloned into the *Xenopus*-preferred pCS2+ vector for mRNA synthesis using Gateway (Dave Turner, University of Michigan, Ann Arbor, MI). To visualize actin retrograde flow, neuronal cultures were incubated in 100 pM tetramethylrhodamine-conjugated kabiramide-C (TMR-KabC, kind gift from Gerard Marriott, University of California, Berkeley) for 3 min, then washed with 1x modified Ringer's (MR) solution. Blebbistatin (Sigma-Aldrich, St. Louis, MO) was used as a selective inhibitor of non-muscle myosin-II. Heparin (Sigma-Aldrich) was used to block binding of soluble laminin (LN) to poly-d-lysine (PDL, Sigma-Aldrich) coated coverslips.

Embryo injection and cell culture. *Xenopus laevis* embryos were obtained as described previously (Gomez et al., 2003) and staged according to Nieuwkoop and Faber (Nieuwkoop, 1994). For protein expression experiments, two dorsal blastomeres of eight-cell-stage embryos were injected with 0.25–0.5 ng GFP-dSH2 *in vitro*-transcribed, capped mRNA (mMessage Machine, Ambion, Austin, TX) or 60-80 pg PXN–GFP, GFP-γ-actin, or Td-Tomato F-tractin DNA. Neural tubes were dissected from 1-day-old embryos and explant cultures containing a heterogeneous population of spinal neurons were prepared as previously describe (Gomez et al., 2003). Explants were plated onto acid-washed No. 1.5 glass coverslips coated with 50 µg/ml PDL, 10 µg/ml LN (Sigma-Aldrich), 10 µg/ml Fibronectin (FN, Sigma-Aldrich), and 5 µg/ml Tenascin (TN, EMD Millipore, Billerica, MA). To visualize LN adsorption to the substratum, PDL coated coverslips were treated with 25 µg/ml fluorescent (HiLyte 488) LN (Cytoskeleton, Inc,

Denver, CO) for 15 min, then washed with phosphate-buffer saline (PBS, Sigma-Aldrich) before imaging. To block LN adsorption, coverslips were pre-treated with 2 μg/ml Heparin (Sigma-Aldrich) for 15 min, followed by 25 μg/ml fluorescent LN with Heparin for 15 min. Cultures were imaged or fixed 16–24 hours after plating. All methods were approved by the University of Wisconsin School of Medicine Animal Care and Use Committee.

Stripe assay. Silicone masks (Karlsruhe Institute of Technology, Karlsruhe, Germany) with 90 μm wide parallel lanes were attached to acid-washed coverslips. A solution of 10 μg/ml LN with 50% HiLyte 488 LN (to detect border in live cultures) was passed through the channels and allowed to bind for 1 hr then was rinsed with excess PBS to remove unbound protein. After the mask was removed, 50 μg/ml PDL was applied to the entire coverslip for 45 min. Patterned substrata were used immediately for spinal explant cultures. After 18-24 hours, cultures with explants near the LN-PDL border were loaded with TMR-KabC. Alexa-546 phalloidin (1:100; Invitrogen) to label filamentous actin (F-actin).

Image acquisition and analysis. For both live and fixed fluorescence microscopy, high-resolution images were acquired using either a 60X/1.45 NA objective lens on an Olympus Fluoview 500 laser-scanning confocal system mounted on an AX-70 upright microscope or a 100X/1.5 NA objective lens on a Nikon total internal reflection fluorescence (TIRF) microscope. For *in vivo* imaging, high resolution images were acquired using a 60x/1.1 NA water immersion objective lens on the confocal. On the confocal, samples were imaged at 2–2.5X zoom (pixel size = 165–200 nm). Images were collected on the TIRF with a Coolsnap HQ2 camera (Roper scientific) using 2 x 2 binning (pixel size = 127 nm). For bright field time-lapse microscopy, low-magnification phase-contrast images were acquired using a 20X objective on a Nikon microscope equipped with an x–y motorized stage for multi-positional imaging. Multi-positional images were capture at 1 min. intervals. Live explant cultures were sealed within perfusion chambers as described previously (Gomez et al., 2003) to allow rapid exchange of solutions.

Images were analyzed using ImageJ software (W. Rasband, National Institutes of Health, Bethesda, MD). Point contacts were identified as discrete areas containing PXN–GFP or GFP-dSH2 that were at least two times brighter than the surrounding background and remained fixed in place for a minimum of 30 seconds. (Woo et al., 2006). For display purposes, some images were pseudo-colored. TMR-KabC labeled growth cones were imaged at 2 Hz by TIRF microscopy for 2 min to measure actin RF. TMR-KabC RF rates were quantified by kymography by sampling three to seven lines per growth cone along filopodia and radiating equally around the axis of outgrowth. We find that kymography is the most accurate method to measure RF, but recognize that it is limited to linear F-actin movements. While off axis flow may slightly influence our absolute rate values, we expect these movements will be consistent across experimental groups so believe that kymography does provide accurate relative differences. Moreover, RF measurements made *in vivo* were performed on relatively flat growth cones with the confocal pinhole aperture set to one Airy unit, which provides an optical section of 600-700 nm, depending on the fluorophore. At this optical section depth, axial position changes of actin puncta will have minimal affect on RF rate calculations. Statistical analysis was carried out using Prism software. Analysis was completed with an unpaired Student's T-test for comparison of two experimental groups, or a one-way ANOVA with a Bonferroni's multiple-comparison test for comparison of 3 or more experimental groups. For comparisons of percentage change in RF, standard error was calculated as post-treatment standard deviation divided by pre-treatment mean.

Dynamic adhesion maps. Dynamic adhesion map images were prepared from image stacks as detailed previously (Santiago-Medina et al., 2011). Briefly, an image stabilization algorithm was applied if necessary and to improve edge detection an unsharp mask routine was applied, followed by thresholding to highlight the puncta of interest. Next, an 8-bit binary filter was applied to equalize point contact intensities. Image stacks were then converted to 16-bit and

user-defined subsets were summed so that intensity encodes pixel lifetime. Final images were contrast enhanced and pseudo-colorized.

Results

Rates of axon outgrowth and actin retrograde flow are inversely proportional and substratum-dependent

We have previously shown that growth cone point contact adhesion dynamics regulate the rate and direction of axon outgrowth (Woo et al., 2006, Myers et al., 2011). Point contacts are thought to support forward axonal translocation in part by stabilizing leading edge protrusions. However, point contacts contain a number of adaptor proteins that link integrin receptors to the actin cytoskeleton (Woo et al., 2006, Myers et al., 2011, Myers et al., 2011), which may further support axon extension by clutching RF. To test whether point contacts correlate with RF, we first determined the rates of RF in *Xenopus Laevis* spinal neuron growth cones on different substrata. We have previously shown that the culture substratum governs point contact assembly and dynamics in *Xenopus* spinal neuron growth cones (Robles et al., 2006), which may correlate with clutching of RF. We cultured spinal neurons on 50 µg/ml PDL, 1, 5, 10 and 25 µg/ml LN, PDL plus 10 µg/ml LN, 10 µg/ml Fibronectin (FN), or 5 µg/ml Tenascin (TN), which are conditions that support point contact adhesion formation to varying degrees (Robles et al., 2006) and associated axon outgrowth rates (Figure 1). Axon outgrowth rates were quantified over a 30 minute (min) time period using low magnification phase contrast imaging.

To investigate the effect of substratum adhesion on RF we used tetramethylrhodamine-conjugated kabiramide C (TMR-KabC) (Petchprayoon et al., 2005). TMR-KabC is a small, cell permeable molecule that binds to the barbed-ends of F-actin and has been used previously at low doses to track RF (Keren et al., 2008, Santiago-Medina et al., 2011, Santiago-Medina et al., 2013). To speckle the barbed-ends of actin filaments, we treated neurons for 3 min with 100 pM TMR-KabC, which partially labels actin barbed-ends, but does not affect the basal rate of neurite outgrowth or growth cone morphology (Santiago-Medina et al., 2013). Immediately

after TMR-KabC labeling, we imaged growth cones on each substratum at 2 Hz by TIRF microscopy for 2 min. F-actin RF rates were quantified by kymography by sampling three to seven lines per growth cone radiated equally from the axis of outgrowth (Figure 1A-D, see Methods). This analysis showed a substratum-dependent, inverse relationship between RF rates and axon outgrowth. Growth cones on LN, which assemble many point contacts and extend rapidly (Robles et al., 2006), have significantly lower RF rates as compared to growth cones plated on PDL, FN, and TN, which assemble few or no point contacts and extend slowly (Figure 1E, Movie 1). We also found that RF and axon outgrowth rates varied with LN substratum concentration (Figure 1F), suggesting that higher ligand density, which promotes point contact assembly (not shown), clutches RF to enhance axon outgrowth. We confirmed the differential RF rates on PDL versus LN by imaging GFP-actin speckles in *Xenopus* spinal neurons (Figure 1G-I). It is noteworthy that the rates of RF measured with GFP-actin were slightly, but significantly slower compared to RF measured using TMR-KabC for neurons on PDL (Figure 1J), which may be due to partial inhibition of actin polymerization by fluorescent actin fusion proteins (Riedl et al., 2008). In addition to rates of RF, we also found that RF on LN was significantly more variable compared to RF on PDL (Figure 1K). These results suggest that dynamic and local clutching during point contact formation, stabilization, and turnover may differentially regulate the rate of RF within growth cone sub-domains. Adhesion proteins such as talin, α-actinin, paxillin, and vinculin likely contribute to these linkages (Woo et al., 2006, Myers et al., 2011, Myers et al., 2011). Together these results suggest that point contacts within the growth cone periphery serve two functions. First, previous data suggest point contacts stabilize new protrusions to prevent retraction mediated by contractile forces, and second, we show point contacts clutch RF to allow actin polymerization to drive further membrane protrusion.

Leading edge RF in growth cones is believed to be significantly powered by myosin-II motor-mediated F-actin contraction, with some contribution by actin polymerization-mediated pushing forces against the leading edge plasma membrane (Lin et al., 1997, Bridgman et al., 2001, Brown et al., 2003, Mogilner et al., 2003, Medeiros et al., 2006, Craig et al., 2012). Consistent with this notion, treatment of *Aplysia* growth cones with the myosin ATPase inhibitor blebbistatin slows the rate of RF by one half, which is further attenuated by actin depolymerization with cytochalasin D (Medeiros et al., 2006). However, myosin-II also contributes to point contact formation in growth cones on LN, as blebbistatin reduces growth cone point contact size and number (Woo et al., 2006). Therefore, we hypothesized myosin-II inhibition would affect RF less on LN as compared to PDL, since inhibition of myosin-II would be counterbalanced by loss of point contacts on LN. We examined the effects of myosin-II inhibition by imaging TMR-KabC labeled growth cones on PDL (Figure 1L) and LN (not shown) for 2 min intervals every 5 min after acute treatment with 50 uM blebbistatin over a 15 min period. Inhibition of myosin-II in growth cones on PDL reduces RF to less than 50% of basal rates after 15 min (Figure 1M). As hypothesized, the effects of blebbistatin are more modest in growth cones on LN (Figure 1M), consistent with the counteracting effects of reduced clutching by point contacts. This analysis also validates TMR-KabC as an accurate probe to measure myosin-II mediated RF.

Acute LN stimulation accelerates axon outgrowth over a time course that correlates with point contact formation and reduced retrograde flow

To temporally link point contact assembly with clutching of RF and acceleration of axon outgrowth, we acutely stimulated neurons on PDL with LN. We have previously shown in neurons cultured on PDL that growth cone point contacts form and neurite outgrowth accelerates rapidly in response to acute LN stimulation over a time course that follows LN

binding to the substratum (Woo et al., 2006). To confirm this, we imaged paxillin-GFP (PXN-GFP) expressing neurons on PDL by TIRF microscopy and observed the assembly of point contacts and accelerated axon outgrowth after 15 min treatment with 25 µg/ml LN (Figure 2A, Movie 2). The time course for the increased rate of neurite outgrowth was quantified with low magnification phase contrast imaging (Figure 2B). Next, *Xenopus* spinal neurons, loaded with TMR-KabC, were acutely treated with 25 µg/ml LN and imaged for 2 min at 2 Hz every 5 min after LN treatment (Movie 3). Analysis of the rate of RF in growth cones by kymography (Figure 2C) shows that RF slows within 5 min post LN treatment, in a temporal pattern that mirrors the *de novo* assembly of point contacts and accelerated neurite outgrowth (Figure 2D). This temporal correlation supports the notion that mechanical coupling between point contact adhesions and actin filaments, through a molecular clutch, slows retrograde flow and promotes axon elongation.

To confirm that the assembly of point contacts is necessary to reduce RF in response to an immobilized LN substratum, we used co-application of heparin to block adsorption of LN to the culture surface. This experiment dissociates the effects of soluble LN versus an immobilized LN substratum. Heparin is a negatively charged, heavily sulfated glycosaminoglycan, that has been used to prevent non-specific adsorption of Netrin to surfaces, but not specific interactions of Netrin with its cell surface receptors (Moore et al., 2012). Since LN contains a heparin binding site localized to the ß-chain, and the integrin binding region is localized to the α-chain, we hypothesized that pre-treatment of neurons with heparin would not inhibit LN-activation of integrin receptors (Beck et al., 1990). We first tested if we could block the adsorption of LN to a PDL substratum with pre-treatment of 2 µg/ml heparin. When not pre-blocked, we find that soluble LN binds rapidly to a PDL substratum and approaches saturation within 10-15 min (Figure 3A) (Woo et al., 2006). On the other hand, pre-treatment with 2 µg/ml heparin significantly inhibits LN binding (Figure 3A). Next, we sought to

determine how bound versus soluble LN affected axon outgrowth, point contact formation, and RF. As described previously, stimulation with LN for 15 min strongly promotes point contact formation (Figure 3B, C) and axon extension (Figures 3D). However, 15 min treatment with soluble, non-adsorbed (heparin co-treatment, Figure 3E) LN does not support point contact formation (Figure 3C, E), nor axon extension (Figure 3D), and often leads to axon stalling or retraction (Figure 3E, Movie 4). Therefore, soluble, non-absorbed LN could activate cell signals that increase RF. For example, active Src is linked to actin polymerization (Tehrani et al., 2007), which may contribute to “pushing” of actin filaments rearward from the leading edge. Moreover, integrin receptors can activate RhoA (Woo et al., 2006, Vicente-Manzanares et al., 2009) and downstream Rho-associated coiled coil-containing kinase (ROCK), which phosphorylates the myosin regulatory light chain at Ser19, resulting in myosin-II-mediated contractility of the actin network. Therefore, to test how soluble LN influences RF, TMR-KabC labeled neurons were first treated with 2 ug/ml heparin, which alone does not significantly change RF. Interestingly, while RF significantly slows in response to substratum immobilized LN (Figure 3F, H), addition of soluble LN applied with heparin significantly increased RF (Figure 3G, H). Consistent with the activation of RF without increased adhesion, addition of LN with heparin resulted in a robust retraction of many axons (Fig 3D). To verify soluble LN is leading to downstream activation of myosin-II, we repeated the heparin and LN co-treatment experimental paradigm in the presence of 50 μg/ml blebbistatin. We found that myosin-II inhibition blocked the increase of RF elicited by soluble LN (Figure 3G). These data suggest soluble LN is activating actin network contractility. This result is in sharp contrast to bound LN, suggesting that without clutching by point contacts, soluble LN strongly stimulates RF and induces axon retraction.

Local clutching modulates actin retrograde flow at growth cone point contacts

Growth cones are more dynamic and motile on LN compared to PDL and undergo cyclical periods of robust membrane protrusion and retraction. Leading edge protrusions are stabilized by new adhesion formation (Woo et al., 2006, Myers et al., 2011, Myers et al., 2011, Santiago-Medina et al., 2013), whereas membrane retractions often occur in response to adhesion disassembly. Therefore, we examined whether differences in rates of RF correlate with sites of leading edge protrusion versus retraction. As predicted, we find that the rate of RF is significantly slower during membrane protrusion (Figure 4A) compared to a stationary leading edge (Figure 4B), but significantly faster during leading edge retraction (Figures 4C, D). These results suggest that clutching of RF to point contact adhesions may direct axon outgrowth through local regulation of protrusion.

Growth cones on LN exhibit more variable RF rates compared to PDL (Figure 1G), suggesting that local clutching by point contact adhesions may have a stronger influence on RF near adhesions. To determine whether RF rates differ near point contacts, we simultaneously imaged point contact adhesions with PXN-GFP or GFP-dSH2 (Robles et al., 2006), together with TMR-KabC in *Xenopus* spinal neurons on LN (Figure 4E, Movie 5). F-actin bundles that co-localized with stable point contacts (>1min in duration) were used to generate “on” point contact kymographs (Figure 4F). Areas within the leading edge devoid of point contacts were used to generate “off” point contact kymographs (Figure 4G). F-actin bundles “on” point contacts showed a significant attenuation of RF velocity relative to F-actin bundles not associated with point contacts (Figure 4H). These data suggest that leading edge RF can be locally restrained at point contact adhesions in growth cones on LN and is not simply regulated as an ensemble contractile actin network.

Since RF can be differentially modulated within growth cones on homogenous LN, it is possible that changes in the adhesive substrata encountered by growth cones directs axon

extension through local differences in clutching of RF. To test this as a possible mechanism of axon guidance, we cultured neurons on substratum patterns of PDL and LN (Figure 5A-C), which we have shown previously promotes growth cone turning (Gomez et al., 2001). Similar to chemotropic turning assays, patterned substrata have been used to elucidate mechanisms of chemical and mechanical guidance responses (Walter et al., 1987, Gomez and Letourneau, 1994, Evans et al., 2007, Knoll et al., 2007, Treloar et al., 2009, San Miguel-Ruiz and Letourneau, 2014). *Xenopus* spinal cord explants were cultured on striped patterns of PDL and LN created using a silicone mask as described (San Miguel-Ruiz and Letourneau, 2014). As expected, a clear preference for growth on LN was evident at low magnification (Figure 5A-C). Growth cones spanning the PDL/LN border were loaded with TMR-KabC and imaged by TIRF microscopy (Figure 5D-F). Growth cones were selected if three kymograph lines could be generated within individual growth cones partially on each substrata. Therefore, F-actin RF velocities were compared from individual growth cones interacting with two distinct substrata (Figure 5F). Using this experimental paradigm, we found that RF was significantly slower within local regions of growth cones on LN compared to PDL (Figure 5G). It is interesting to note that for growth cones spanning borders, the average rate of RF on PDL was significantly slower compared to homogenous PDL (10.35±.22 vs 12.11±0.23, $P<.0001$). These data suggest that F-actin clutching can be locally controlled at sites of ECM attachment, but that clutching of the entire F-actin network also contributes globally to rates of RF.

Soluble axon guidance cues modulate the rates of F-actin RF

Growth promoting and inhibiting axon guidance cues can influence actin polymerization (Vitriol et al., 2012) and point contact formation (Woo et al., 2006, Myers et al., 2011), but it is not known how soluble cues regulate RF. We previously showed that on LN, brain derived neurotrophic factor (BDNF) promotes point contact formation and enhances neurite outgrowth (Myers et al., 2011), while Semaphorin3A (Sema3A) had the opposite effect (Woo et al., 2006,

Bechara et al., 2008). Therefore, we tested how BDNF and Sema3A affect RF rates on PDL and LN in growth cones labeled with TMR-KabC. We found that treatment with 100 ng/ml BDNF for 15 min did not significantly affect the RF rates in growth cones on PDL, but caused a marked decrease in RF on LN (Figure 6A-D, M, Movie 6). This effect was observed specifically in the subpopulation of growth cones that exhibited protrusive responses to BDNF, as unresponsive growth cones showed little change in RF in response to BDNF (not shown). Since BDNF promotes point contact formation and strongly enhances axon extension on LN, but not PDL (Myers et al., 2011), these data suggest that point contact induced F-actin clutching is a key regulatory mechanism for attractive growth cone responses.

In contrast to BDNF, Sema3A is a repulsive axon guidance factor that disrupts existing growth cone point contacts and prevents new point contact formation (Woo et al., 2006, Bechara et al., 2008). Therefore, if clutching of RF depends on point contacts, we expect that RF rates on LN, but not PDL, will be potentiated in response to Sema3A treatment. To test this, we imaged TMR-KabC labeled growth cones plated on PDL or LN before and after treatment with a sub-collapsing dose of Sema3A (400 ng/ml) for 15 min. Growth cones that stalled in response to Sema3A were analyzed for changes in RF. At this dose, growth cone morphology was only modestly altered, indicating that Sema3A did not depolymerize F-actin. In contrast to the LN-specific effects of BDNF on RF, Sema3A increased RF in growth cones on both PDL (Figure 6E-H) and LN (Figure 6I, J, Movie 7). However, Sema3A treatment caused a greater increase in RF rates in growth cones on LN (Figure 6M). The partial effect of Sema3A treatment on growth cones on PDL may be due to activation of both actin polymerization (Jurney et al., 2002) and RhoA-dependent myosin contraction (Wu et al., 2005, Brown and Bridgman, 2009). In addition to activation of contraction, the stronger stimulation of RF for growth cones on LN may be due to acute disruption of point contacts, which would release the clutching forces normally restraining RF. Therefore, in coordination with ECM-mediated

adhesion, attractive and repulsive axon guidance cues like BDNF and Sema3A may regulate axon outgrowth and guidance by locally modulating rates of RF.

Axonal growth cones exhibit slower actin retrograde flow *in vivo*

Our *in vitro* assays suggest that clutching leading edge RF may control neurite outgrowth and guidance within developing embryos. To begin to investigate the role for RF as a potential regulator of axon guidance *in vivo*, we expressed Td-Tomato F-tractin, a peptide that specifically binds F-actin (Johnson and Schell, 2009, Saengsawang et al., 2012), in Rohon-Beard sensory neurons and commissural interneurons within the developing *Xenopus* neural tube by targeted blastomere injection (Figure 7A). Specific classes of F-tractin-labeled neurons were identified via cell body position and axonal projection patterns in the exposed spinal cord preparations (Santiago-Medina et al., 2011) viewed at low magnification (Figure 7B). Growth cones of Rohon-Beard sensory neurons extending along the dorsal fascicle of the neural tube, as well as growth cones of commissural interneurons extending ventrally toward the floor plate, were imaged at high speed and resolution to measure RF (Figure 7C, Movie 8). Confocal optical sections were collected at a single focal plane (~700 nm) from growth cones that remained in focus for the duration of the imaging sequence, allowing us to accurately track linear movements of GFP-actin puncta. Quantification of kymographs revealed that growth cones *in vivo* exhibit significantly slower RF compared to growth cones cultured on both PDL and LN (Figure 7D). While the rate of RF *in vivo* could be slower due to reduced myosin-II activity, it is possible that strong F-actin clutching within the three dimensional space of the developing embryo contributes to slow RF rates. Clutching of RF *in vivo* may occur through growth cone receptor interactions with ECM or cell adhesion molecule ligands present in the spinal cord (Myers et al., 2011). We confirmed that RF measurements made *in vivo* depend on myosin-II activity by treating embryos with blebbistatin (Figure 7F-H), which reduced RF.

However, note that the effects of blebbistatin on RF *in vivo* are less pronounced than we observed on LN *in vitro* (Figure 1), which may be due to limited access to blebbistatin *in vivo*. Alternatively, adhesion complexes that clutch RF *in vivo* may also be disrupted by inhibition of myosin-II, which would oppose the effects of inhibition of myosin-II on RF. Td-Tomato F-tractin was specifically used in these experiments since 488 nm excitation light photo-inactivates blebbistatin, precluding use of GFP-actin.

Discussion

Mechanical forces produced within growth cones are coordinated by extracellular factors to guide axon extension (Tyler, 2012, Kerstein et al., 2015). Protrusive forces are thought to be largely directed by regulated actin polymerization, but here we show that modulation of F-actin RF by clutching to point contact adhesion sites may be an equally important determinant for axon outgrowth and guidance (see Model). Using TMR-KabC and GFP-actin to measure RF, we show that RF in growth cones depends on culture substratum and varies inversely with the rate of outgrowth (Model 1A, B). We find that RF is slow and variable in highly motile growth cones on LN and *in vivo*. The variability of RF rates locally within individual growth cones on LN suggests there is local modulation of clutching, which we demonstrate occurs at sites of paxillin-containing point contact adhesions. Differential rates of RF also correlate with locations of leading edge protrusion and retraction, suggesting localized clutching may regulate axon guidance (Model 1C, D). Consistent with this notion, we show that local differences in RF rates occur within growth cones spanning substratum boundaries. Finally, we show that soluble axon guidance cues that modulate point contact adhesion assembly and disassembly also affect RF rates on LN, suggesting axons associated with ECM *in vivo* may be guided by local modulation of F-actin clutching.

While clutching of RF has been hypothesized as a guiding force for developing axons (Mitchison and Kirschner, 1988, Suter et al., 1998, Bard et al., 2008, Shimada et al., 2008, Toriyama et al., 2013, Garcia et al., 2015), our study provides the first evidence of clutch-dependent axon extension and guidance on an ECM substratum. The clutch hypothesis was initially described by Mitchison and Kirschner (Mitchison and Kirschner, 1988), and has been largely examined for clutching to cell adhesion molecules (CAM). In *Aplysia* growth cones, a local reduction in RF upon contact with immobilized Aplysia CAM (apCAM) coated beads correlates with the targeted invasion of microtubules from the central domain toward the

restrained bead, suggesting preferential growth in the direction of clutched RF (Suter et al., 1998). However, due to the slow growth rate of Aplysia axons, studying the effect of clutching on overall outgrowth or local guidance is limited. In this study, we show that clutching to point contact adhesions is necessary for LN, as well as BDNF and Sema3A induced changes in RF, which correlates with local protrusion and retraction. Similar to apCAM, L1 clutches and attenuates RF through the adapter protein shootin to promote axonal outgrowth downstream of Netrin-1 (Shimada et al., 2008, Toriyama et al., 2013). More recently, local coupling of F-actin to N-cadherin through α-catenin was found to clutch RF locally on N-cadherin micropatterns (Bard et al., 2008, Garcia et al., 2015). Therefore, it appears CAM protein complexes function to link F-actin and restrain RF to promote axon outgrowth through distinct adaptor proteins. However, whether integrin-ECM adhesion complexes use similar mechanisms has not been examined. While cell-cell adhesive interactions play key roles in axon tract formation, pioneering growth cones often navigate through a complex ECM (Myers et al., 2011). Immobilized ECM proteins form a rigid substrata which enable traction forces necessary for force generation (Gardel et al., 2008, Moore et al., 2009, Koch et al., 2012, Moore et al., 2012). Additionally, pioneering axons secrete matrix metalloproteases to remodel their local ECM, making substratum interactions highly dynamic (Santiago-Medina et al., 2015). Our study is the first to show that modulation of clutching of F-actin RF at point contact adhesions regulates local protrusion and retraction at the growth cone leading edge downstream of permissive and repulsive axon guidance cues.

Experiments testing the effects of soluble versus substratum-associated LN suggest signaling pathways regulate growth cone motility downstream of integrin receptor activation and clustering. Integrin clustering is known to occur in response to immobilized, but not soluble ligands (Cluzel et al., 2005). Integrin clustering leads to recruitment and phosphorylation of adhesion adaptor proteins, such as paxillin and FAK (Robles et al., 2006, Myers et al., 2011).

The additional downstream signals activated by substratum-bound LN may be due to integrin receptor clustering that provides “mechanical” activation of growth cones. It is unclear how integrin receptor clustering on immobilized LN promotes additional signaling in growth cones. However, clustered integrins do activate RhoA and Rho-associated coiled coil-containing kinase (ROCK) (Cluzel et al., 2005), which increases MLC2 phosphorylation at Ser19 (Woo et al., 2006) to promote F-actin contractile forces (Vicente-Manzanares et al., 2009). The RhoA-ROCK-myosin-II signaling cascade acts as a feedback control to further stabilize and mature adhesions in the lamellipodia of migrating cells (Chrzanowska-Wodnicka and Burridge, 1996, Vicente-Manzanares et al., 2009). Interestingly, previous work showed a similar requirement of immobilized Netrin and myosin contractile forces in the activation of FAK and p130-Cas (Moore et al., 2012). Inhibition of myosin-II prevented activation of FAK and p130-Cas downstream of stimulation with substratum-associated Netrin (Moore et al., 2012). P130-Cas forms a complex with the adaptor molecule Crk to induce downstream activation of Rho GTPases, such as Rac1 and Cdc42 (Liu et al., 2007). These data suggest the importance of mechanosensitive signaling molecules in point contact adhesions. The early targeting of adaptor proteins to activated and clustered integrins may promote local myosin-II-mediated F-actin contractile forces. These mechanical forces may promote further phosphorylation and clustering of putative mechanosensitive molecules (Moore et al., 2010, Ciobanasu et al., 2014). Several molecules that target to growth cone point contacts have been shown to function as mechanosensors including talin (del Rio et al., 2009), FAK (Wang et al., 2001), vinculin (Grashoff et al., 2010) and p130-Cas (Sawada et al., 2006). These proteins are unfolded by “stretching” of the protein, which is believed to expose cryptic protein binding and phosphorylation sites leading to further maturation of adhesions (Vicente-Manzanares et al., 2009, Moore et al., 2010).

In motile growth cones, actin treadmilling is believed to be driven by both pulling forces from myosin-II motor-mediated F-actin sliding and pushing forces at the membrane from barbed-end actin polymerization at the leading edge (Forscher et al., 1988, Lin et al., 1995, Brown et al., 2003). In contrast, the distal lamellipodium of migrating, non-neuronal cells lacks myosin II-mediated contractile forces and RF is largely powered by leading edge actin polymerization (Ponti et al., 2004, Vicente-Manzanares et al., 2009). In fibroblasts, myosin-II is localized proximal to the lamellipodium within the lamellum region where it organizes actin and contributes to RF. However, actomyosin filaments in neuronal growth cones are not so rigidly organized structures and are much more dynamic. The unique morphology and dynamics of growth cones suggest they possess distinct mechanisms governing traction forces at the leading edge. Indeed, myosin-II is highly expressed in the growth cone central domain, transition zone, and to a lesser extent along f-actin bundles in the peripheral domain (Bridgman et al., 2001, Medeiros et al., 2006, Burnette et al., 2008). Our findings verify the function of myosin-II in the growth cone peripheral domain as blebbistatin treatment reduces RF rates at the leading edge. Together with previous evidence (Bridgman et al., 2001), our findings suggest that chemotropic factors could target myosin-II to regulate RF and direct growth cone motility.

It is important to note that we find that the rates of RF are only partially reduced by inhibition of myosin-II (Figure 1H-I). Moreover, we find that the effects of myosin-II inhibition on RF rates are greater for growth cones on PDL compared to LN and compared to growth cones *in vivo* (Figure 1I). This difference may be due to the disruption of point contact adhesions of growth cones on LN and *in vivo* by myosin-II inhibition (Woo et al., 2006), which would balance the loss of myosin-II motor activity. Interestingly, these data suggest that the rate of actin polymerization is greater on LN compared to PDL, since the rate of RF is higher on LN compared to PDL under conditions where adhesions are lost and myosin-II is inactivated.

Heightened actin polymerization on LN is consistent with integrin-activated signals, such as Src/FAK tyrosine kinase signaling (Figure 3) that can activate Cdc42 and Rac1 (Woo et al., 2006, Myers et al., 2012).

Local differences in RF rates within growth cones at sites of point contact adhesions (Figure 4E-I) suggest that local clutching can slow RF regionally within the actin filament network. Discontinuities of RF correlate with areas of leading edge protrusion and retraction (Figure 4A-D), suggesting localized clutching may influence the direction of outgrowth. Sites of local protrusion are associated with areas of increased actin polymerization (Mallavarapu and Mitchison, 1999, Krause and Gautreau, 2014), which is expected to increase RF (Van Goor et al., 2012). Therefore, our observations of reduced RF at sites of membrane protrusion suggest that clutching forces are highest in protrusive areas, which is consistent with traction force microscopy showing elevated traction forces at focal adhesions (Gardel et al., 2008) and in the direction of cell migration (Munevar et al., 2001).

We have previously demonstrated that soluble axon guidance cues modulate growth cone motility in part through modulation of integrin point contact adhesion dynamics (assembly and turnover) (Woo et al., 2006, Woo et al., 2009, Myers et al., 2011). Specifically, BDNF promotes axon outgrowth by stimulating adhesion assembly and turnover (Myers et al., 2011), while Sema3A destabilizes adhesions (Woo et al., 2006). Consistent with links between point contact adhesions and RF, we show here that BDNF slows RF specifically in growth cones on LN (Figure 6, 8C), while Sema3A increases RF most robustly in growth cones on LN (Figure 6, 8D). These results further imply that soluble cues may differentially affect axon guidance depending on the cell substratum. Growth cones use a variety of insoluble protein substrata to support traction forces during axon extension *in vivo*, including a variety of ECM proteins and cell adhesion molecules. Actin RF is also restricted through associations with cell adhesion molecules, such as IgCAM and L1 (Suter et al., 1998, Shimada et al., 2008), which can be

regulated by axon guidance cues. We show here that RF occurs *in vivo,* but is slower relative to RF observed on homogenous LN *in vitro*. The identity of extracellular substrata and intracellular adaptor proteins is unclear *in vivo*, but RF rates are closer to those observed on cell adhesion molecules. It is known that combinatorial activities of permissive, attractive, and repulsive guidance cues encountered simultaneously *in vivo* are integrated by growth cones to regulate axon pathfinding behaviors necessary to build complex neural networks (Dudanova et al., 2013). Future studies should attempt to specifically interfere with clutching forces *in vivo* to determine if modulation of RF plays a significant role in axon pathfinding *in vivo.*

Figure 1. The rate of axon outgrowth is inversely proportional to actin retrograde flow rates. (A-D) Actin RF in motile growth cones was visualized by TIRF microscopy using TMR-KabC, a barbed-end binding actin probe. Kymographs were generated from 2 min time-lapse sequences of TMR-KabC labeled growth cones cultured on indicated substrata. Dashed yellow lines indicate example lines used to calculate flow rates. **(E)** The rate of RF (left axis) and axon outgrowth (right axis) is inversely related for spinal neurons plated on different substrata, Poly-d-Lysine (PDL, n=16 GCs, 68 axons), 10 µg/ml Laminin (LN, n=15 GCs, 95 axons), PDL plus LN (n=16 GCs, n=185 axons), 10 µg/ml Fibronectin (FN, n=16 GCs, n=70 axons), 5 µg/ml Tenascin (TN, n=8 GCs, n=37 axons). **(F)** The rate of RF (left axis) and axon outgrowth (right axis) axis is inversely related for neurons plated on increasing concentrations of LN: 1 µg/ml (n=11 GCs, n=80 axons), 5 µg/ml (n=9 GCs, n=101 axons), 10 µg/ml (n=10 GCs, 63 axons), and 25 µg/ml (n=12 GCs, n=249 axons). **(G)** 2D image of a GFP-actin expressing growth cone on PDL with kymograph sample line through leading edge (red line). Scale, 5 µm. **(H-I)** Kymographs were created from growth cones on PDL (H) and 10 µg/ml LN (I). **(J)** Growth cones labeled with TMR-KabC and GFP-actin exhibited significantly lower RF rates on LN (n=17 GCs) relative to PDL (n=20 GCs). **(K)** The coefficient of variation (standard deviation/ mean) of TMR-KabC RF is significantly greater for growth cones plated on 10 µg/ml LN (n=137) versus PDL (n=105). **(L)** Kymographs generated from 2 min time-lapse sequences of TMR-KabC labeled growth cones captured at indicated times before and after 50 µM blebbistatin treatment. **(M)** The rate of RF after blebbistatin treatment was significantly attenuated on PDL (n=9 GCs) and LN (n=8 GCs) (***$p<0.001$), but the percent reduction (not shown) was more significantly reduced in growth cones on PDL ($p<0.001$). ***$p<0.001$, *$p<0.05$.

Figure 1.

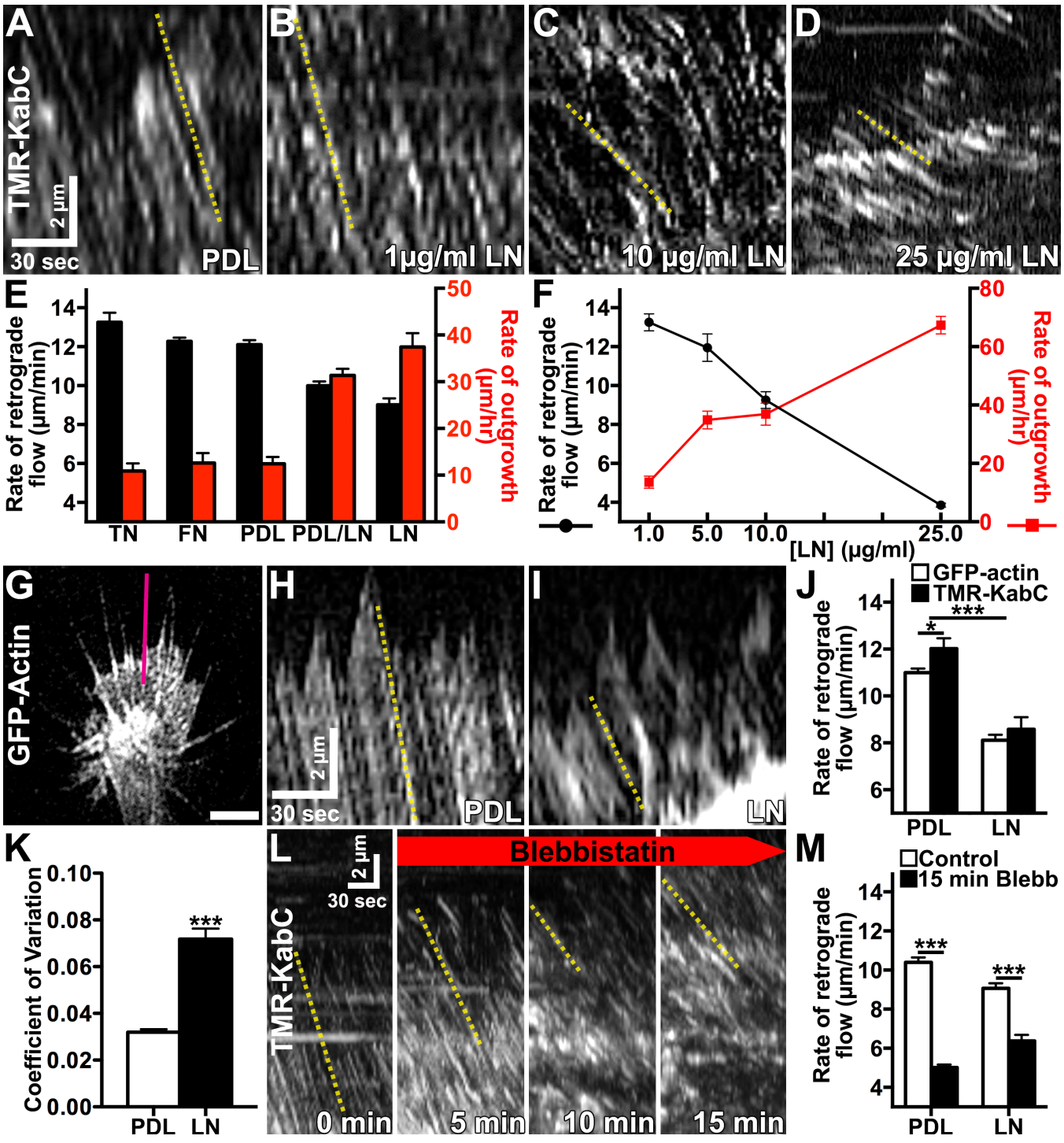
A
TMR-KabC
2 µm
30 sec
PDL
B
1µg/ml LN
C
10 µg/ml LN
D
25 µg/ml LN
E
Rate of retrograde flow (µm/min)
Rate of outgrowth (µm/hr)
TN
FN
PDL
PDL/LN
LN
F
[LN] (µg/ml)
1.0
5.0
10.0
25.0
G
GFP-Actin
H
I
J
GFP-actin
TMR-KabC
K
Coefficient of Variation
L
Blebbistatin
0 min
5 min
10 min
15 min
M
Control
15 min Blebb

Figure 2. Acute LN stimulation accelerates axon outgrowth over a time course that correlates with point contact formation and reduced retrograde flow. (A-A”’) Confocal images of a growth cone expressing PXN-GFP on PDL before and at indicated times after addition of 25 μg/ml LN. Within 10 min of LN addition, many point contact adhesions form (red arrowheads). Scale, 5 μm. **(B)** Low magnification phase contrast images showing most axons accelerate (color-matched arrowheads) after 15 min treatment with 25 μg/ml LN. Scale, 50 μm. **(C)** Kymographs generated from 2 min time-lapse sequences of TMR-KabC labeled growth cones captured at indicated times before and after LN addition. Dashed yellow lines indicated calculated example flow rates. **(D)** The average rate of axon outgrowth (n=56) versus RF (n=10 GCs) at times before and after LN stimulation shows an inverse relationship. ***$p<0.001$, **$p<0.01$, *$p<0.05$.

Figure 2.

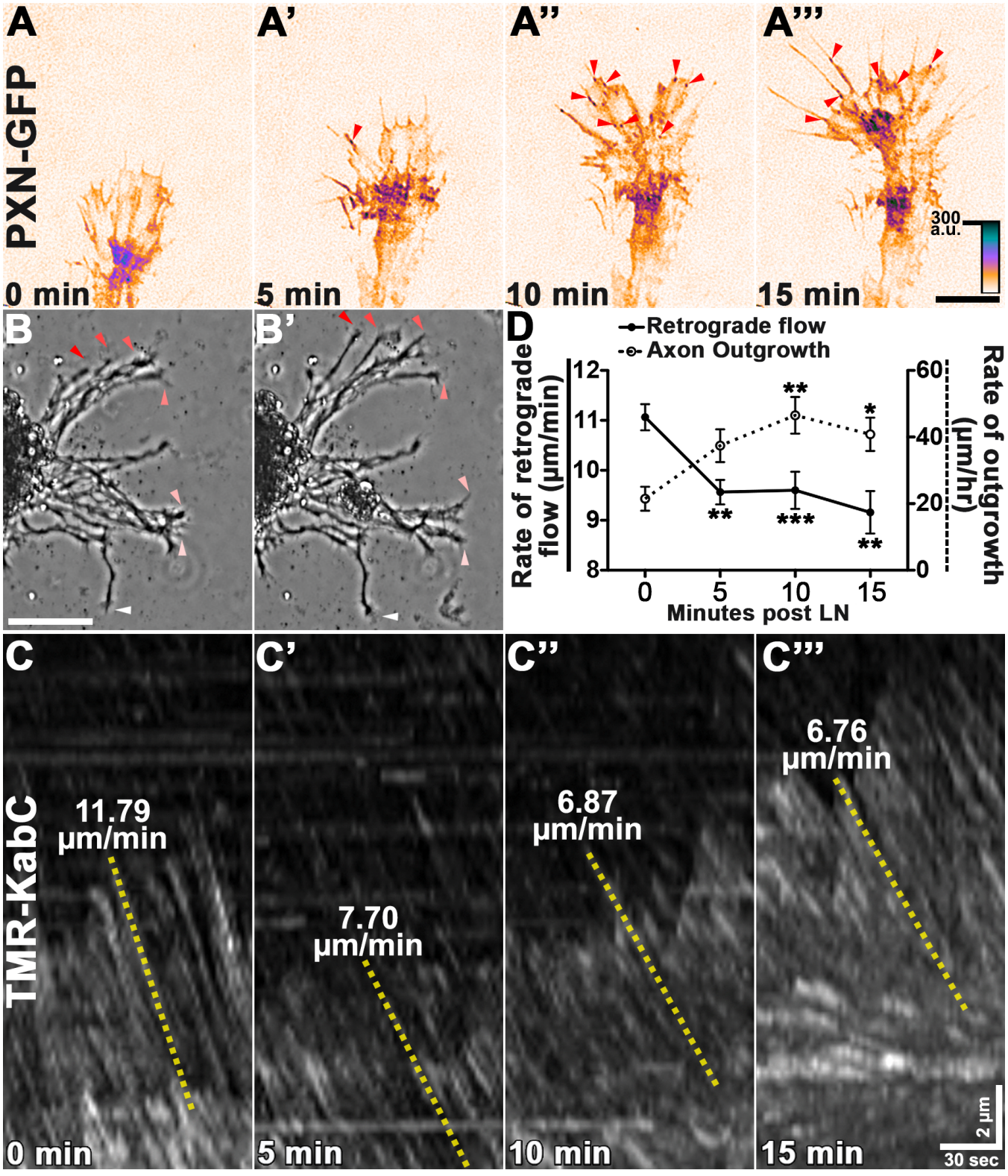
A
A'
A''
A'''
PXN-GFP
0 min
5 min
10 min
15 min
300
a.u.
B
B'
D
Retrograde flow
Axon Outgrowth
Rate of retrograde flow (µm/min)
Rate of outgrowth (µm/hr)
12
11
10
9
8
60
40
20
0
0
5
10
15
Minutes post LN
**
**
***
**
*
C
C'
C''
C'''
TMR-KabC
11.79 µm/min
7.70 µm/min
6.87 µm/min
6.76 µm/min
0 min
5 min
10 min
15 min
2 µm
30 sec

Figure 3. Point contact formation is required for LN induced axon outgrowth. (A, A') TIRF images of PXN-GFP expressing growth cone on PDL before (A) and 15 min after addition of LN (A').**(B)** The mean intensity of fluorescent LN on PDL-coated glass coverslips treated for 15 min with 25 µg/ml LN alone, 2 µg/ml heparin alone, and LN plus heparin. **(C)** Axon outgrowth on PDL (n=80) is stimulated by 15 min treatment with LN (n=52), but is strongly inhibited by soluble LN (LN plus heparin, n=25). **(D, D')** TIRF images of PXN-GFP expressing growth cone on PDL before (E) and 15 min after (E') addition of LN plus heparin. **(E, F)** Kymographs generated from 2 min time-lapse sequences of TMR-KabC labeled growth cones on PDL before (E, F) and after stimulation with LN (E') and LN plus heparin (F'). Dashed yellow lines indicate example lines used to calculate flow rates. **(G)** Average rates of TMR-KabC RF in growth cones plated on PDL before and 15 min after indicated stimulations. Adsorbed LN significantly slows RF, while soluble LN significantly accelerates RF (n=9 GCs). Scale, 5 µm. ***p<0.001, **p<0.01, *p<0.05.

Figure 3.

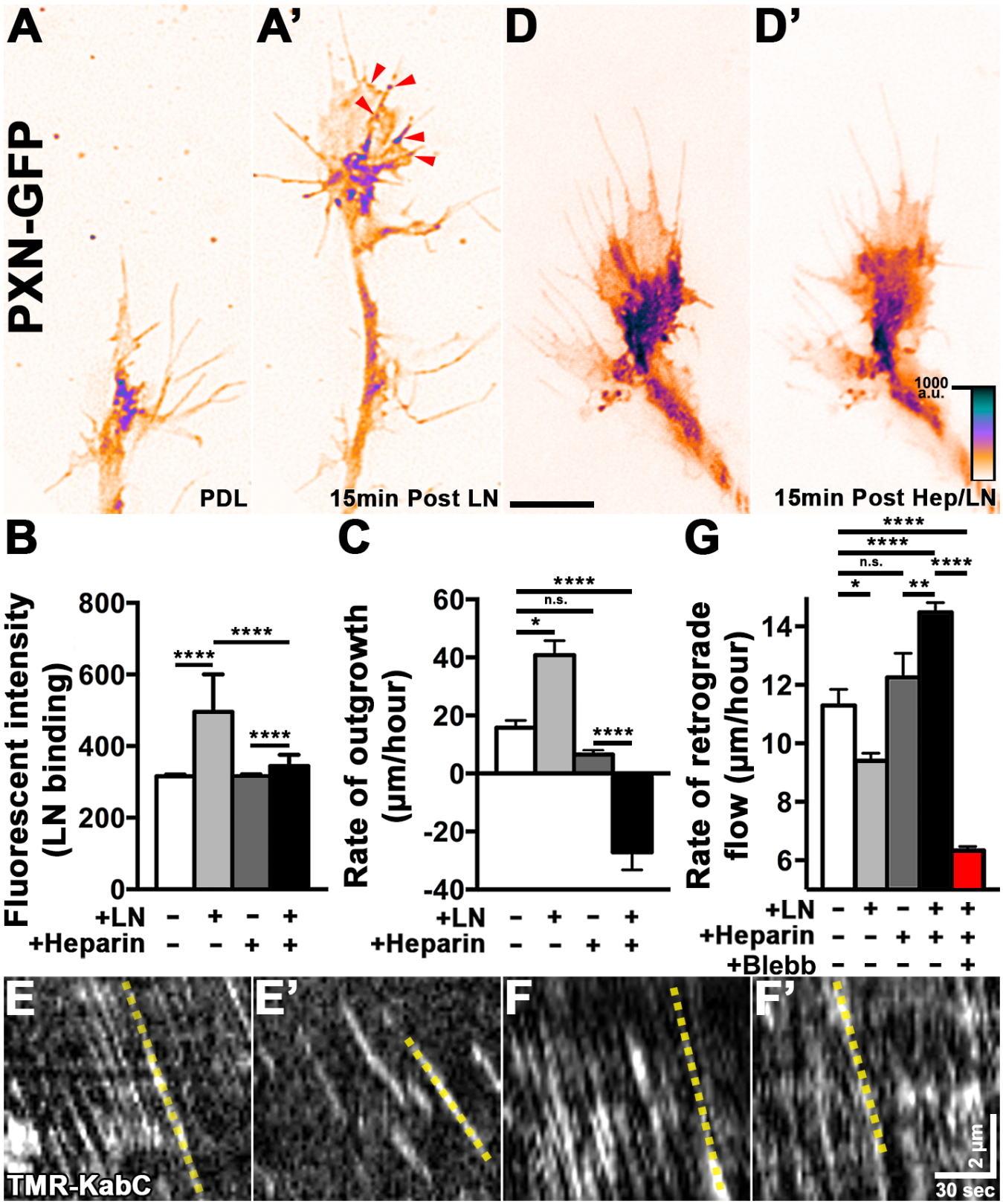
A
A'
D
D'
PXN-GFP
PDL
15min Post LN
15min Post Hep/LN
1000 a.u.
B
Fluorescent intensity (LN binding)
800
600
400
200
0
****
****
****
+LN - + - +
+Heparin - - + +
C
Rate of outgrowth (µm/hour)
60
40
20
0
-20
-40
****
n.s.
*
****
+LN - + - +
+Heparin - - + +
G
Rate of retrograde flow (µm/hour)
14
12
10
8
6
****
****
n.s.
****
*
**
+LN - + - + +
+Heparin - - + + +
+Blebb - - - - +
E
E'
F
F'
TMR-KabC
2 µm
30 sec

Figure 4. F-actin retrograde flow rates correlate with leading edge protrusion/retraction and is reduced at adhesion sites. (A-C) Representative kymographs generated from regions of protruding (A), stationary (B) and retracting (C) leading edge membrane. Dashed yellow lines indicated calculated example flow rates. Yellow line indicates growth cone leading edge. **(D)** The rate of RF is significantly slower in protruding relative to stationary and retracting membranes (n=15 GCs). **(E)** 2D TIRF image of a growth cone expressing PXN-GFP (green) and labeled with TMR-KabC (red). Note strong TMR-KabC labeling at the leading edge where F-actin barbed-ends are concentrated. **(F-G)** Kymographs generated from 2 min time-lapse sequences of TMR-KabC and PXN-GFP double-labeled growth cones using sampling lines over adhesions (F) and off adhesions (G). Horizontal green lines in (F) represent stable PXN-containing adhesions. **(H)** The average RF rates over adhesions (n=38) are significantly slower than off adhesions (n=25) and compared to randomly sampled (n=63) RF rates. Scale, 5 μm. ***$p<0.001$, **$p<0.01$, *$p<0.05$.

Figure 4.

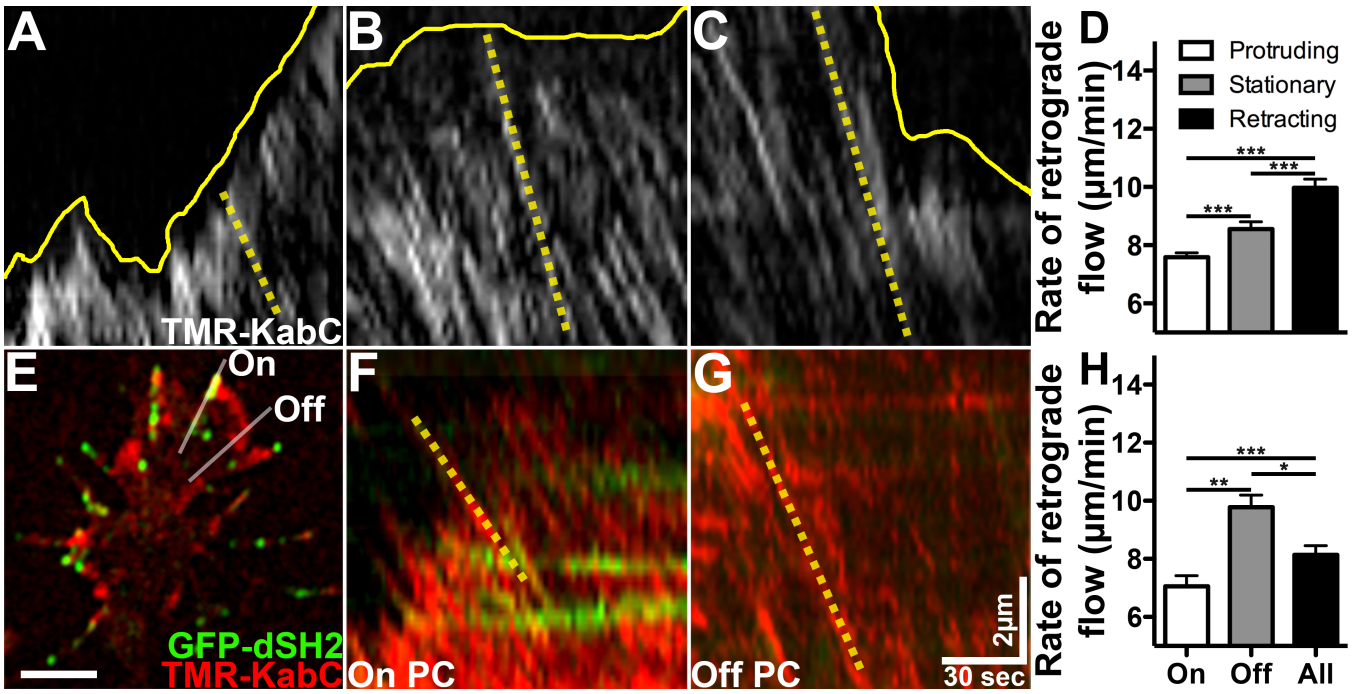
A
B
C
D
TMR-KabC
Protruding
Stationary
Retracting
Rate of retrograde flow (µm/min)
14
12
10
8
6
***
***
***
E
On
Off
F
G
H
GFP-dSH2
TMR-KabC
On PC
Off PC
2µm
30 sec
**
*
On
Off
All

Figure 5. F-actin retrograde flow is locally regulated within growth cones at PDL/LN substrata borders. (A-C) Low magnification images of *Xenopus* spinal cord explants labeled for F-actin using Alexa546-Phalloidin (A) cultured on a patterned substratum of alternating lanes of PDL and LN (B). Borders were visualized using fluorescent (HiLyte 488) LN (green). Pseudo-colored image merge (C) shows strong preference for LN. Scale, 50 μm. **(D-E)** High magnification TIRF image of a growth cone labeled with TMR-KabC (D) spanning a PDL/LN border (E). LN was labeled with Succinimidyl Ester 647 (SE-647). **(F)** Merged image of TMR-KabC labeled growth cone (magenta) spanning border between LN (green) and PDL (unlabeled) with representative lines used to generate kymographs. **(G)** The average rates of RF in growth cones spanning a PDL/LN border are significantly faster over PDL compared to LN (n=27 GCs). However, differences between LN (n=15 GCs) and PDL (n=10 GCs) are more dramatic on homogenous substrata (Note RF rates on homogenous substrata are data duplicated from Fig 1 for comparison). Scale, 5 μm. ***$p<0.001$, *$p<0.05$.

Figure 5.

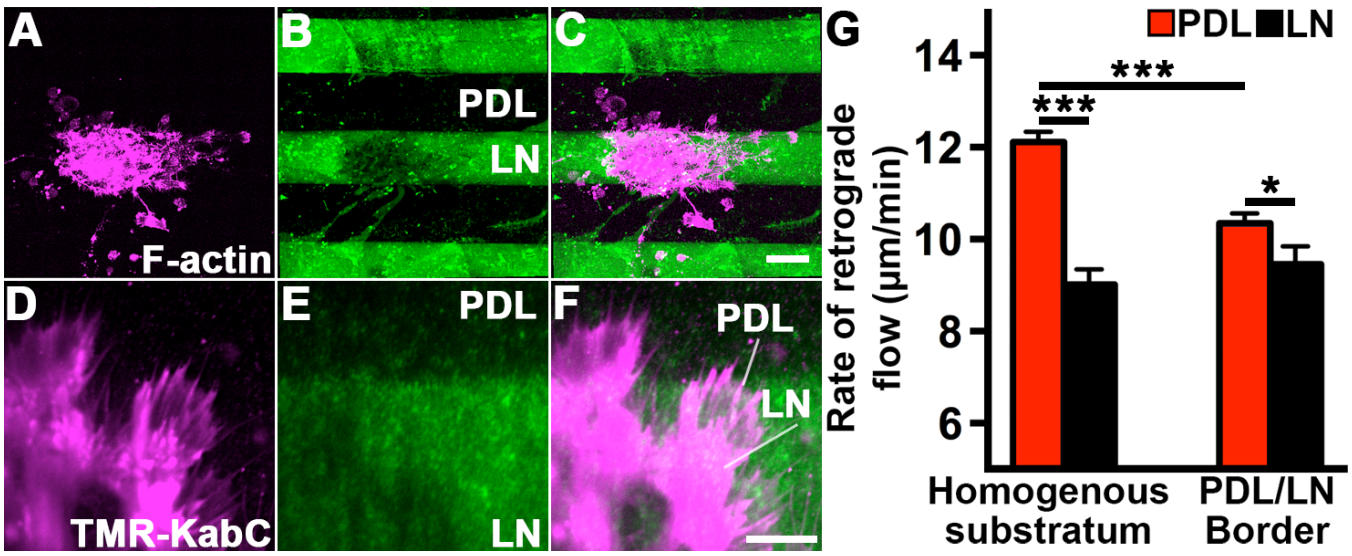
A
F-actin
B
PDL
LN
C
D
TMR-KabC
E
PDL
LN
F
PDL
LN
G
PDL LN
Rate of retrograde flow (µm/min)
14
12
10
8
6
***
***
*
Homogenous substratum
PDL/LN Border

Figure 6. Soluble axon guidance cues modulate the rates of F-actin RF. (A, B) 2D TIRF images of a TMR-KabC labeled growth cone on LN before (A) and 15 min after BDNF treatment (B). Note this growth cone expands in response to BDNF. **(C, D)** Kymographs generated from 2 min time-lapse sequences of TMR-KabC labeled growth cones captured before (C) and after BDNF treatment (D). Dashed yellow lines indicated calculated example flow rates. **(E, F)** 2D TIRF images of a TMR-KabC labeled growth cone on PDL before (E) and 15 min after Sema3A treatment (F). Note this growth cone retracts slightly in response to Sema3A treatment. **(G, H)** Kymographs generated from 2 min time-lapse sequences of TMR-KabC labeled growth cones captured before (G) and after Sema3A treatment (H). **(I, J)** 2D TIRF images of a TMR-KabC labeled growth cone on LN before (I) and 15 min after Sema3A treatment (J). Note this growth cone retracts slightly in response to Sema3A treatment. **(K, L)** Kymographs generated from 2 min time-lapse sequences of TMR-KabC labeled growth cones captured before (K) and after Sema3A treatment (L). **(M)** BDNF has little effect on the rate of RF of growth cones on PDL (n=5 protruding GCs), but RF significantly slows in growth cones on LN (n=16 protruding GCs). Sema3A accelerates RF of growth cones on LN (n=11 GCs) more significantly compared to growth cones on PDL (n=11 GCs). Scale, 5 μm. ***$p<0.001$.

Figure 6.

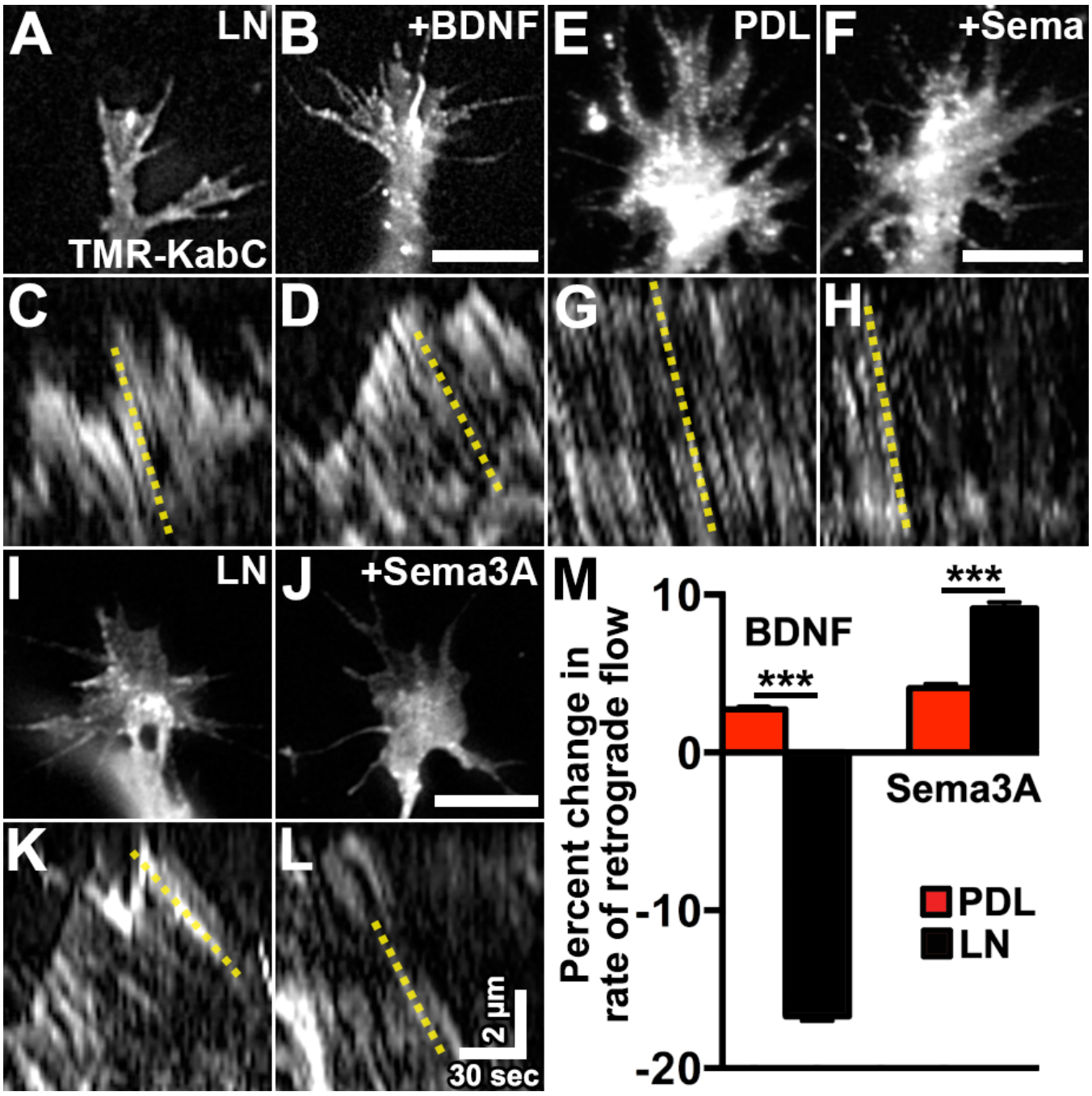
A
LN
TMR-KabC
B
+BDNF
E
PDL
F
+Sema
C
D
G
H
I
LN
J
+Sema3A
K
L
2 µm
30 sec
M
Percent change in rate of retrograde flow
10
0
-10
-20
BDNF
***
***
Sema3A
PDL
LN

Figure 7. Axonal growth cones exhibit slow actin RF *in vivo.* (A) Schematic illustrating blastomere injection of DNA plasmid encoding Td-Tomato F-tractin targeted to the dorsal spinal cord. Embryos were allowed to develop to 24 hours post-fertilization (hpf) before exposing spinal cord for live imaging. **(B)** Low magnification and contrast stretched confocal z-series projection showing F-tractin labeled Rohon-Beard neuron (red arrow) and commissural interneuron (white arrow). An ascending RB axon is tipped by a growth cone (box). Scale, 30 μm. **(C)** High magnification image from time series used to generate kymographs (yellow line) of growth cone from boxed region in (B). Scale, 5 μm. **(D)** The rate of RF *in vivo* (n=19 GCs) is significantly slower than RF rates observed in cultured neurons on PDL and 10 μg/ml LN. **(E, F)** Kymographs generated from 2 min time-lapse sequences of a F-tractin labeled growth cone before (E) and after (F) inhibition of myosin II with 50 μM blebbistatin. Dashed yellow lines indicated example flow lines used to calculate rates. **(G)** The rate of RF after blebbistatin treatment is significantly reduced relative to pre-treatment and DMSO control media. Scale, 10 μm. (***$p<0.001$).

Figure 7.

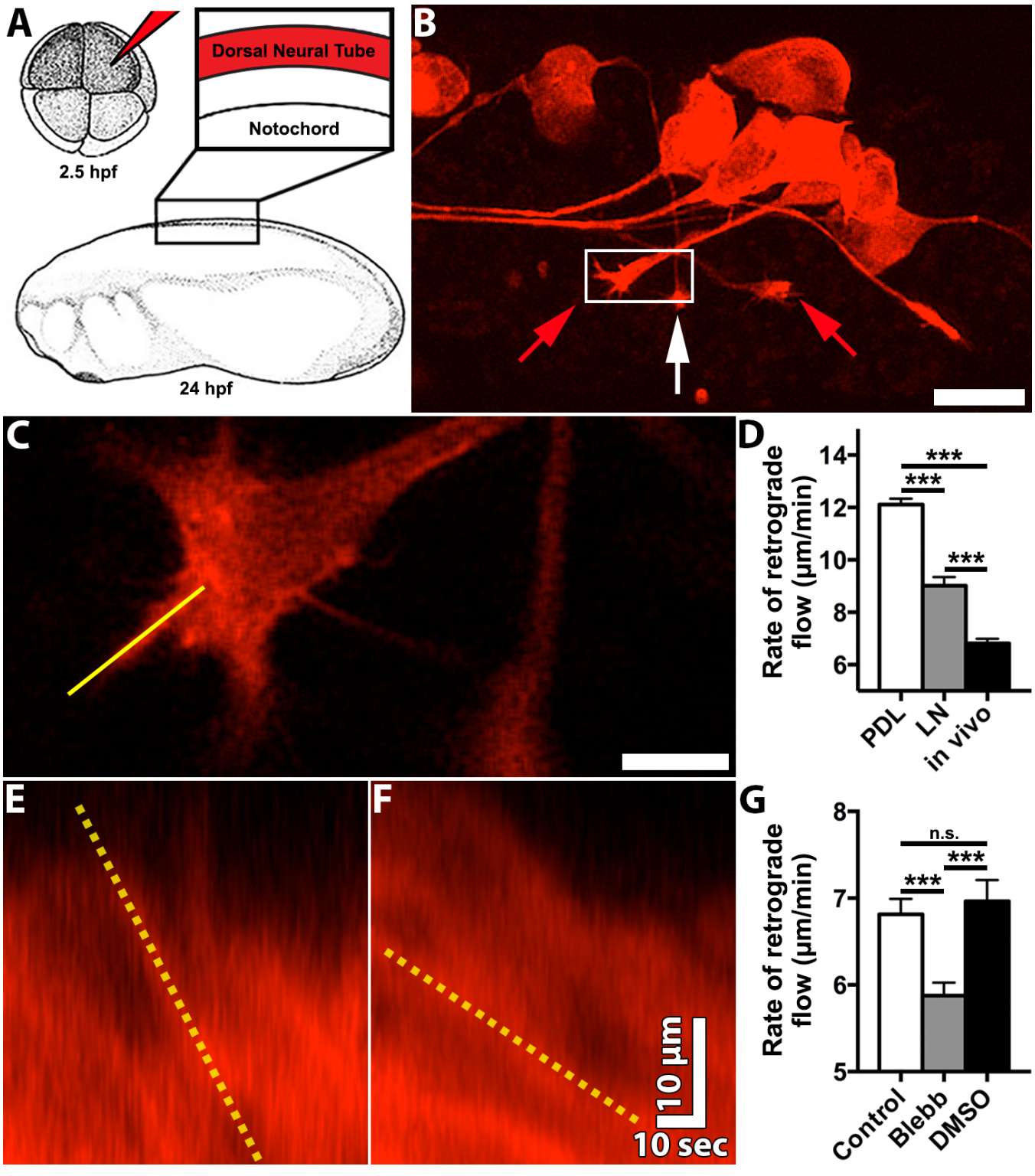
A
Dorsal Neural Tube
Notochord
2.5 hpf
24 hpf
B
C
D
Rate of retrograde flow (µm/min)
14
12
10
8
6
***
***
***
PDL
LN
in vivo
E
F
10 µm
10 sec
G
Rate of retrograde flow (µm/min)
8
7
6
5
n.s.
***
***
Control
Blebb
DMSO

Model 1. Regulation of protrusion through modulation of integrin-dependent F-actin clutching by axon guidance cues. Actin filaments populating the leading edge of growth cones undergo constant RF due to proximal myosin-II mediated contractile forces ($F_{contraction}$) and distal actin polymerization, which pushes against the plasma membrane to propel filaments rearward ($F_{polymerization}$). **(A)** In the absence of integrin activation and clustering, the molecular clutch is disengaged and $F_{contraction}$ and $F_{polymerization}$ drive rapid actin RF. However, even under low clutching conditions, leading edge actin polymerization can at times exceed RF, resulting in modest forward protrusion ($F_{protrusion}$) and some forward translocation of the growth cone. **(B)** In the presence of ECM proteins, integrin receptors are activated, cluster and recruit adhesome-related adaptor and signaling proteins to form point contact adhesions, which link to actin filaments. Point contact adhesions form a slip clutch with actin filaments ($F_{adhesion}$), which restricts RF and generates traction forces ($F_{traction}$) on the ECM. Integrin activation also increases myosin-II activity and actin polymerization, which should increase actin RF. However, faster RF is overcome by point contact mediated clutching, which promotes forward growth cone translocation. **(C)** BDNF increases point contact formation and turnover (Myers and Gomez 2011) and promotes actin polymerization, as well as myosin-II activation (Gehler et al., 2004). However, more point contact adhesions that are rapidly turning over further clutch RF to increase forward protrusion and accelerate axon outgrowth. **(D)** Sema3A, a repulsive axon guidance cue, promotes the disassembly of point contacts (Woo and Gomez 2006), which disrupts F-actin clutching to minimize $F_{adhesion}$ and $F_{traction}$. In addition, Sema3A activates RhoA and ROCK, resulting in phosphorylation of myosin-II at Ser19, to increase $F_{contraction}$ (Gallo, 2006). Loss of point contact clutching and increased $F_{contraction}$ leads to strong activation of RF and subsequent axon stalling and retraction.

Model 1.

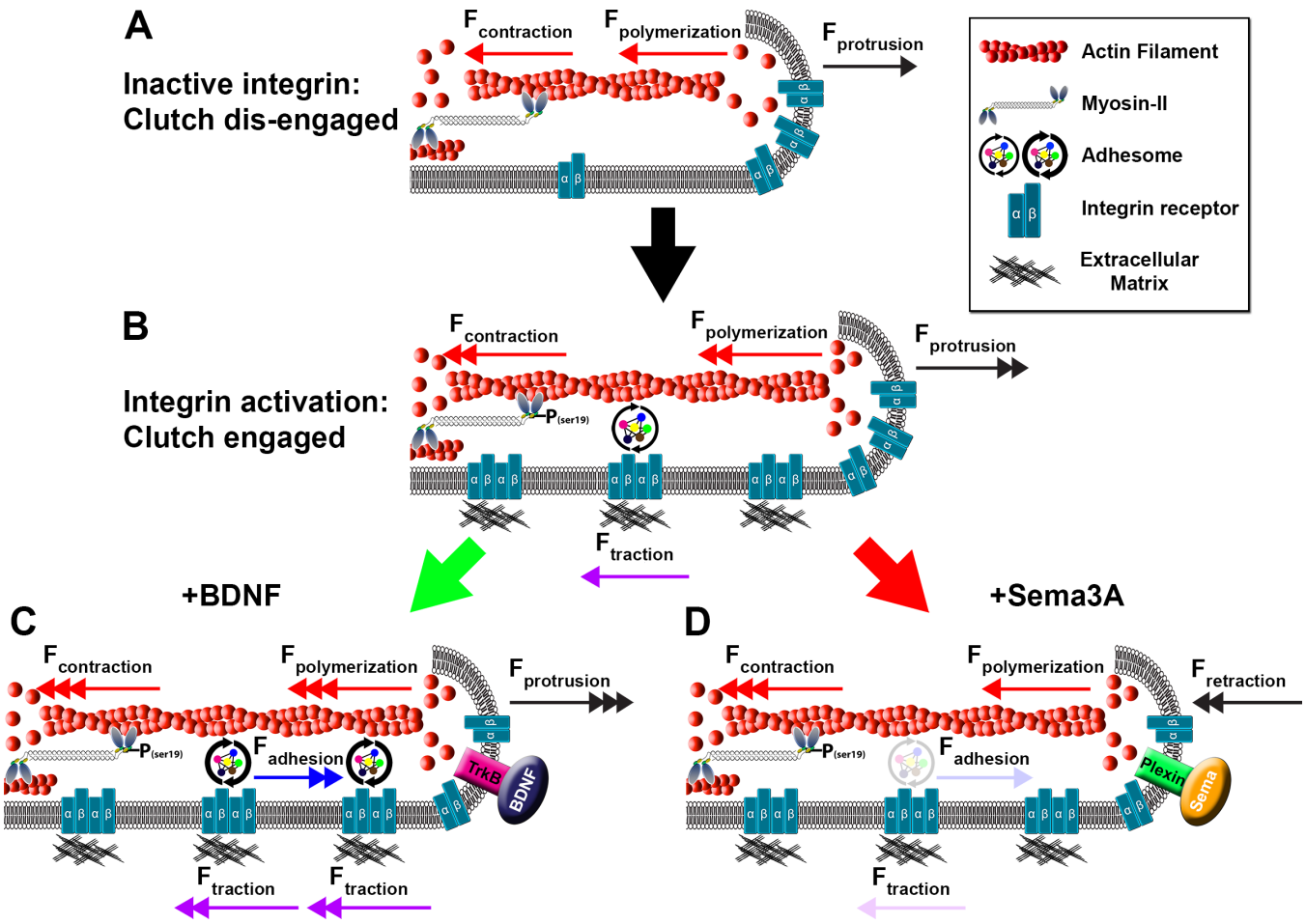
A
Inactive integrin:
Clutch dis-engaged
F contraction
F polymerization
F protrusion
Actin Filament
Myosin-II
Adhesome
Integrin receptor
Extracellular Matrix
B
Integrin activation:
Clutch engaged
P(ser19)
F traction
+BDNF
+Sema3A
C
F adhesion
TrkB
BDNF
D
F retraction
Plexin
Sema

Bibliography

Antar LN, Li C, Zhang H, Carroll RC and Bassell GJ (2006) Local functions for FMRP in axon growth cone motility and activity-dependent regulation of filopodia and spine synapses. Mol Cell Neurosci 32(1-2): 37-48.

Bamburg JR (1999) Proteins of the ADF/cofilin family: essential regulators of actin dynamics. Annu Rev Cell Dev Biol 15: 185-230.

Bard L, Boscher C, Lambert M, Mege RM, Choquet D and Thoumine O (2008) A molecular clutch between the actin flow and N-cadherin adhesions drives growth cone migration. J Neurosci 28(23): 5879-5890.

Bechara A, Nawabi H, Moret F, Yaron A, Weaver E, Bozon M, Abouzid K, Guan JL, Tessier-Lavigne M, Lemmon V and Castellani V (2008) FAK-MAPK-dependent adhesion disassembly downstream of L1 contributes to semaphorin3A-induced collapse. EMBO J 27(11): 1549-1562.

Beck K, Hunter I and Engel J (1990) Structure and function of laminin: anatomy of a multidomain glycoprotein. FASEB J 4(2): 148-160.

Bridgman PC, Dave S, Asnes CF, Tullio AN and Adelstein RS (2001) Myosin IIB is required for growth cone motility. J Neurosci 21(16): 6159-6169.

Brown JA and Bridgman PC (2009) Disruption of the cytoskeleton during Semaphorin 3A induced growth cone collapse correlates with differences in actin organization and associated binding proteins. Dev Neurobiol 69(10): 633-646.

Brown ME and Bridgman PC (2003) Retrograde flow rate is increased in growth cones from myosin IIB knockout mice. J Cell Sci 116(Pt 6): 1087-1094.

Burnette DT, Ji L, Schaefer AW, Medeiros NA, Danuser G and Forscher P (2008) Myosin II activity facilitates microtubule bundling in the neuronal growth cone neck. Dev Cell 15(1): 163-169.

Carlier MF and Pantaloni D (2007) Control of actin assembly dynamics in cell motility. J Biol Chem 282(32): 23005-23009.

Choi CK, Vicente-Manzanares M, Zareno J, Whitmore LA, Mogilner A and Horwitz AR (2008) Actin and alpha-actinin orchestrate the assembly and maturation of nascent adhesions in a myosin II motor-independent manner. Nat Cell Biol 10(9): 1039-1050.

Chrzanowska-Wodnicka M and Burridge K (1996) Rho-stimulated contractility drives the formation of stress fibers and focal adhesions. J Cell Biol 133(6): 1403-1415.

Cluzel C, Saltel F, Lussi J, Paulhe F, Imhof BA and Wehrle-Haller B (2005) The mechanisms and dynamics of (alpha)v(beta)3 integrin clustering in living cells. J Cell Biol 171(2): 383-392.

Ciobanasu C, Faivre B and Le Clainche C (2014) Actomyosin-dependent formation of the mechanosensitive talin-vinculin complex reinforces actin anchoring. Nat Commun 5: 3095.

Craig EM, Van Goor D, Forscher P and Mogilner A (2012) Membrane tension, myosin force, and actin turnover maintain actin treadmill in the nerve growth cone. Biophys J 102(7): 1503-1513.

del Rio A, Perez-Jimenez R, Liu R, Roca-Cusachs P, Fernandez JM and Sheetz MP (2009) Stretching single talin rod molecules activates vinculin binding. Science 323(5914): 638-641.

Dent EW, Gupton SL and Gertler FB (2011) The growth cone cytoskeleton in axon outgrowth and guidance. Cold Spring Harb Perspect Biol 3(3).

Dudanova I and Klein R (2013) Integration of guidance cues: parallel signaling and crosstalk. Trends Neurosci 36(5): 295-304.

Evans AR, Euteneuer S, Chavez E, Mullen LM, Hui EE, Bhatia SN and Ryan AF (2007) Laminin and fibronectin modulate inner ear spiral ganglion neurite outgrowth in an in vitro alternate choice assay. Dev Neurobiol 67(13): 1721-1730.

Flynn KC, Hellal F, Neukirchen D, Jacob S, Tahirovic S, Dupraz S, Stern S, Garvalov BK, Gurniak C, Shaw AE, Meyn L, Wedlich-Soldner R, Bamburg JR, Small JV, Witke W and Bradke F (2012) ADF/cofilin-mediated actin retrograde flow directs neurite formation in the developing brain. Neuron 76(6): 1091-1107.

Forscher P and Smith SJ (1988) Actions of cytochalasins on the organization of actin filaments and microtubules in a neuronal growth cone. J Cell Biol 107(4): 1505-1516.

Gardel ML, Sabass B, Ji L, Danuser G, Schwarz US and Waterman CM (2008) Traction stress in focal adhesions correlates biphasically with actin retrograde flow speed. J Cell Biol 183(6): 999-1005.

Garcia M, Leduc C, Lagardere M, Argento A, Sibarita JB and Thoumine O (2015) Two-tiered coupling between flowing actin and immobilized N-cadherin/catenin complexes in neuronal growth cones. Proc Natl Acad Sci U S A 112(22): 6997-7002.

Giannone G, Mege RM and Thoumine O (2009) Multi-level molecular clutches in motile cell processes. Trends Cell Biol 19(9): 475-486.

Gomez TM and Letourneau PC (1994) Filopodia initiate choices made by sensory neuron growth cones at laminin/fibronectin borders in vitro. J Neurosci 14(10): 5959-5972.

Gomez TM, Harrigan D, Henley J and Robles E (2003) Working with Xenopus spinal neurons in live cell culture. Methods Cell Biol 71: 129-156.

Gomez TM, Robles E, Poo M and Spitzer NC (2001) Filopodial calcium transients promote substrate-dependent growth cone turning. Science 291(5510): 1983-1987.

Grashoff C, Hoffman BD, Brenner MD, Zhou R, Parsons M, Yang MT, McLean MA, Sligar SG, Chen CS, Ha T and Schwartz MA (2010) Measuring mechanical tension across vinculin reveals regulation of focal adhesion dynamics. Nature 466(7303): 263-266.

Johnson HW and Schell MJ (2009) Neuronal IP3 3-kinase is an F-actin-bundling protein: role in dendritic targeting and regulation of spine morphology. Mol Biol Cell 20(24): 5166-5180.

Jurney WM, Gallo G, Letourneau PC and McLoon SC (2002) Rac1-mediated endocytosis during ephrin-A2- and semaphorin 3A-induced growth cone collapse. J Neurosci 22(14): 6019-6028.

Keren K, Pincus Z, Allen GM, Barnhart EL, Marriott G, Mogilner A and Theriot JA (2008) Mechanism of shape determination in motile cells. Nature 453(7194): 475-480.

Kerstein PC, Nichol RHt and Gomez TM (2015) Mechanochemical regulation of growth cone motility. Front Cell Neurosci 9: 244.

Knoll B, Weinl C, Nordheim A and Bonhoeffer F (2007) Stripe assay to examine axonal guidance and cell migration. Nat Protoc 2(5): 1216-1224.

Krause M and Gautreau A (2014) Steering cell migration: lamellipodium dynamics and the regulation of directional persistence. Nat Rev Mol Cell Biol 15(9): 577-590.

Kubo Y, Baba K, Toriyama M, Minegishi T, Sugiura T, Kozawa S, Ikeda K and Inagaki N (2015) Shootin1-cortactin interaction mediates signal-force transduction for axon outgrowth. J Cell Biol 210(4): 663-676.

Lin CH, Espreafico EM, Mooseker MS and Forscher P (1996) Myosin drives retrograde F-actin flow in neuronal growth cones. Neuron 16(4): 769-782.

Lin CH and Forscher P (1995) Growth cone advance is inversely proportional to retrograde F-actin flow. Neuron 14(4): 763-771.

Liu G, Li W, Gao X, Li X, Jurgensen C, Park HT, Shin NY, Yu J, He ML, Hanks SK, Wu JY, Guan KL and Rao Y (2007) p130CAS is required for netrin signaling and commissural axon guidance. J Neurosci 27(4): 957-968.

Lowery LA and Van Vactor D (2009) The trip of the tip: understanding the growth cone machinery. Nat Rev Mol Cell Biol 10(5): 332-343.

Mallavarapu A and Mitchison T (1999) Regulated actin cytoskeleton assembly at filopodium tips controls their extension and retraction. J Cell Biol 146(5): 1097-1106.

Marsick BM, Flynn KC, Santiago-Medina M, Bamburg JR and Letourneau PC (2010) Activation of ADF/cofilin mediates attractive growth cone turning toward nerve growth factor and netrin-1. Dev Neurobiol 70(8): 565-588.

Medeiros NA, Burnette DT and Forscher P (2006) Myosin II functions in actin-bundle turnover in neuronal growth cones. Nat Cell Biol 8(3): 215-226.

Mitchison T and Kirschner M (1988) Cytoskeletal dynamics and nerve growth. Neuron 1(9): 761-772.

Mogilner A and Oster G (2003) Polymer motors: pushing out the front and pulling up the back. Curr Biol 13(18): R721-733.

Moore SW, Biais N and Sheetz MP (2009) Traction on immobilized netrin-1 is sufficient to reorient axons. Science 325(5937): 166.

Moore SW, Roca-Cusachs P and Sheetz MP (2010) Stretchy proteins on stretchy substrates: the important elements of integrin-mediated rigidity sensing. Dev Cell 19(2): 194-206.

Moore SW, Zhang X, Lynch CD and Sheetz MP (2012) Netrin-1 attracts axons through FAK-dependent mechanotransduction. J Neurosci 32(34): 11574-11585.

Munevar S, Wang YL and Dembo M (2001) Distinct roles of frontal and rear cell-substrate adhesions in fibroblast migration. Mol Biol Cell 12(12): 3947-3954.

Myers JP and Gomez TM (2011) Focal adhesion kinase promotes integrin adhesion dynamics necessary for chemotropic turning of nerve growth cones. J Neurosci 31(38): 13585-13595.

Myers JP, Santiago-Medina M and Gomez TM (2011) Regulation of axonal outgrowth and pathfinding by integrin-ECM interactions. Dev Neurobiol 71(11): 901-923.

Nie D, Di Nardo A, Han JM, Baharanyi H, Kramvis I, Huynh T, Dabora S, Codeluppi S, Pandolfi PP, Pasquale EB and Sahin M (2010) Tsc2-Rheb signaling regulates EphA-mediated axon guidance. Nat Neurosci 13(2): 163-172.

Nieuwkoop PD, Faber, J. (1994). Normal Table ofXenopus laevis (Daudin). New York City, Garland Publishing Inc.

Petchprayoon C, Suwanborirux K, Tanaka J, Yan Y, Sakata T and Marriott G (2005) Fluorescent kabiramides: new probes to quantify actin in vitro and in vivo. Bioconjug Chem 16(6): 1382-1389.

Ponti A, Machacek M, Gupton SL, Waterman-Storer CM and Danuser G (2004) Two distinct actin networks drive the protrusion of migrating cells. Science 305(5691): 1782-1786.

Riedl J, Crevenna AH, Kessenbrock K, Yu JH, Neukirchen D, Bista M, Bradke F, Jenne D, Holak TA, Werb Z, Sixt M and Wedlich-Soldner R (2008) Lifeact: a versatile marker to visualize F-actin. Nat Methods 5(7): 605-607.

Robles E, Woo S and Gomez TM (2005) Src-dependent tyrosine phosphorylation at the tips of growth cone filopodia promotes extension. J Neurosci 25(33): 7669-7681.

Robles E and Gomez TM (2006) Focal adhesion kinase signaling at sites of integrin-mediated adhesion controls axon pathfinding. Nat Neurosci 9(10): 1274-1283.

Saengsawang W, Mitok K, Viesselmann C, Pietila L, Lumbard DC, Corey SJ and Dent EW (2012) The F-BAR protein CIP4 inhibits neurite formation by producing lamellipodial protrusions. Curr Biol 22(6): 494-501.

San Miguel-Ruiz JE and Letourneau PC (2014) The role of Arp2/3 in growth cone actin dynamics and guidance is substrate dependent. J Neurosci 34(17): 5895-5908.

Santiago-Medina M, Gregus KA and Gomez TM (2013) PAK-PIX interactions regulate adhesion dynamics and membrane protrusion to control neurite outgrowth. J Cell Sci 126(Pt 5): 1122-1133.

Santiago-Medina M, Gregus KA, Nichol RH, O'Toole SM and Gomez TM (2015) Regulation of ECM degradation and axon guidance by growth cone invadosomes. Development 142(3): 486-496.

Santiago-Medina M, Myers JP and Gomez TM (2011) Imaging adhesion and signaling dynamics in Xenopus laevis growth cones. Dev Neurobiol.

Sawada Y, Tamada M, Dubin-Thaler BJ, Cherniavskaya O, Sakai R, Tanaka S and Sheetz MP (2006) Force sensing by mechanical extension of the Src family kinase substrate p130Cas. Cell 127(5): 1015-1026.

Shimada T, Toriyama M, Uemura K, Kamiguchi H, Sugiura T, Watanabe N and Inagaki N (2008) Shootin1 interacts with actin retrograde flow and L1-CAM to promote axon outgrowth. J Cell Biol 181(5): 817-829.

Smilenov LB, Mikhailov A, Pelham RJ, Marcantonio EE and Gundersen GG (1999) Focal adhesion motility revealed in stationary fibroblasts. Science 286(5442): 1172-1174.

Suter DM, Errante LD, Belotserkovsky V and Forscher P (1998) The Ig superfamily cell adhesion molecule, apCAM, mediates growth cone steering by substrate-cytoskeletal coupling. J Cell Biol 141(1): 227-240.

Symons MH and Mitchison TJ (1991) Control of actin polymerization in live and permeabilized fibroblasts. J Cell Biol 114(3): 503-513.

Tehrani S, Tomasevic N, Weed S, Sakowicz R and Cooper JA (2007) Src phosphorylation of cortactin enhances actin assembly. Proc Natl Acad Sci U S A 104(29): 11933-11938.

Thievessen I, Thompson PM, Berlemont S, Plevock KM, Plotnikov SV, Zemljic-Harpf A, Ross RS, Davidson MW, Danuser G, Campbell SL and Waterman CM (2013) Vinculin-actin interaction couples actin retrograde flow to focal adhesions, but is dispensable for focal adhesion growth. J Cell Biol 202(1): 163-177.

Toriyama M, Kozawa S, Sakumura Y and Inagaki N (2013) Conversion of a signal into forces for axon outgrowth through Pak1-mediated shootin1 phosphorylation. Curr Biol 23(6): 529-534.

Treloar HB, Ray A, Dinglasan LA, Schachner M and Greer CA (2009) Tenascin-C is an inhibitory boundary molecule in the developing olfactory bulb. J Neurosci 29(30): 9405-9416.

Turney SG and Bridgman PC (2005) Laminin stimulates and guides axonal outgrowth via growth cone myosin II activity. Nat Neurosci 8(6): 717-719.

Tyler WJ (2012) The mechanobiology of brain function. Nat Rev Neurosci 13(12): 867-878.

Van Goor D, Hyland C, Schaefer AW and Forscher P (2012) The role of actin turnover in retrograde actin network flow in neuronal growth cones. PLoS One 7(2): e30959.

Vicente-Manzanares M, Ma X, Adelstein RS and Horwitz AR (2009) Non-muscle myosin II takes centre stage in cell adhesion and migration. Nat Rev Mol Cell Biol 10(11): 778-790.

Vitriol EA and Zheng JQ (2012) Growth cone travel in space and time: the cellular ensemble of cytoskeleton, adhesion, and membrane. Neuron 73(6): 1068-1081.

Walter J, Henke-Fahle S and Bonhoeffer F (1987) Avoidance of posterior tectal membranes by temporal retinal axons. Development 101(4): 909-913.

Wang HB, Dembo M, Hanks SK and Wang Y (2001) Focal adhesion kinase is involved in mechanosensing during fibroblast migration. Proc Natl Acad Sci U S A 98(20): 11295-11300.

Weitzdoerfer R, Dierssen M, Fountoulakis M and Lubec G (2001) Fetal life in Down syndrome starts with normal neuronal density but impaired dendritic spines and synaptosomal structure. J Neural Transm Suppl(61): 59-70.

Woo S and Gomez TM (2006) Rac1 and RhoA promote neurite outgrowth through formation and stabilization of growth cone point contacts. J Neurosci 26(5): 1418-1428.

Woo S, Rowan DJ and Gomez TM (2009) Retinotopic mapping requires focal adhesion kinase-mediated regulation of growth cone adhesion. J Neurosci 29(44): 13981-13991.

Wu KY, Hengst U, Cox LJ, Macosko EZ, Jeromin A, Urquhart ER and Jaffrey SR (2005) Local translation of RhoA regulates growth cone collapse. Nature 436(7053): 1020-1024.

Yamashiro S and Watanabe N (2014) A new link between the retrograde actin flow and focal adhesions. J Biochem 156(5): 239-248.

Zhang XF, Hyland C, Van Goor D and Forscher P (2012) Calcineurin-dependent cofilin activation and increased retrograde actin flow drive 5-HT-dependent neurite outgrowth in Aplysia bag cell neurons. Mol Biol Cell 23(24): 4833-4848.

Chapter 3

Adhesion Dynamics are Modulated by Substrata Elasticity to Regulate Cell-type Specific Human Neuritogenesis

Abstract

The extracellular microenvironment of the developing nervous system is a dynamic and complex landscape of both chemical and mechanical signals that regulate cell proliferation, differentiation, and migration. The regulatory roles of chemical cues in neuronal morphogenesis have been described, however, little is known about how mechanical forces influence neurite development. Extrinsic mechanical forces arise from cell adhesion to the extracellular matrix (ECM) and cell-cell adhesion, while intrinsic forces are generated by myosin-mediated contraction and polymerization/depolymerization of the cytoskeleton. Furthermore, mechanical regulation of human neurite development has not been investigated. Here we examined the role of mechanical forces on neurite development of human forebrain (hFB) neurons and human motor neurons (hMN) derived from induced pluripotent stem cells (iPSC). These two populations of neurons extend axons into distinct environments. hMN axons, upon exiting the spinal cord, must navigate into more rigid peripheral tissues. Conversely, hFB neurons remain within the elastic central nervous system (CNS). Using polyacrylamide and collagen hydrogels of varying elasticity we found hMN neuritogenesis was strongly promoted on more rigid substrata. On polyacrylamide, hMN reached maximal growth on 25 kPa, which is within the ranger of muscle. Interestingly, hFB neurites exhibit little differential outgrowth in two-dimensional environments, but grew longer neurites in soft three-dimensional collagen. We found that the observed differential growth rates are in part due to greater adhesion of the growth cone leading edge to more rigid environments, suggesting hMN growth cones form more stable adhesions leading to greater motility. Furthermore, we found RhoA, an important adhesion regulating GTPase, activity was higher on rigid substrata in hMNs. Interestingly, activation of RhoA stabilized leading edge protrusions and increased hMN neurite outgrowth on soft substrata, while decreasing outgrowth on more rigid substrata. These data suggest RhoA acts as a mechanosensor on elastic substrata to balance intracellular

contractile and adhesive forces. Finally, we found that mechanosensitive adhesion proteins FAK, Src, and p130-CAS are upregulated on more rigid substrata in hMN growth cones. Taken together, these data illustrate the mechanistic role adhesion cycling plays to regulate neurite outgrowth in different biophysical environments for peripheral projecting neurons.

Introduction

During development of the nervous system, neurites must navigate through a complex extracellular space consisting of varying environmental cues. Extracellular ligand binding to cell surface receptors direct axon morphogenesis via activation of various signaling pathways which induce changes cytoskeletal dynamics, local protein synthesis, and membrane trafficking control (Leung et al., 2006, Tojima et al., 2010, Dent et al., 2011). The study of long projecting axon guidance has principally focused on how soluble chemical ligands, deposited in the extracellular environment, induce morphological changes within growth cones to regulate extension and directed growth [reviewed in (Tessier-Lavigne and Goodman, 1996, Lowery et al., 2009)]. However, a growing breadth of research indicate secreted growth factors and chemokines are likely immobilized *in vivo* to induce morphological responses. Guidance responses induced by factors such as netrin induced growth cone turning appear to depend on ligand immobilization (Moore et al., 2010, Moore et al., 2012). Other factors such as bone morphogenic proteins (BMPs) and semaphorins can bind to extracellular matrix (ECM) proteins such as fibronectin, tenascin, and laminin (Hynes, 2002, Hynes, 2009). Additionally, adhesion receptors, such as integrin receptors, can exist as co-receptors for growth factor receptors like vascular endothelial growth factor (VEGF) receptor (Rahman et al., 2005). Importantly, these interactions between the ECM, growth factors, and cell surface receptors serve multiple function as both adhesive ligands and to induce biochemical signals. Moreover, a plethora of recent studies have found the elasticity of the substrata can affect neurite outgrowth, guidance, and branching [reviewed in (Kerstein et al., 2015)].

Developing axons in the central (CNS) and peripheral (PNS) nervous system must traverse a wide range of tissue of varying elasticities. A number of recent studies illustrate the the ability of substrata elasticity, or rigidity, to tightly regulate neurite growth and guidance [reviewed in (Kerstein et al., 2015)]. Elasticity, quantified as the Young's modulus or elastic

modulus (pascals, Pa), is measured as the deformability of a material in response to mechanical force. Using magnetic resonance elastrography, human tissue elasticity has be found to be significantly variable, including within the brain and spinal cord (McCracken et al., 2005, Kruse et al., 2008, Tyler, 2012). In fact, human and rodent brains appear to have a wide variance of elastic modulus ranging from 0.1 kPa to 16 kPa (Tyler, 2012). Therefore, central projecting cortical neurons must grow in a variety of elastic conditions, and fine tune their growth rates accordingly. These fluctuation in rigidity have been found to affect CNS hippocampal neurite development, as neurites grew faster on extremely soft substratum (Kostic et al., 2007). Furthermore, mouse primary spinal cord neurons were shown to have more complex axonal branching on less rigid substrata (Flanagan et al., 2002). However, due to the range of different substrata and elastic moduli used, the effect of rigidity on CNS neurite development is still not entirely clear.

In contrast to neurite growth within the CNS, motor neurons and dorsal root ganglion (DRG) neurons are required to project into more rigid peripheral tissue. Substrata elasticity appears to strongly affect neurite development of peripheral innervating neurons using chick DRG neurons (Balgude et al., 2001, Willits et al., 2004, Sundararaghavan et al., 2009), mouse DRG (Cheng et al., 2011), rat DRG (Koch et al., 2012), and Xenopus spinal cord (Kerstein et al., 2013). However, the effects of rigidity on neurite length appear to differ depending on elastic material, ECM protein, and range of elasticity. Moreover, neuritogenesis of motor neurons in different elastic environments has not been specifically investigated. Motor axon development consists of four stereotyped events: initiation in soft CNS, spinal cord exiting at stereotyped exit points, axon fasciculation growth in the periphery, and synaptogenesis at the neuromuscular junction [reviewed in (Pfaff et al., 2008)]. Our laboratory has recently shown *Xenopus* spinal neurons form invadopodia like growth cone protrusions, which can release matrix metalloproteinases (MMPs) to break down ECM, and are critical for axon exiting from

the spinal cord (Santiago-Medina et al., 2015). We hypothesize this process of ECM remodeling changes the biophysical properties of the basal lamina surrounding the spinal cord, and subsequently affects neurite outgrowth. Upon exiting, motor neuron axons then grow in very rigid environments, such as bone (15-30 GPa), connective tissue and arteries (0.1-1MPa), and muscle (10-100 kPa) (Tyler, 2012, Franze, 2013). Finally, synaptogenesis at the neuromuscular junction requires mechanical force dependent synapse matching between the presynaptic bouton and muscle. Therefore, substrata elasticity appears to play a critical role in navigating axons during all steps of motor neuron morphogenic development (Siechen et al., 2009).

The molecular mechanisms that could differ between CNS and PNS projecting neurons are still relatively unknown. Similar to non-neuronal and cancer cell migration, growth cone adhesions play a crucial role in sensing and responding to mechanical stimuli. In response to mechanical stimuli, receptor-like protein tyrosine phosphatase alpha (RPTP-α) has been found to co-localize with $\alpha_v\beta_6$ integrins and activate Src kinase and Cas to regulate neurite growth rate (Kostic et al., 2007). Another recent study found growth cone adhesions are critical for controlling neurite outgrowth on different elasticities (Koch et al., 2012). Peripheral projecting DRG growth cones were found to have more adhesions, which correlated with longer neurites on rigid relative to softer substrata. Moreover, this study discovered central projecting hippocampal neurons had fewer growth cone adhesions, which correlated with a lack of mechanosensitive responses. While these data give us some indication of the molecular modulators of mechanotransduction during neurite outgrowth the exact molecular differences between neuronal subtypes remains elusive. Another open question in the field is whether central and peripheral projecting human neurite development is similarly regulated by mechanical stimuli.

Here, we used induced pluripotent stem cell (iPSC) derived human motor neurons (hMN) and human forebrain neurons (hFB) to examine substrata elasticity on neurite development and guidance. We show that hMN preferentially grow longer neurites on more rigid polyacrylamide hydrogels and three dimensional collagen after 2 DIV. Conversely, hFB did not appear to have neurite lengths differences dependent upon substrata rigidity on polyacrylamide. Interestingly, the rate of hFB neurite outgrowth was significantly more rapid on soft substrata relative to rigid substrata. Additionally, in three-dimensional collagen hFB projected longer neurites on soft substrata. One mechanism of mechanosensitive motility in non-neuronal cells includes regulating adhesion to the ECM. Similarly, we observed more stable adhesion of hMN growth cones to rigid environments. Moreover, RhoA-GTPase activity was a principle determinant of mechanosensitive neurite growth for hMN. Pharmacological activation of RhoA stabilized leading edge protrusions and increased hMN neurite outgrowth on soft substrata, while decreasing adhesivity and outgrowth on more rigid substrata. These data strongly suggest RhoA functions to balance intracellular contractile and adhesive forces for optimal growth of hMN neurites. Finally, we found that mechanosensitive adhesion proteins, focal adhesion kinase (FAK), Src, and p130-CAS, have increased activity on rigid substrata in hMN. These data illustrate a novel mechanistic role of RhoA and adhesion in regulating human neurite outgrowth dependent on environmental substrata.

Materials and methods

Plasmid constructs and reagents. GFP transfected in human neurons was provided by Erik Dent (University of Wisconsin, Madison) and sub-cloned into pCAX vector for expression in human neurons (Dave Turner, University of Michigan, Ann Arbor, MI). Lysophosphatidic acid (LPA, Fisher Scientific) and Rho Inhibitor I (Cytoskeleton, Inc.) were used to activate and inhibit RhoA, respectively.

Neuronal differentiation and transfection. Human forebrain neurons (hFB) were differentiated as previously described (Hu et al., 2010, Doers et al., 2014). Human motor neurons (hMN) were differentiated as previously described (Du et al., 2015). Neurospheres were plated onto polyacrylamide hydrogels coated with 50 µg/ml PDL, 25 µg/ml laminin (Sigma-Aldrich), 10 µg/ml fibronectin (Sigma-Aldrich); and 1 mg/ml collagen hydrogels (Corning Discovery Labware) in neurobasal media containing B27 supplements (Life Technologies). Collagen was crosslinked using 1 mM and 10 mM genipin (Sigma-Aldrich). Cultures were imaged or fixed at 24 hours or 48 hours after plating, respectively.

Immunocytochemistry. Cultures were incubated in 5% CO2 and 9% 02 at 37°C then imaged or fixed 24-48 hr after plating. For immunocytochemistry (ICC), neuron cultures were fixed in 4% paraformaldehyde in Krebs sucrose fixative (4% PKS) (Dent and Meiri, 1992), permeabilized with 0.1% Triton X-100, and blocked in 1.0% fish gelatin in CMF-PBS for 1 h at room temperature. Primary antibodies were used at the following dilutions in blocking solution: 1:1000 acetylated tubulin (Sigma-Aldrich), 1:500 all pY-FAK antibodies (Biosource), 1:500 all pY-Src antibodies (Biosource), 1:100 pY-p130-CAS (Cell Signaling Technologies). Alexa-Fluor-conjugated secondary antibodies were purchased from Invitrogen and used at 1:250 in blocking solution. Included with secondary antibodies was Alexa-647 phalloidin (1:50 –1:100; Invitrogen) to label filamentous actin (F-actin).

RhoA G-LISA. Rho G-LISA activation assay colorimetric kit (Cytoskeleton Inc.) was used to measure RhoA activity in hMN. hMN from 0.5 kPa and 25 kPa laminin coated polyacrylamide hydrogels were lysed and diluted to 0.5mg/ml using lysis buffer and then loaded on to their G-LISA plate for protein analysis. This was followed by detection with RhoA-GTP antibody and HRP, and reading absorption at 490 nm with a microplate reader.

Image acquisition. For fixed fluorescence microscopy, low-magnification images were acquired using either a 20X/0.50 NA or 60X/1.45 objective lens on an Olympus Fluoview 500 laser-scanning confocal system mounted on an AX-70 upright microscope. For live differential interference contrast (DIC) microscopy, high-magnification images were acquired using a 40X/ 1.3 NA objective lens on a Nikon total internal reflection fluorescence (TIRF) microscope. On the confocal, samples were imaged at 2–2.5X zoom (pixel size = 165–200 nm). Images were collected on the TIRF with a Coolsnap HQ2 camera (Roper scientific) with 2x2 binning (pixel size = 127 nm). Second Harmonic Generation (SHG) was used to image collagen fibril structure before and after genipin treatment.

Image analysis. Images were analyzed using ImageJ software (W. Rasband, National Institutes of Health, Bethesda, MD). Neurite length was quantified as the distance of a single projection measured from the edge of the neurosphere explant. The ten longest neurites were used because of neurite density. Neurite outgrowth was quantified as the total distance of growth cone leading edge forward translocation after 30 minutes. GFP-hMN labeled growth cones were imaged at 2 Hz by TIRF microscopy for 2 min to measure actin RF. Leading edge morphology were quantified by kymography by sampling three to seven lines per growth cone radiating equally around the axis of outgrowth.

Sholl analysis (Sholl and Uttley, 1953). Images were analyzed using the Sholl Analysis plugin in ImageJ. An ellipse was fit to hFB and hMN neurospheres and initial radius set to 50μm away

from neurosphere edge. The outer radius was set beyond the extent of the longest neurite, and the radius step size (spacing between consecutive circles) was set to 5 μm.

Statistical analysis. Analysis was carried out using Prism software. Analysis was completed with an unpaired Student's T-test for comparison of two experimental groups, or a One-way or Two-way ANOVA with a Bonferroni's multiple-comparison test for comparison of 3 or more experimental groups. For quantitative immunocytochemistry experiments phosphor-tyrosine of specific proteins signal was in ratio to succinimidyl ester 647 (SE-647) and rigid was normalized to soft to illustrate fold changes.

Results

Two-dimensional neurite extension of human neurons is regulated by substrata elasticity

Previous studies using animal models have shown the biophysical properties of the substrata affect neurite development. Multiple studies have found preferential growth for neurons on softer substrata, such as mouse spinal cord (Flanagan et al., 2002), mouse hippocampal (Kostic et al., 2007), rat spinal cord (Jiang et al., 2008), and Xenopus Laevis spinal cord (Kerstein et al., 2013). Conversely, other studies have found maximal growth on moderately more rigid substrata, such as rat DRG (Koch et al., 2012) and mouse DRG (Cheng et al., 2011). However, these studies have differed in the flexible substrata (agarose, collagen, polyacrylamide, polydimethylsiloxane, or silk fibroin hydrogel, and extracellular matrix coating (poly-d/l-lysine, laminin, or fibronectin), as well as a fluid definition of soft versus rigid [reviewed in (Kerstein et al., 2015)]. Additionally, there has been no investigation to whether human neurite extension and guidance is similarly regulated by substrata elasticity. Therefore, we examined neuritogenesis of human neurons on varying physiologically relevant elasticities.

Neurites growing outside the CNS must sense and respond to more diverse elastic substrata relative to central projecting neurites. However, rigidity fluctuations found within the CNS have also been shown vary during neurodevelopment (Koser et al., 2016). To test whether central and peripheral projecting human neurites respond differentially to substrata elasticity, we cultured hMN and hFB on PDL and laminin coated polyacrylamide of differing elasticity (0.2 kPa, 0.5 kPa, 1 kPa, 2 kPa, 4 kPa, 8 kPa, 15 kPa, 25 kPa, 50 kPa, and 125 kPa). Initially, we found hMN and hFB did not regularly adhere to the softest substrata (0.2 kPa). However, hMN and hFB neurites were present after 1-2 DIV on all other substrata. hMN extended longer neurites on rigid substrata (Figure 1A-D, I), reaching peak lengths on 25 kPa (Figure 1C, I), a physiologically correlative rigidity to muscle tissue. Additionally, neurite

number appeared to be greater on rigid for hMN. Sholl analysis data revealed an increased number and length of neurite projections on rigid substrata (Figure 1L). Additionally, there was a greater number of neurites closer to the neurosphere, suggesting substrata rigidity could have an effect on neurite initiation (Figure 1L). In contrast to hMN, elasticity appeared to have less of an effect on neurite extension for hFB cultures with the longest neurites growing on 1 kPa, 2 kPa, 15 kPa, 50 kPa, and 125 kPa (Figure 1E-H, J). Further evaluation using sholl analysis found rigidity did appear to have an affect on neurite number, with fewer neurites extending on soft substrata (Figure 1M). However, the longer extending neurites grew similar distances (Figure 1M). This could either indicate rigidity affects neurite formation, or central projecting neurons prefer to extend neurites via cell-cell adhesion mechanisms and the neurites, once formed, stay within the neurosphere. These data are in accordance with previous data which discovered no preferential growth in response to varying elasticities for hippocampal neurons cultured on laminin (Koch et al., 2012). However, a contrasting study found hippocampal neurites preferred more elastic conditions (0.5 kPa) over rigid (4 kPa) when cultured on fibronectin (Kostic et al., 2007). Therefore, we cultured hFB on different elastic substrata coated with the ECM molecule, fibronectin (Supplemental Figure S1). In contrast to previous evidence we determined that hFB neurites did not have a trend of altered neurite length on different elastic polyacrylamide coated with fibronectin (Supplemental Figure S1).

Neuronal differentiation and neuritogenesis involves a stereotyped sequence of events and involves an array of signaling cascades to initiate and extend a neurite (da Silva and Dotti, 2002). These signaling pathways can be activated downstream of mechanical force to affect initiation, extension, or both. Additionally, the mechanical environment can independently affect cell fate (Musah et al., 2014). To delineate between the effects of substrata elasticity on neurite extension from other cell processes we quantified the rate of neurite outgrowth for hMN and hFB. As previously stated, we observed a significant disparity on neurite length for hMN at 0.5

kPa and 25 kPa. These two elasticities are physiologically comparable to CNS (0.5 kPa) and peripheral tissue (25 kPa) (Tyler, 2012). Therefore, we examined time-lapsed neurite outgrowth of hMN and hFB under soft (0.5 kPa) and rigid (25 kPa) conditions. Neurite outgrowth rates on soft were significantly slower than rigid substrata for hMN (Figure 1O-P, S), suggesting that differential neurite lengths were predominately due to differences in neurite extension. Contradictory to our neurite length results, time-lapse imaging of hFB revealed a reduction in neurite outgrowth rate on rigid substrata compared to soft (Figure 1Q-R, T). Therefore, soft environments increase neurite outgrowth rate, while rigid environments induce greater neurite number, resulting in a similar number of long projecting neurites for hFB. These findings confirm the hypothesis that CNS and peripheral projecting neurite extension rate is influenced by environmental rigidity.

Three-dimensional neurite extension of human neurons is regulated by substrata elasticity

To further investigate the effect of substrata elasticity on neurite outgrowth, we next examined neurite length in three-dimensional collagen hydrogels. Numerous studies have used collagen matrices to generate variable elastic cell culture conditions to study cell shape, polarity, and durotaxis (Greenburg and Hay, 1982, Willits et al., 2004, Sundararaghavan et al., 2009). Three-dimensional collagen matrices can affect neuronal processes such as neuritogenesis and nerve regeneration (Bozkurt et al., 2007, Gil and del Rio, 2012). To test whether altering elasticity has an effect on three-dimensional neurite development, hMN and hFB were cultured on 1.5 mg/ml fibrillar collagen. This concentration produces a dense collagen matrices to assay neurite outgrowth with three-dimensional varying mechanical forces. Neurites were present after 1 DIV for hMN and hFB (Data not shown). However,

neurites appeared to grow more slowly in three-dimensional collagen relative to polyacrylamide and were fixed after 4 DIV for analysis.

Collagen matrices are relatively soft, with an elastic modulus less than 5 kPa (Roeder et al., 2002). To investigate neurite growth responses to different rigidities in three-dimensions, collagen matrices were treated with 1 mM or 10 mM genipin, a collagen cross linking molecule, for 18 hours. Genipin has been shown to crosslink cellular and extracellular matrix tissue in addition to biomaterial scaffolds causing an increase in rigidity (Sundararaghavan et al., 2008). Using SHG, we compared structural properties of collagen matrices without (Figure 2A) and with (Figure 2B) 10 mM genipin and found genipin induced increased fibril size (Figure 2C) and decreased fibril count (Figure 2D), suggesting increased collagen crosslinking into large fibrils. Importantly, genipin and collagen cross interaction produces autofluorescence when excited at 590 nm. This autofluorescence is directly correlated with increased rigidity, and allowed us to quantify differences in collagen matrix elasticity (Sundararaghavan et al., 2008). There was a significant increase in autofluorescence after 1 mM genipin treatment confirming our assay induces increased rigidity (Figure 2E).

We observed increased neurite lengths extending from hMN while growing in genipin crosslinked collagen relative to control (Figure 2 F-G, J). Furthermore, we quantified neurite growth depth in 3D collagen. The more extended neurites projecting from hMN on rigid collagen also grew deeper into collagen (Figure 2K-L, N). These data correspond with neurite length differences on polyacrylamide and confirm that peripheral projecting neurons extend more rapidly in less elastic conditions. Using the same experimental paradigm, we probed neurite length for hFB in different three-dimensional elastic conditions. Cultured hFB neurons embedded in control collagen matrices (Figure 2H) and with 1 mM genipin (Figure 2I). In contrast to hMN, more rigid conditions caused reduction in hFB neurite length after 4 DIV relative to control, indicating hFB prefer soft conditions in three-dimensional collagen matrices

(Figure J). These data contradict the result we observed with two-dimensional cultures on flexible polyacrylamide (Figure 1J). However, hFB neurites appeared to grow deeper in to rigid collagen (Figure M-O). This could be due to increased exploratory neurite growth for hFB neurons on rigid substrata. These differential effects for hFB could be due to preferred growth on collagen as an ECM substrata or specific three-dimensional relative to two-dimensional mechanosensitive growth. Taken together, it appears the elastic environment affects the development of neurites projecting from both hMN and hFB in three-dimensional matrices.

Elasticity dependent neurite extension of human neurons is mediated by growth cone leading edge adhesivity

Migrating cells respond to the biophysical properties of the extracellular microenvironment by expression of mechanosensitive proteins that change their conformational structure in response to acute forces directed upon cell [reviewed in (Schiller et al., 2013, Kerstein et al., 2015)]. A number of biochemical outputs of mechanosensing have been described to regulate cell shape and behavior. Among these outputs is the modulation of adhesion complex proteins located around integrin receptors, which have been discovered to be critical components of mechanosensing. Integrin receptors are involved in detection of elastic fluctuations as well as providing the initial substrate for adhesion complexes to form in response to other signals (Sun et al., 2016). This dual role of integrin based adhesions creates a homeostatic feedback, which is required for increasing or decreasing cell motility during neurodevelopment, cell migration, and in metastatic cancer cells (Huttenlocher et al., 1996, Cox and Huttenlocher, 1998, Yamahashi et al., 2015). Furthermore, our laboratory has shown adhesion modulation, downstream of signals such as calcium, is an important mediator of growth cone mechanical force response (Kerstein et al., 2013). Consequently, we next

attempted to correlate leading edge growth cone adhesivity on varying elasticities with rate of outgrowth and neurite length differences we observed in Figures 1 and 2.

We assay for differences in leading edge adhesivity by examining protrusion and retraction of GFP expressing hMN using kymography. Cultured hMN on soft (0.5 kPa) and rigid (25 kPa) polyacrylamide were imaged using TIRF microscopy after 1 DIV (Figure 3A). Morphological events were quantified by sampling three to seven lines per growth cone (Figure 3B-B'). This analysis showed hMN growth cones had longer lived protrusions on rigid substrata compared to soft (Figure 3C-E). The more stable protrusions on rigid were also correlated with extended duration of retraction, as well as a reduced rate of retraction (Figure 3E-F). These data indicate that on rigid substrata hMN protrusions are more stable. In addition, while the growth cone retracts, possibly due to actin depolymerization, the leading edge adheres more to the substrata. We hypothesize that rigid substrata is a more attractive environment for hMN due to adhesion stabilization. Also, we found that the rate of protrusion did not differ between soft or rigid (Figure 3F). This could denote similar rates of actin polymerization on either substrata, further implying growth cone adhesion as a key regulatory mechanism of mechanical force dependent motility.

Recent evidence correlated a lack of growth cone adhesions with the loss of mechanosensitive responses for CNS neurons, implying the absence of integrin based adhesions in CNS neurons could underly the results observed in Figure 1J (Koch et al., 2012). Therefore, we correlated hFB leading edge morphology with environmental rigidity. Elasticity appeared to a significantly less important effect on adhesivity of the leading edge, evidenced by no significant differences observed in the duration of protrusion (Figure G-H). However, there was a longer duration of retraction on soft substrata indicating some reduced role of adhesivity. Furthermore, the duration of protrusion and retraction were reduced in hFB relative to hMN, suggesting an overall reduction of adhesive influence on hFB outgrowth (Figure 3E,

H). The rate of protrusion and retraction was greater on soft substrata, which correlated with more rapid outgrowth (Figure 1T), relative to rigid (Figure 3J). These data indicate CNS growth cone motility is more dependent on direct regulation of the cytoskeleton, whereas peripheral projecting neurite development is principally governed by modulating the adhesivity of the growth cone to the substrata.

RhoA GTPase activity in hMN is upregulated on rigid substrata

As substrata adhesion appears to have a critical role in neurite growth on flexible substrata (Figure 3), we sought to elucidate the signaling molecules involved in adhesion mediated mechanotransduction in hMN. In migrating cells and growth cones, adhesions have been found to be tightly regulated by Rho family GTPases, such as Rac1, RhoA, and CDC42 (Woo et al., 2006, Myers et al., 2012, Ridley, 2015). Briefly, upon integrin activation and clustering, signaling molecules Src and FAK phosphorylate nascent adhesion proteins paxillin and p130-CAS (Sawada et al., 2006, Cohen-Hillel et al., 2009). Paxillin and p130-CAS localize guanine nucleotide exchange factors (GEF), ß-Pix and DOCK180 to adhesions, respectively (Ridley, 2015). These events are involved in nascent adhesion formation and yield increased Rac1 mediated actin branching and polymerization during lamellipodial protrusion (Kiyokawa et al., 1998, ten Klooster et al., 2006). After nascent adhesion formation, Rac1 activity decreases while RhoA activity is simultaneously increased, due to inhibitory crosstalk [reviewed in (Ridley, 2015)]. RhoA is critical for stress fiber and focal adhesion maturation via downstream activation of Rho-associated protein kinase (ROCK) and myosin-II activity (Vicente-Manzanares et al., 2009). It has been proposed adhesion maturation is mediated by myosin-II contractile forces on F-actin transmitted into the adhesion, thereby activating stretch gated adhesion molecules, such as p130-CAS, talin, and vinculin (Sawada et al., 2006, del Rio et al., 2009, Moore et al., 2010). In neurons, it has been principally believed Rac1 and RhoA

have antagonistic roles, with Rac1 stimulating neurite outgrowth through adhesion stabilization and actin polymerization, and RhoA inhibiting growth by inducing contraction of the actin cytoskeleton. However, more recent evidence in neurons, in agreement with non-neuronal cell migration evidence, suggest RhoA plays a much more complicated role and can induce positive growth effects (Woo et al., 2006).

Therefore, we attempted to better understand the role of RhoA in hMN growth cone mechanotransduction. Mechanical forces in the environment have been shown to influence Rho GTPase activity through upstream modulation of GEFs and GTPase activating proteins (GAP) which activate and deactivate GTPases, respectively (Lawson and Burridge, 2014). To determine the role of RhoA on mechanotransduction during neurite development, we first performed a G-LISA small GTPase activation assay. This allowed us to measure the level of GTP bound (activated) RhoA in hMN on soft and rigid substrata (Supplemental Figure S2). In short, cells were cultured for 2 DIV and lysed. The cell lysate was incubated in a RhoA-GTP affinity plate and detected via antibody recognition (Supplemental Figure S2A). We found an increase in RhoA-GTP for hMN cultured on rigid substrata relative to soft (Supplemental Figure S2B). These results denote a correlation between higher RhoA activity, growth cone leading edge stability, and neurite outgrowth for peripheral projecting hMN on rigid substrata.

Modulating RhoA activity in hMN controls mechanosensitive neurite growth responses

To further examine the function of RhoA as a mechanosensitive signaling molecule in hMN, we attempted to pharmacologically manipulate RhoA to probe for effects on neurite length, rate of outgrowth, and growth cone morphology. Lysophosphatidic acid (LPA) has been shown to induce strong growth cone collapse at high doses (O'Connor et al., 2012). LPA acts as an extracellular signaling molecule by binding to cell surface G-protein coupled receptors to initiate biochemical signaling (Kranenburg et al., 1999). One output of LPA is RhoA-GTPase

activity (Kranenburg et al., 1999). Previous studies observing the inhibitory effects of LPA have been on glass and culture plastic, which is more rigid than human tissue (Moolenaar et al., 1997, Jeon et al., 2012). How LPA affects neurite extension on flexible substrata has not been tested. To test the effects of RhoA overactivation on human neurite development we exposed hMN on soft and rigid polyacrylamide substrata to chronic LPA treatment. After 24 hours in culture hMN were treated with control media, 10 nM, 100 nM, or 1 μM LPA for 24 hours and fixed (Supplemental Figure S3). Relative to control neurons, which had stunted neurites on soft substrata, chronic LPA treatment caused a significant increase in neurite length on soft (Figure 4A-B,G). This effect was dose dependent with greater neurite length directly correlated with higher LPA concentration (Supplemental Figure S3A-D, I). As previously stated, hMN extend neurites optimally on rigid substrata reaching peak velocity on 25 kPa (Figure 1I, 4D). However, after chronic LPA treatment, hMN neurite length was significantly reduced on rigid substrata (Figure 4E, G). This reduction was correlated with increasing concentration of LPA (Supplemental Figure S3E-I), which has been observed previously on rigid substrata such as culture glass or plastic. These experiments further indicate RhoA may act as a sensor to regulate mechanosensitive growth responses, as hMN grew optimally on soft substrata due to chronic RhoA overactivation. Interestingly, these data contradict multiple studies in which LPA has been shown to be inhibitory (Moolenaar et al., 1997, Jeon et al., 2012).

As stated previously, during cell migration RhoA activation is increased downstream of mechanosensitive signals on rigid substrata (Lawson et al., 2014). Therefore, to further test the role of RhoA in growth cone mechanotransduction, we assayed neurite outgrowth on soft and rigid substrata in the presence of chronic RhoA pharmacological inhibition using Rho Inhibitor I (C3 Transferase), which inhibits RhoA, RhoB, and RhoC (Herr et al., 2014). Differentiated hMN were exposed to Rho Inhibitor I after 24 hours in vitro. Previous evidence found inhibition of RhoA downstream signaling molecules, such as ROCK and myosin II, causes increased

neurite length on culture glass, suggesting blocking actin contractility induces greater neurite outgrowth (Gu et al., 2013, Roloff et al., 2015). Similarly, we found on rigid substrata (25 kPa) there was an increase in neurite length after 24 hours (Figure 5F-G). In contrast, neurite length was decreased on soft in response to chronic Rho inhibition (Figure 5C, G). These data further implicate RhoA activity as a key regulatory factor governing biophysical based responses during neuritogenesis. RhoA appears to be optimally activated on rigid substrata and modulating the balance of RhoA GTP/GDP can control neurite extension by artificially activating/inactivating RhoA mediating signaling.

Rho GTPases such as RhoA, CDC42, and Rac1 have been implicated to control multiple steps in neuronal maturation including neural progenitor cell proliferation, neuronal migration, and plasticity of neurons (Stankiewicz and Linseman, 2014). Therefore, to parse apart the effects of RhoA manipulation on neurite outgrowth from other cellular processes, hMN cultures were acutely stimulated with LPA. To assess the effects of acute LPA treatment we treated neurons with 100nM LPA for 30 minutes on varying elastic substrata. Initially, as previously shown (Figure 1N-R), growth cone motility was greater on rigid substrata relative soft (Figure 5H-I). However, LPA treatment appeared to reverse this trend as growth cone translocation was more rapid on soft substrata post LPA relative to rigid (Figure 5H'', I''), correlating with increased neurite lengths previously observed. In fact, LPA was found to induce retraction of many neurites on rigid (data not shown). The RhoA dependent effects were also seen with Rho inhibition. Consistent with the neurite length results, Rho inhibition resulted in slower growth cone translocation and outgrowth on soft (Figure 5J). This was reversed on rigid substrata, as Rho inhibition yielded accelerated growth cone forward movement (Figure 5K). These results indicate modulation of RhoA activity is involved in determining force dependent neurite outgrowth rates through growth cone translocation specifically.

Mediating adhesion is a key component of RhoA effects on growth cone motility (Woo et al., 2006). We attempted to correlate acute RhoA activation with changes in leading edge morphogenic responses. hMN were transfected with GFP and cultured on laminin coated polyacrylamide dishes with elasticities of soft and rigid as previously described (Figure 3A-B). On soft substrata, the leading edge membrane was unstable with more rapid protrusion and retraction (Figure 5L, N). Acute RhoA overactivation via LPA disrupted this cycling between protrusion and retraction and promoted leading edge adhesion and stability (Figure 5L'). We observed an increase leading edge protrusion duration and distance, in addition to increased retraction duration (Figure 5N-P). In contrast, on rigid substrata LPA treatment slowed forward leading edge translocation by perturbing adhesivity (Figure 5M). We observed decreased protrusion distance in growth cones cultured on rigid substrata, suggesting LPA treatment adversely affects protrusive activity on rigid (Figure 5P). Taken together, these data indicate RhoA acts as a crucial mechanosensor in human nerve growth cones. RhoA is optimally activated on rigid substrata, downstream of mechanical signals, in peripheral projecting motor neurons and direct modulation of RhoA can alter mechanical force matching between motor neurites and the environment.

Tyrosine phosphorylation of mechanosensitive adhesion proteins correlates with rigidity dependent neurite outgrowth

Our results reveal a role for adhesion regulation during human neurite outgrowth on flexible substrata. A number of signaling cascades could be involved in adhesion mediated mechanotransduction within growth cones. During initial integrin mediated mechanosensing, FAK is recruited to the integrin complex, where it is then autophosphorylated at y397, providing a binding site for the SH2 domain of Src, which leads to its activation via autophosphorylation at y418 (Toutant et al., 2002, Wang et al., 2005, Bae et al., 2014, Zhang et al., 2014). Our

laboratory previously demonstrated that phosphorylated y418 FAK, which can be activated by mechanical stimuli, is essential for growth cone adhesion assembly and disassembly (Myers et al., 2011). We tested FAK activity in hMN growth cones and observed higher phosphorylation of FAK at y397 on rigid substrata relative to soft (Figure 5A-B, K). In a similar role to FAK, we have shown Src is crucial in regulating neurite extension by modulating adhesion dynamics during growth cone motility (Robles et al., 2005). To elucidate the effect of substrata rigidity on Src signaling, we immunolabeled hMN growth cones with antibodies that specifically recognize Src autophosphorylation (activation) at y418, and the inhibition site at y529 (Robles et al., 2005). We observed an increase in phosphorylation of Src at y418 on rigid substrata relative to soft substrata (Figure 5C-D, L). In contrast, we found inhibition of Src activity via phosphorylation at y529 was higher on soft substrata relative to rigid (Figure E-F, M). Together, our findings indicate greater activation of adhesion signaling molecules FAK and Src, suggesting they are involved in leading edge stabilization and increased neurite outgrowth on rigid substrata for hMN.

To further identify the adhesion proteins involved in mechanically dependent human neurite development, we investigated the activity of the mechanosensitive substrate of FAK and Src, p130-CAS. Downstream of integrin activation, myosin-II induced actin retrograde flow leads to stretching of p130-CAS, further stabilizing adhesions (Sawada et al., 2006, Bae et al., 2014). This stretching event is required to expose cryptic phosphorylation sites for Src, and subsequently FAK, to activate p130-CAS. These phosphorylation events are required for cell spreading and motility in fibroblasts (Zhang et al., 2014). Moreover, p130-CAS has been found to be a key regulator of axon guidance (Liu et al., 2007). To quantify differences in p130-CAS activity in hMN growth cones on different elasticities we immunolabeled for phospho-specific antibodies for two activations sites, y165 and y410. We found p130-CAS phosphorylation was higher in hMN growth cones for both phosphorylation sites on rigid substrata (Figure 5I-J, N-

O), confirming our hypothesis p130-CAS activity is higher downstream of FAK and Src on rigid substrata. Our observations indicate mechanically dependent adhesion signaling and scaffold proteins are important for hMN neurite development on flexible substrata.

Phosphorylation of mechanosensitive adhesion proteins on different elasticities is reversed downstream of RhoA activation

To test how RhoA may modulated growth cone adhesivity through FAK, Src, and p130-CAS we cultured hMN on polyacrylamide gels of different elasticities coated with laminin and pharmacologically manipulated RhoA. As described previously, hMN rate of outgrowth was higher on rigid substrata, and this correlated with increased phosphorylation of activation sites for FAK, Src, and p130-CAS (Figure 5). In Figure 4 we identified RhoA as a mechanosensor and regulator of neurite length, outgrowth, and leading edge protrusion on flexible substrata. As previously stated, multiple lines of evidence suggest myosin-II contraction of the actin network, downstream of RhoA, stabilizes adhesions (Cox et al., 2001, Machacek et al., 2009). Therefore, hMN on soft (0.5 kPa) and rigid (25 kPa) substrata were stimulated with 100 nM LPA for 1 hr, fixed, and labeled by immunocytochemistry with phosphotyrosine specific antibodies to FAK, Src, and p130-CAS. LPA treatment lead to no significant difference to the levels of FAK y397 on soft and rigid substrata (Fig. 6C-D, M), which is in contrast what we observed with control media wash (Figure 6A-B, M), suggesting that RhoA overactivation on soft substrata increases phosphorylation levels close to that of rigid substrata. Furthermore, we observed LPA treatment lead to a decrease in Src phosphorylation at y418 on rigid compared to soft (Figure 6G-H, N), which is in opposition to Src activation with control media wash (Figure 6E-F, N). Finally, we found RhoA overactivation did not have an effect on p130-CAS phosphorylation at y165 (Figure 6I-L, O). Taken together, these data show that RhoA acts upstream of FAK and Src to control growth cone mechanotransduction in hMN. However,

because LPA treatment did not result in differential p130-CAS phosphorylaton relative to control, we hypothesize another mechanism, besides mechanical stretching of adhesion proteins, could underly the overactivation effects of RhoA. The possible mechanism will be discussed further in the discussion.

Discussion

Here we show, for the first time in human neurons, the biophysical properties of the environment play a critical role in neurite development in PNS and CNS projecting neurons. Using polyacrylamide (Figure 1) and collagen (Figure 2) hydrogels we showed hMN neurites respond to the elastic environment in two-dimensional and three-dimensional cultures, respectively. Neurite lengths were longer on more rigid substrata for hMN reaching maximal length at 25 kPa, which is within the range of muscle tissue (Tyler, 2012). In contrast, substrata elasticity did not have a clear affect on hFB neurite growth in two-dimensional environments. On polyacrylamide, hFB rate of outgrowth was more rapid on soft substrata, however, this did not appear to affect neurite length after 2 DIV (Figure 1). Additionally, hFB grew longer neurites in soft three-dimensional matrices, further complicating our understanding of human CNS neuronal morphogenesis in different elastic environments. We also identified a link between RhoA mediated adhesion dynamics and mechanical force dependent neurite growth in hMN. It appears the leading edge of hMN growth cones adhere more to rigid substrata (Figure 3) and this correlated with increased activation of RhoA, FAK, Src, and p130-CAS (Figures 4-5). We found modulating RhoA activity can switch mechanosensitive responses as LPA caused hMN to extend longer neurites on soft substrata (Figure 4). Finally, were observed FAK, Src, but not p130-CAS, activity is regulated downstream of RhoA (Figure 6), suggesting that similar to non-neuronal cells, hMN growth cone mechanotransduction acts as a feedback homeostatic regulator of neurite outgrowth.

There are still many unanswered questions to understanding how biophysical properties regulate motor axon development. However, responding to substrata composition appears to be critical during all steps of motor axon development. For example, how motor axons, which initiate in the CNS, are instructed to defasciculate and grow through the basal lamina and into the periphery is still an open question. Motor axons must exit the spinal cord at defined points

dependent on motor neuron subtypes [reviewed in (Bonanomi and Pfaff, 2010). Essentially, these can be broken down to ventral, including spinal motor neurons that innervate striated muscle, and dorsal, including neurons exiting from the hindbrain, exiting motor neurons (Guthrie, 2007). For ventral motor neurons the interaction between Cxcr4, a G protein coupled receptor expressed by motor neurons, and Cxcl12, a chemokine expressed by mesenchymal cells flanking the spinal cord, is required for exiting (Lieberam et al., 2005). Disruption of this interaction inhibits motor neuron axons from exiting the spinal cord, and they project dorsal and exit at inappropriate regions (Lieberam et al., 2005). In addition to this chemoattractive interaction, our laboratory hypothesizes growth cones must locally break down the ECM to exit the spinal cord, and this may be regulated by the biophysical properties of the ECM. We have recently discovered motor neuron growth cone basal and apical protrusions, termed invadosomes, are required for three-dimensional neurite guidance (Santiago-Medina et al., 2015). Importantly, we showed these structures are required for motor neuron axon exiting of the spinal cord. These structures, similar to cancer cell invadopodia, can break down ECM, suggesting remodeling of ECM components *in vivo*. In metastatic cancer cells and migrating fibroblasts these ECM remodeling events are regulated by the biophysical environment (Artym et al., 2015, Doyle et al., 2015, Li et al., 2015). Moreover, the release of MMPs has been shown to be directly regulated by elasticity (Haage and Schneider, 2014), providing further evidence that *in vivo*, substrata rigidity may play an instructive role for motor neuron axon exiting from the spinal cord. However, the initiating factor between mechanosensing and ECM remodeling remains less understood. Our results in collagen matrices further suggest environmental mechanics affect neurite development in three-dimensional environments, perhaps through modulation of invadopodia or MMP release. Future studies should investigate the affect of mechanosensing in motor neuron growth cones and MMP activity.

The ability of motor neuron growth cones to sense the significant disparate elasticities upon leaving the CNS and respond accordingly is poorly understood. Upon leaving the spinal cord motor axons grow in a rostral-caudal segmentation pattern [reviewed in (Bonanomi et al., 2010)]. This spatial organization is governed by positioning of somites surrounding the spinal cord (Keynes and Stern, 1984). Axonal growth cones must sense the fluctuations in ECM at somatic boundaries. Somites have stereotyped biophysical composition with increasing rigidity toward the posterior somite boundary (McMillen et al., 2016). Interestingly, motor axons avoid these areas of increasing rigidity leading to axon fasciculation and extension on the anterior side of the somite. Cells in the posterior half of the somite additionally secrete inhibitory cues Sema3A/3F, Ephrin-B1, F-Spondin, T-cadherin, and chondroitin sulfate proteoglycans (Bonanomi et al., 2010). While the posterior inhibitory responses have been previously thought to be exclusively due to chemical gradients of these guidance cues, our results and others indicate the composition and mechanical properties of the ECM is crucial in promoting fasciculation and guidance. It is likely the biophysical mediated effects on neurite outgrowth we observed act in conjunction with these inhibitory cues *in vivo*. Specifically, guidance cues Semaphorin and Ephrin likely modulate adhesion related mechanotransduction in motile growth cones to induce morphological changes. For example, Semaphorin 3A regulates traction forces and actin RF by modulating adhesion dynamics and endocytosis of membrane bound integrin receptors (Woo et al., 2006, Tojima et al., 2010, Myers et al., 2011, Nichol IV et al., 2016). The inhibitory effects of Ephrins have been demonstrated using immobilized ligand border assays, indicating the observed effects of Ephrins on adhesion dynamics have a biophysical component (Woo et al., 2009). Guidance molecules such as EphrinB2 have been identified as adhesive ligands and can control matrix rigidity during cell migration and tissue development, respectively (Pfaff et al., 2008, Wilkinson et al., 2008). EphB ligand binding activates downstream effectors of adhesion dynamics, including Src and Rho-GEF (Park and

Lee, 2015). How semaphorin and ephrins interact with the ECM to regulate substrata rigidity and cell signaling during axon growth *in vivo* is still largely unknown.

The mechanochemical regulation of growth cones guides axon extension toward the postsynaptic target at the neuromuscular junction as well. Axonal projections from motor neurons in the same region of the spinal cord innervate the same muscle (Landmesser, 2001). Growing axons branch and innervate muscle in an identical rostral-caudal location to their cell bodies within the spinal cord (Bonanomi et al., 2010). Upon reaching target muscle, axons branch to innervated their proper synaptic partner. Axonal branching is affected by substrata rigidity, as mouse spinal cord neurons branched more on softer substrata (Flanagan et al., 2002). The matching spinal neuron location to muscle innervation has been characterized and is dependent on ephrinA as there are observed impairments in neuromuscular topography of mouse mutants lacking ephrin-A2/A5 or overexpressing ephrinA5 (Feng et al., 2000). This is likely due to EphrinA mediated disruption of growth cone adhesion (Woo et al., 2009), or by activating MMP induced cleavage of cell surface ephrinA ligands (Hattori et al., 2000). As previously stated, both of these events can be governed by mechanical properties of the environment. Innervating axons likely encounter different muscle rigidities dependent upon spatial and temporal muscle development. An exciting recent publication used techniques to modulate substrata elasticity *in vivo* (Koser et al., 2016). These techniques could provide useful to tightly regulate temporal changes in muscle rigidity during motor axon innervation. A caveat to our study and others is the lack of characterization of elastic measurements of muscle during development. The observed muscle elasticities reported previously have been in cultured myocytes and cardiac muscle from adult mice (Mathur et al., 2001, Collinsworth et al., 2002, Engler et al., 2006) and adult humans using magnetic resonance elastrography (Tyler, 2012). Further characterization of developing muscle rigidity fluctuations is critical to understanding our results. Importantly, human iPSCs can be differentiated into muscle fibers

(Chal et al., 2015), allowing researchers to investigate the effect of muscle rigidity with motor neuron axon branching and synaptogenesis.

There is compelling evidence that motor neuron axon spinal cord exiting, growth into periphery, and branching and synaptic targeting is regulated by the biophysical properties of the microenvironment. The open question is whether elasticity plays a permissive or instructive role for developing motor neurons. Additionally, it is less clear if growing axons sense and respond to fluctuations in the environment by altering adhesion and cytoskeletal factors, or growth cones themselves remodel the ECM locally to allow for maximal outgrowth, or both. Here, we identified key adhesion and cytoskeleton regulatory proteins, RhoA, FAK, Src, and p130-CAS, as being mechanosensitive in hMN. However, the temporal and spatial dynamics of activation of these proteins, and how that affects adhesion formation and turnover, still needs to be elucidated.

A lot can be deduced from non-neuronal and cancer cell migration literature. Motile cells can detect and react to the mechanical properties of the extracellular microenvironment through integrin based adhesions (Sun et al., 2016). However, the initial step of mechanosensing, whether integrin receptors directly sense the environment or they are activated downstream of mechanosensitive ion channels or lipid signaling, is still relatively unknown. It is clear integrin based adhesions are modulated by mechanical force, and subsequently transmit traction forces onto the ECM promoting force reciprocity between the ECM and the cytoskeleton. Whatever the initial step, integrin activation and clustering leads to recruitment of multiple signaling and scaffold molecules to the nascent adhesion (Sun et al., 2016). \Among the proteins recruited, Src and FAK phosphorylate paxillin and p130-CAS (Sawada et al., 2006, Cohen-Hillel et al., 2009). Paxillin and p130-CAS localize the GEFs ß-Pix and DOCK180 to adhesions, respectively (Ridley, 2015). Both DOCK180 and ß-Pix alter Rac1 mediated lamellipodia formation and cell spreading through induction of actin

polymerization (Kiyokawa et al., 1998, ten Klooster et al., 2006). Concomitantly, FAK recruits Arp2/3 thereby promoting actin dynamics through the GEF Trio (Medley et al., 2003). Other proteins, such as vinculin, talin, and α-actinin are recruited to adhesion sites to clutch F-actin (Humphries et al., 2007, Choi et al., 2008). The coupling between integrin adhesions and F-actin is required for the assembly and turnover of nascent adhesions. After nascent adhesion formation RhoA, which is initially inactivated via p190RhoGAP, a Rho-specific GAP activated downstream of integrin in a Src-dependent manner, is activated by several Rho-GEFs [reviewed in (Lawson et al., 2014)]. RhoA ultimately leads to increased actomyosin contraction through ROCK (Totsukawa et al., 2000). It was initially hypothesized that the effects of RhoA on adhesion during mechanotransduction was due to myosin-II increasing actin RF and subsequently increasing mechanical force on the adhesion to stretch mechanosensitive adhesion proteins, such as p130-CAS, talin, and vinculin (Chrzanowska-Wodnicka et al., 1996, Sawada et al., 2006, del Rio et al., 2009, Zhang et al., 2014). This rationale was due to the observation that focal adhesion maturation was diminished by blocking RhoA or myosin-II (Chrzanowska-Wodnicka et al., 1996). However, two lines of evidence have recently challenged this view. Adhesion maturation and size was discovered to be independent of traction forces (Beningo et al., 2001) and RhoA-ROCK-myosin-II mediated contraction did not always correlate with adhesion maturation (Tan et al., 2003). However, the complete loss of myosin-II contractility abolishes focal adhesion formation. Consequently, the tension produced by actin RF on adhesions does have an affect on adhesion formation, but may not be as important as initially believed.

The observation that myosin-II contractility is dispensable for adhesion maturation in response to mechanical force might appear to be in discord with our results showing increased Src and FAK activity after RhoA activation (Figure 6). However, the increased neurite length and outgrowth we observed after RhoA activation might be due to another function of myosin-

II. In myosin-II depleted cells, adhesion maturation was reinitiated after re-expression of myosin-II that was still able to bind and crosslink actin, but was defective as a motor protein (Choi et al., 2008). The crosslinking function of myosin-II, which is also regulated by RhoA, could prove a more important function than the force generating activity. In short, during myosin-II bundling of actin filaments, near clustered integrin adhesion sites, proteins that are bound to the actin filament are brought together, allowing interactions and localization around integrin receptors (Vicente-Manzanares et al., 2009). This leads to increased adhesion signaling, as well as increase integrin avidity, both leading to formation and maturation of adhesions (Vicente-Manzanares et al., 2009). Our results suggest that in hMN growth cones the actin crosslinking function of myosin-II may underly the increased leading edge stabilization and neurite lengths we observed after LPA induced RhoA activation (Figure 4). We showed LPA treatment reverses the effect of elasticity on phosphorylation of FAK and Src (Figure 6). However, we did not observe this effect for the phosphorylation of p130-CAS, which has been proven to be dependent upon intracellular mechanical force induced by myosin-II contractility (Sawada et al., 2006, Zhang et al., 2014). We conclude the overactivation of RhoA on soft substrata, where RhoA activity is lower under control conditions, increased myosin-II crosslinking allowing adhesion proteins to localize around integrin receptors leading to more stable adhesion. Yet, differences in myosin-II contractility was not enough to induce stretching of p130-CAS. Conversely, on rigid substrata RhoA overactivation could promote such increased contractility that the crosslinking effects of myosin-II are overshadowed leading to repulsive responses. In future studies, the temporal and spatial regulation of actin RF and adhesion formation and turnover after RhoA overactivation should be investigated to delineate the role of RhoA-myosin-II mediated crosslinking and contractility. Additionally, whether myosin-II crosslinked anti-parallel actin filaments exist in the growth cone leading edge, where adhesions initiate, has not been characterized.

The results discussed here link adhesion dynamics to being a major factor governing mechanotransduction in human growth cones during neurite development. Nonetheless, the initial step of mechanosensing in neuronal growth cones remains unidentified. Whether integrin receptors themselves are mechanically gated is not known. Adhesion regulation is a key regulator and output of mechanical responses, but may not be the initiating factor. Mechanically gated ion channels are an intriguing set of molecules that could initiated force induced signaling pathways. In addition to many other functions, mechanosensitive channels are important mediators of cell motility. Mechanosensitive channels control Ca2+ signaling to regulate cell migration and growth cone motility (Jacques-Fricke et al., 2006, Wei et al., 2009, Kerstein et al., 2013). Mechanosensitive ion channels and Ca2+ signals localize to areas of high traction force indicating local force may act to gate these channels around adhesions (Gomez et al., 2001, Doyle et al., 2004, Franze et al., 2009). Previously, our laboratory found substratum elasticity modulates Ca2+ influx through mechanosensitive channels as rigid substrata elicit higher frequency of Ca2+ transients, and subsequently inhibits axon extension (Kerstein et al., 2013). How mechanical forces are transduced into mechanosensitive channel gating remains unknown, but possibly involves coupling with the cytoskeleton or local lipid compositions (Clark et al., 2007, Hayakawa et al., 2008). Force activated Ca2+ signals act to modulate adhesion dynamics and growth cone motility through calpain (Kerstein et al., 2013). Calpain is a Ca2+-dependent protease that cleaves adhesion and actin binding proteins to modulate their function (Robles et al., 2003, Kerstein et al., 2013). Targets of calpain include FAK (Chan et al., 2010), which we show is upregulated in human motor neurons under optimal growth conditions (Figure 5). The link between mechanosensitive ion channel activation and RhoA is less well understood. Ca2+ influx regulates RhoA via induced phosphorylation of p190Rho-GAP. However, this may be indirectly through Ca2+ modulation of adhesions. Due to the complexities of homeostatic feedback around adhesions, the initiating factor during growth

cone mechanotransduction may not be due to a single molecule but coordinated interactions between mechanically gated channels, integrin clustering, adhesion protein signaling, and cytoskeletal dynamics.

Less may be deduced about how these mechanosensitive signaling pathways described here control mechanical dependent neurite guidance within the CNS. While our neurite length results in three-dimensional collagen (Figure 2) and other studies have found effects of substrata rigidity on CNS neurite projections the results are varied and unclear (Flanagan et al., 2002, Kostic et al., 2007). Two studies using mouse (Kostic et al., 2007) and rat (Koch et al., 2012) hippocampal neurons found increased neurite length on soft substrata and no effect of substrata on neurite length, respectively. The disparate results were likely due differences in ECM substrata coating, as preferential growth was observed specifically on fibronectin. We repeated these experiments using hFB and found no difference between substrata used on neurite lengths. Collagen did show a robust effect on neurite length for hFB. In the developing CNS, collagen, laminin, and fibronectin are mainly expressed in the basal lamina surrounding the brain (Barros et al., 2011). However, fibril forming collagens, such as collagen I used here, are not highly expressed in the brain or spinal cord parenchyma. Other non-fibril-forming collagens and collagen-like proteins are widely expressed in the developing CNS (Fox, 2008, Myers et al., 2011). Though expressed primarily in the basal lamina associated with the pia matter, laminin is also thought to be present in the subplate, ventricular zone, and marginal zone of the developing cerebral wall (Schmid and Anton, 2003). Laminin also appears to serve as a substratum to migrating neurons during early cortical development (Hunter et al., 1992). In addition to the basal lamina, fibronectin is expressed in radial glia and affects migration of cortical plate neurons during cortical lamination (Sheppard et al., 1995). Our results on collagen suggest the three-dimensional environment is the most important regulator of CNS neurite development. We conclude this because of low collagen abundance

in the brain parenchyma, and we did not observe these results in two-dimensional cultures on laminin and fibronectin. In light of this, the majority of mechanical dependent neurite growth in the CNS may be due to cell-cell adhesion and specific interactions with supporting glia. In addition, collagen, laminin, and fibronectin bind to a unique array of integrin receptors to activate different signaling pathways. Future studies should elucidate the difference between integrin receptor subtypes expressed in human cortical neurons to better understand neurite development on flexible substrata.

Figure 1. Human hMN, but not hFB, neurite development depends on substrata elasticity. (A-H) Low magnification confocal images of hMN (A-D) and hFB (E-H) neurospheres immunolabeled for βIII-tubulin (magenta) and F-actin (phalloidin, green). Neurospheres were cultured on polyacrylamide gels of varying elasticity (ranging from 0.2 kPa to 125 kPa), coated with poly-d-lysine and laminin (LN), for 2 DIV. Scale bar, 100 μm. **(I)** Quantification of hMN neurite lengths on different elasticities. Due to the density of neurites, the ten longest neurites were measured for analysis and comparison between experimental groups. Note that neurites maximally extend on rigid substrata, reaching optimal growth on 25 kPa. **(J)** Quantification of neurite lengths on varying elasticities for hFBs. Note the absence of a differential growth trend dependent on substrata rigidity. **(K)** Example of an inverted contrast image of a neurosphere used for sholl analysis to quantify neurite number and length. Analyses were performed using the ImageJ Sholl analysis plugin (Start radius 50 μm from neurosphere exterior, ending radius 700 μm, step size 5 μm, radius span 5 μm). **(L-M)** Sholl analysis quantification of hMN (L) and hFB (M) on soft (0.5 kPa, red line), intermediate (8 kPa, cyan line), and rigid (25 kPa, blue line). Using Two-way ANOVA (rigidity and length) we found significant difference between elasticities for both both neuronal subtypes. Inset indicates the mean number of total intersections on soft, intermediate, and rigid substrata at all distances. Significance determined by One-way ANOVA. **(N-Q)** Time-lapse representative images of hMN (N-O) and hFB (P-Q) extending neurites on soft and rigid polyacrylamide gels over a 30 min period. Color matched open arrows indicate growth cone initial location at start of time lapse. Closed arrows indicate translocation of growth cone after 30 min. Scale bar, 50 μm. **(R-S)** Rate of neurite outgrowth for hMN (R) and hFB (S) cultured on soft and rigid LN coated polyacrylamide gels. Significance determined by Student's t test. All data sets are mean±s.e.m. ***$p<0.001$ **$p<0.01$.

Figure 1.

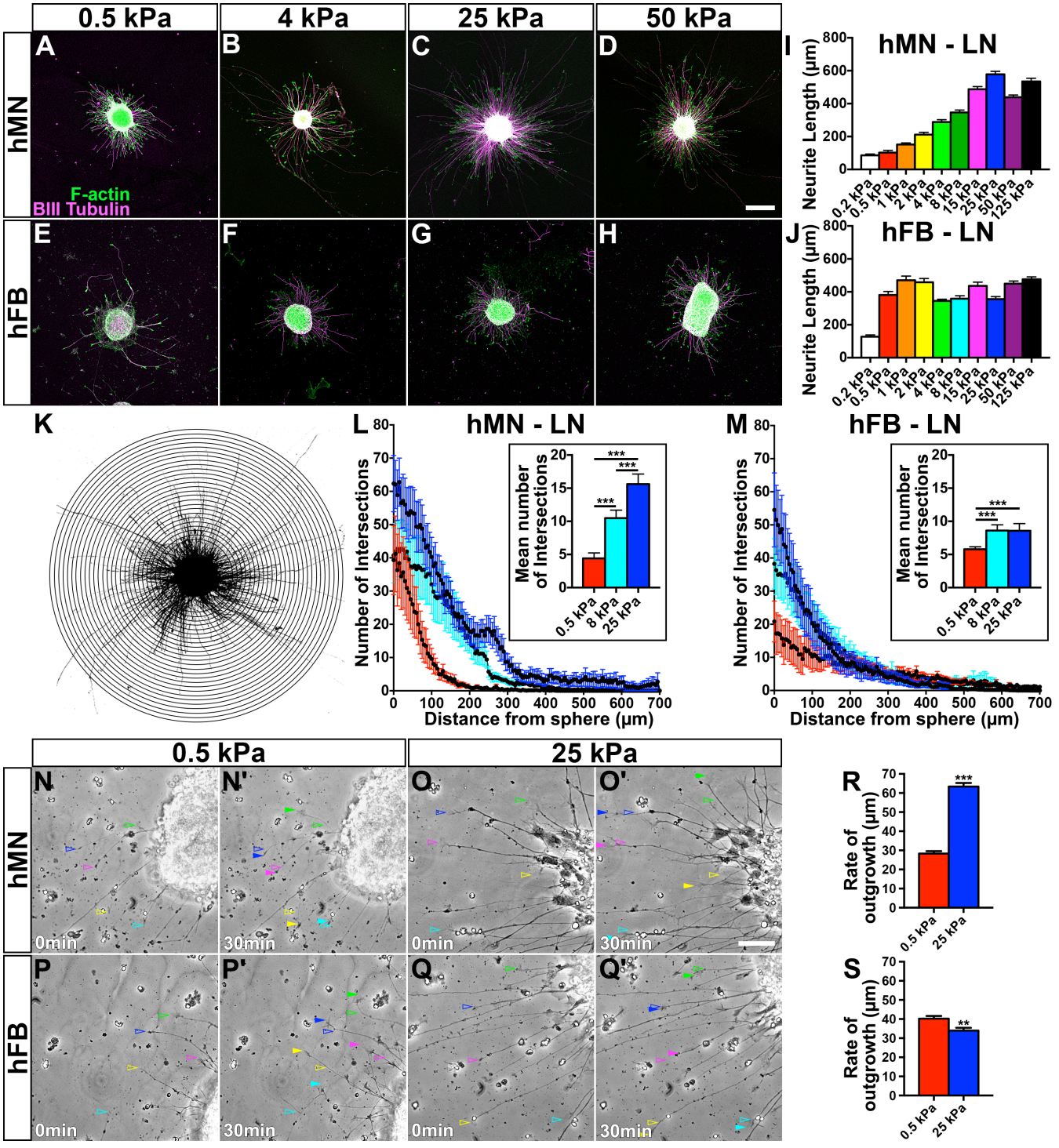
0.5 kPa
4 kPa
25 kPa
50 kPa
hMN
hFB
A
B
C
D
E
F
G
H
F-actin
BIII Tubulin
I
hMN - LN
Neurite Length (µm)
J
hFB - LN
0.2 kPa
0.5 kPa
1 kPa
2 kPa
4 kPa
8 kPa
15 kPa
25 kPa
50 kPa
125 kPa
K
L
hMN - LN
M
hFB - LN
Number of Intersections
Distance from sphere (µm)
Mean number of Intersections
***
N
N'
O
O'
P
P'
Q
Q'
0min
30min
R
Rate of outgrowth (µm)
S
**

Figure 2. Human human neurite development depends on substrata elasticity in three dimensional. (A-B) Single optical section representative images of self-assembled 1.5 mg/ml collagen hydrogel (A) and genipin treated collagen hydrogel (B). Multi-photon second harmonic generation (blue) images are merged with confocal genipin fluorescence (excitation 590nm, red). Magenta signifies colocalization of the collagen fibrils with genipin. Note the difference in fibril size and density. **(C-D)** Collagen fibril size (C) and count (D) in control collagen and 10mM genipin quantification. Note the increase size and decreased density of collagen fibrils in the presence of 10mM genipin. Significance determined by Student's t test. **(E)** Mean intensity of genipin fluorescence in control collagen and collagen with 10mM genipin. Genipin fluorescence directly correlates with changes in rigidity. Significance determined by Student's t test. **(F-I)** Low magnification confocal z-stack images of hMN (F-G) and hFB (H-I) neurospheres immunolabeled for βIII-tubulin (magenta) and F-actin (phalloidin, green). Neurospheres were cultured on collagen hydrogels without (F, H) and with 1mM genipin (G, I) for 4 DIV. Scale bar, 100 μm. **(J)** Quantification of neurite lengths on control collagen and collagen with genipin for hMN and hFB. Note the opposite result on neurite length for hMN and hFB on different elasticities of collagen. Significance determined by Student's t test within neuronal subtype. **(K)** Quantification of the depth into hydrogels for hMN and hFB. Significance determined by Student's t test within neuronal subtype. All data are mean±s.e.m. ***$p<0.001$.

Figure 2.

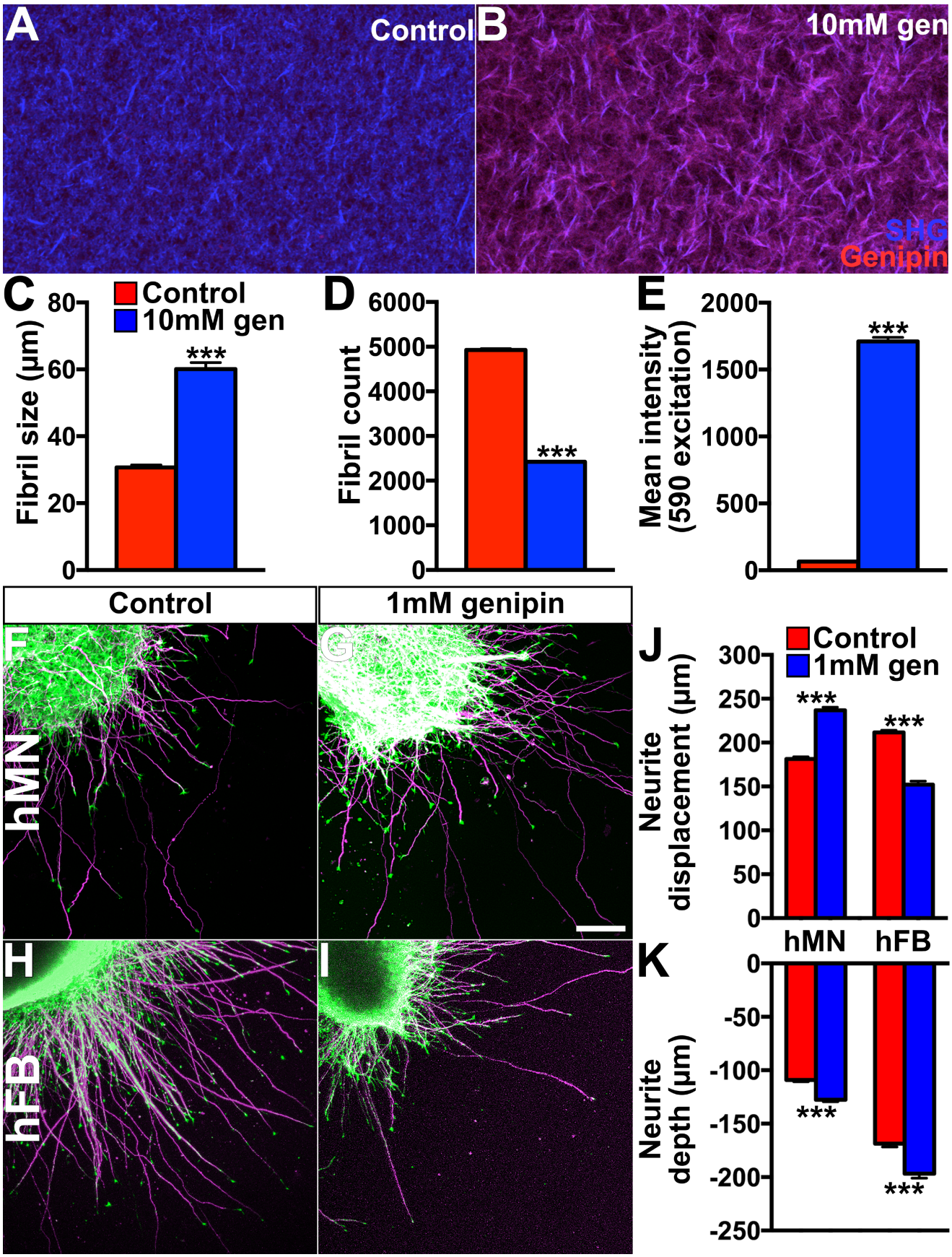
A
Control
B
10mM gen
SHG
Genipin
C
Control
10mM gen
Fibril size (μm)
0
20
40
60
80
***
D
Fibril count
0
1000
2000
3000
4000
5000
6000
***
E
Mean intensity (590 excitation)
0
500
1000
1500
2000
***
Control
1mM genipin
F
G
hMN
H
I
hFB
J
Control
1mM gen
Neurite displacement (μm)
0
50
100
150
200
250
300
***
***
hMN
hFB
K
Neurite depth (μm)
0
-50
-100
-150
-200
-250
***
***

Figure 3. hMN, but not hFB, growth cones have more stable leading edge adhesion to rigid substrata. (A) Example of a GFP expressing hMN growth cone cultured on laminin coated polyacrylamide gel used for morphology analysis. Scale bar, 10 μm. **(B)** Example of a growth cone used for morphology analysis showing initial (red) and final (green) growth cone position. Yellow line is an example of kymograph produced from 2 min time-lapse sequence in the growth cone peripheral domain. **(B')** Kymograph constructed from region specified in time-lapse of growth cone in (B). **(C-D)**, Representative kymographs generated from hMN growth cone leading edge membranes on soft and rigid substrata. Note the greater stability of the leading edge on rigid substrata. Scale bar, 10 μm. **(E)** Quantification of leading edge membrane duration of protrusion and retraction events on soft and rigid substrata for hMN growth cones. Significance determined by Student's t test. **(F)** Rate of membrane protrusion and retraction of hMN growth cone leading edge for neurons cultured on soft and rigid substrata. Significance determined by Student's t test. **(G-I)** Kymographs illustrating growth cone leading edge morphological events from hFB growing on soft and rigid substrata. Scale bar, 10 μm. **(H)** Quantification of leading edge membrane duration of protrusion and retraction events on soft and rigid substrata for hFB growth cones.. Significance determined by Student's t test. **(J)** Rate of membrane protrusion and retraction of hFB growth cone leading edge for neurons cultured on soft and rigid substrata. Significance determined by Student's t test. All data sets are mean±s.e.m. ***$p<0.001$ *$p<0.01$.

Figure 3.

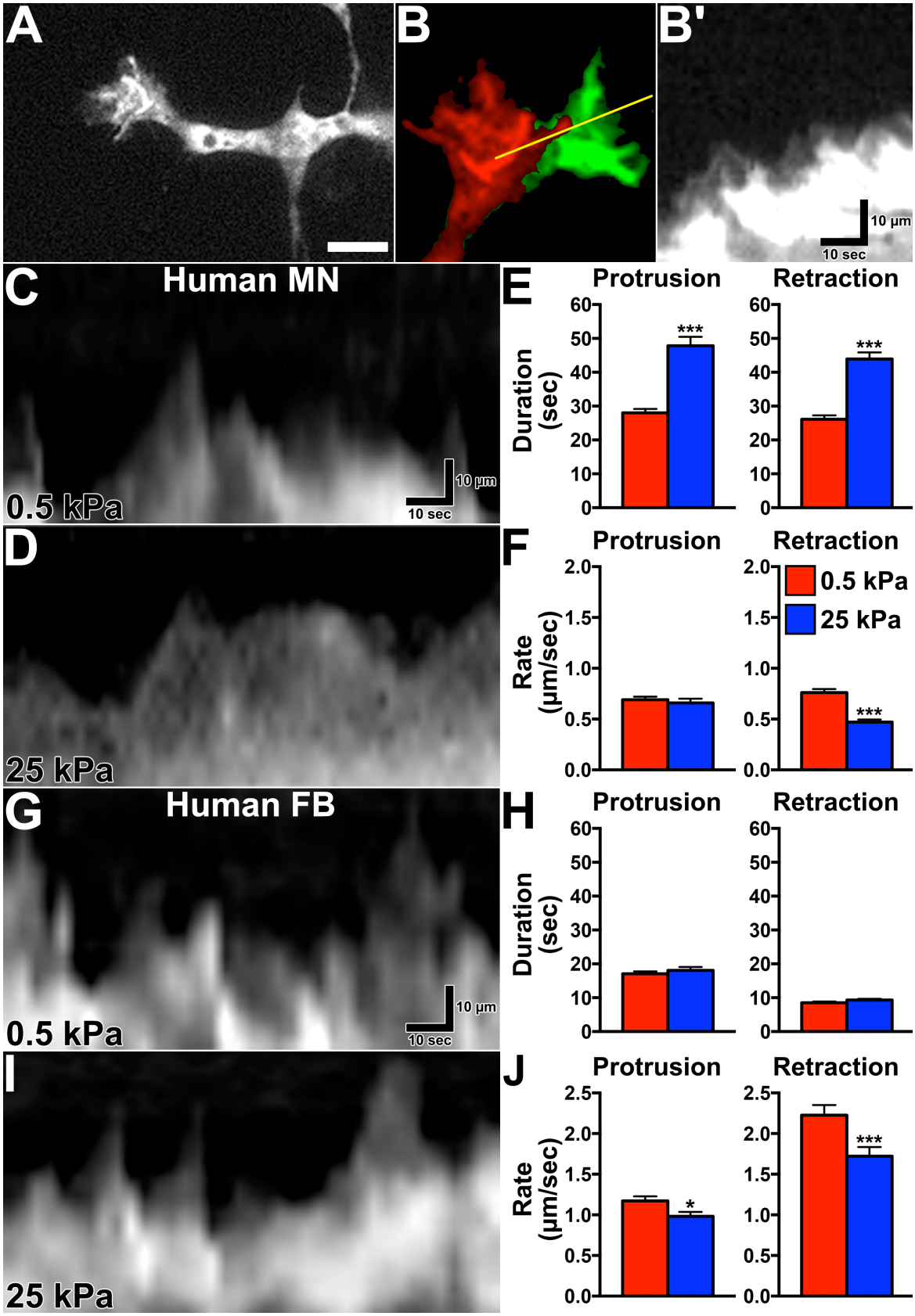
A
B
B'
10 µm
10 sec
C
Human MN
0.5 kPa
10 µm
10 sec
D
25 kPa
E
Protrusion
Retraction
Duration (sec)
***
***
F
Protrusion
Retraction
Rate (µm/sec)
0.5 kPa
25 kPa
***
G
Human FB
0.5 kPa
10 µm
10 sec
H
Protrusion
Retraction
Duration (sec)
I
25 kPa
J
Protrusion
Retraction
Rate (µm/sec)
*
***

Figure 4. RhoA pharmacological manipulation alters hMN neurite growth on different elastic substrata. (A-F) Representative images of hMN neurospheres after 2 DIV on soft (A-C) and rigid (D-F) substrata. hMN were stimulated with control media (A), 100 nM Lysophosphatidic acid (LPA, B), and 1 μg/ml Rho inhibitor I (C) after 24 hours in culture; then fixed after 24 hours and immunolabeled for βIII-tubulin (magenta) and F-actin (phalloidin, green). Scale bar, 100 μm. **(G)** Mean neurite length quantification of neurospheres after chronic pharmacological stimulation reveals RhoA manipulation has opposite effects dependent upon substrata elasticity. Significance determined by One-way ANOVA. **(H-I)** Time-lapse DIC images of individual neurites at time points: 30 min before (H, I) and 0 min (H', I') and 30 min (H", I") post acute 100 nM LPA treatment. Note LPA treatment causes rapid neurite extension soft substrata, but retraction on rigid substrata. Scale bar, 10 μm. **(J-K)** Time-lapse DIC images of individual neurites at time points: 30 min before (H, I) and 0 min (H', I') and 30 min (H", I") post acute 1 μg/ml Rho inhibitor I treatment. Note the increased rate of extension on rigid substrata, and growth cone stalling on soft substrata. **(L-M)** Representative kymographs generated from hMN growth cone leading edge membranes on soft and rigid substrata before and after acute 100 nM LPA treatment. Note the increased stability of the leading edge on soft substrata after LPA treatment. Yellow line indicates growth cone leading edge. Scale bar, 10 μm. **(N-O)** Quantification of leading edge membrane duration of protrusion (N) and retraction (O) events on soft and rigid substrata for hMN growth cones before and after acute 100 nM LPA treatment. Note the increased duration of protrusion and retraction after LPA on soft substrata. Significance determined by Student's t test. **(P)** Distance of membrane protrusion of hMN growth cone leading edge for neurons cultured on soft and rigid substrata. Note the increase in distance after LPA treatment on soft substrata. All data sets are mean ±s.e.m. ***$p<0.001$.

Figure 4.

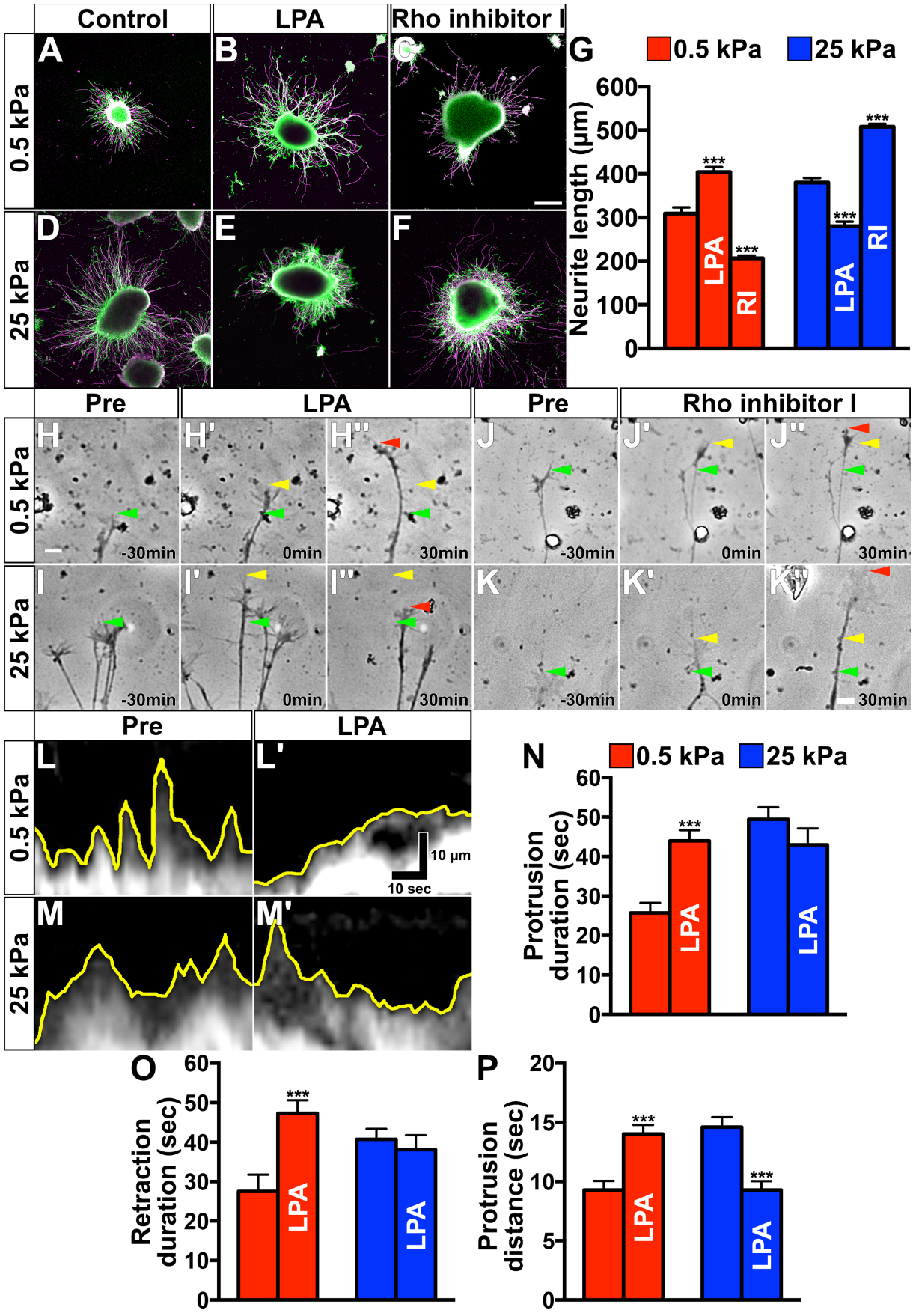
Control
LPA
Rho inhibitor I
0.5 kPa
25 kPa
A
B
C
D
E
F
G
0.5 kPa
25 kPa
Neurite length (μm)
600
500
400
300
200
100
0
***
LPA
RI
Pre
LPA
Pre
Rho inhibitor I
H
H'
H''
J
J'
J''
I
I'
I''
K
K'
K''
-30min
0min
30min
L
L'
M
M'
10 μm
10 sec
N
Protrusion duration (sec)
60
50
40
30
20
10
0
O
Retraction duration (sec)
P
Protrusion distance (sec)
20
15
10
5

Figure 5. Activation of adhesion signaling and scaffold proteins on rigid substrata. (A-J) Representative images of hMN growth cones on soft (0.5 kPa) and rigid (25 kPa) laminin coated polyacrylamide gels. Neurons were cultured for 2 DIV fixed, and immunostained with phospho-specific antibodies to the sites indicated. Fluorescence intensity was measured for activation sites for FAK (y397), Src (y418), and p130-CAS (y165 and 410), and an inhibition site for Src (y529). Immunolabeled images (A-J; green) are merged with fluorescent phalloidin labeling of filamentous actin (F-actin; magenta). Scale bar, 5 μm. **(K-O)** Quantification of phospho-labeled adhesion proteins in ratio with total protein (SE647) in hMN growth cones at specified phosphorylation sites. Rigid substrata data are normalized to soft substrata. Significance determined by Student's t test. All data sets are mean±s.e.m. ***p 0.001.

Figure 5.

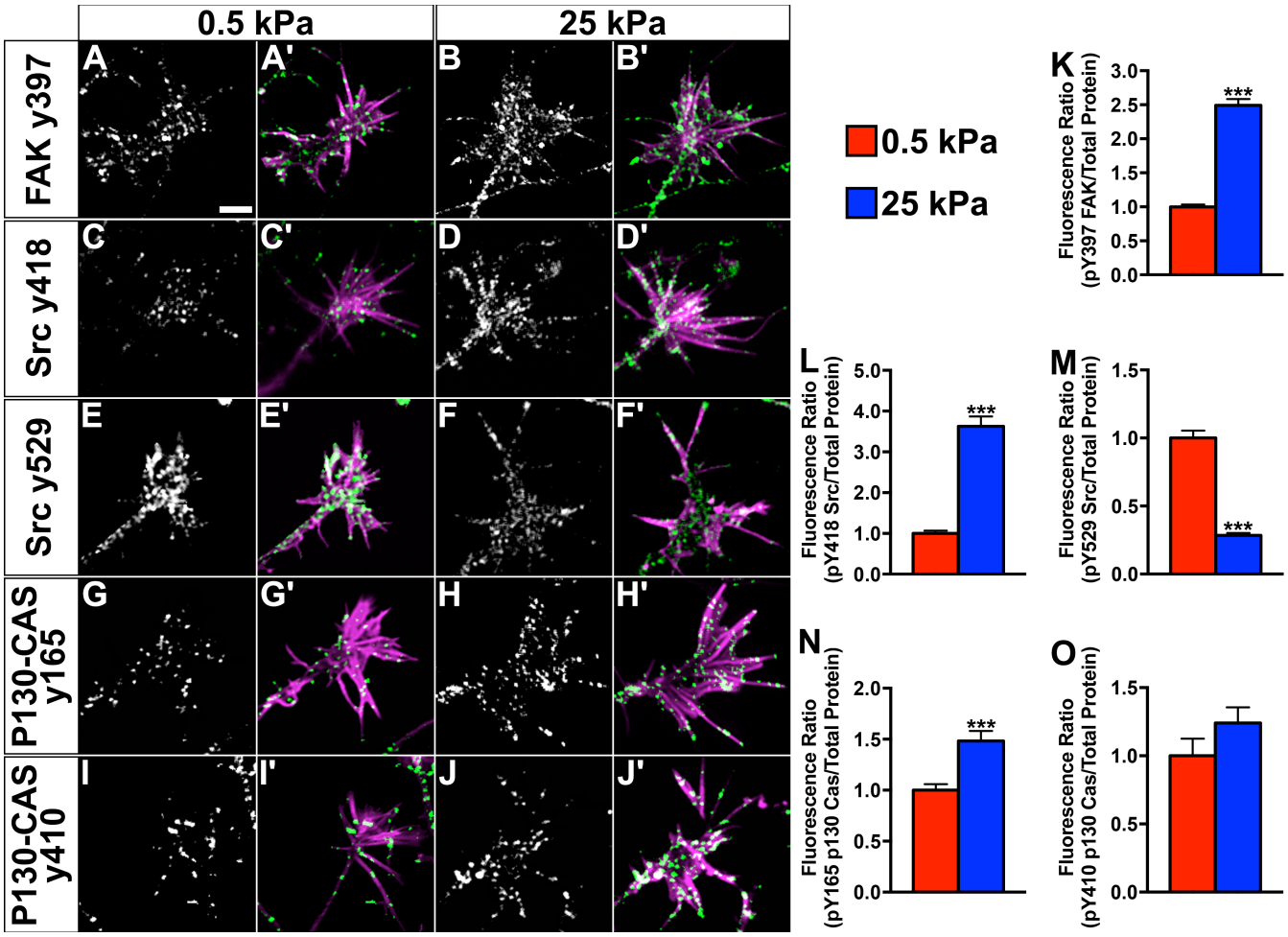
0.5 kPa
25 kPa
FAK y397
Src y418
Src y529
P130-CAS y165
P130-CAS y410
A
A'
B
B'
C
C'
D
D'
E
E'
F
F'
G
G'
H
H'
I
I'
J
J'
0.5 kPa
25 kPa
K
Fluorescence Ratio (pY397 FAK/Total Protein)
3.0
2.5
2.0
1.5
1.0
0.5
0.0
***
L
Fluorescence Ratio (pY418 Src/Total Protein)
5.0
4.0
3.0
2.0
1.0
0.0
***
M
Fluorescence Ratio (pY529 Src/Total Protein)
1.5
1.0
0.5
0.0
***
N
Fluorescence Ratio (pY165 p130 Cas/Total Protein)
2.0
1.5
1.0
0.5
0.0
***
O
Fluorescence Ratio (pY410 p130 Cas/Total Protein)
1.5
1.0
0.5
0.0

Figure 6. Activation of adhesion signaling proteins on soft substrata after LPA treatment. (A-L) Representative images of hMN stimulated with control media (A, B, E, F) or stimulated with LPA (C, D, G, H) for 1 hr, that were cultured on soft or rigid substrata and immunostained with phospho-specific antibodies to the sites indicated. Immunolabeled images (A-H; green) are merged with fluorescent phalloidin labeling of F-actin (magenta). Scale bar, 5 μm. **(M-O)** Quantification of phospho-labeled adhesion proteins in ratio with total protein (SE647) in hMN growth cones at specified phosphorylation sites stimulated for 1 hr with 100 nM LPA on soft and rigid substrata. Rigid substrata data are normalized to soft substrata. Data from Figure 6K are included for comparison. Significance determined by Student's t test within experimental group (unstimulated and LPA). All data sets are mean±s.e.m. ***p 0.001.

Figure 6.

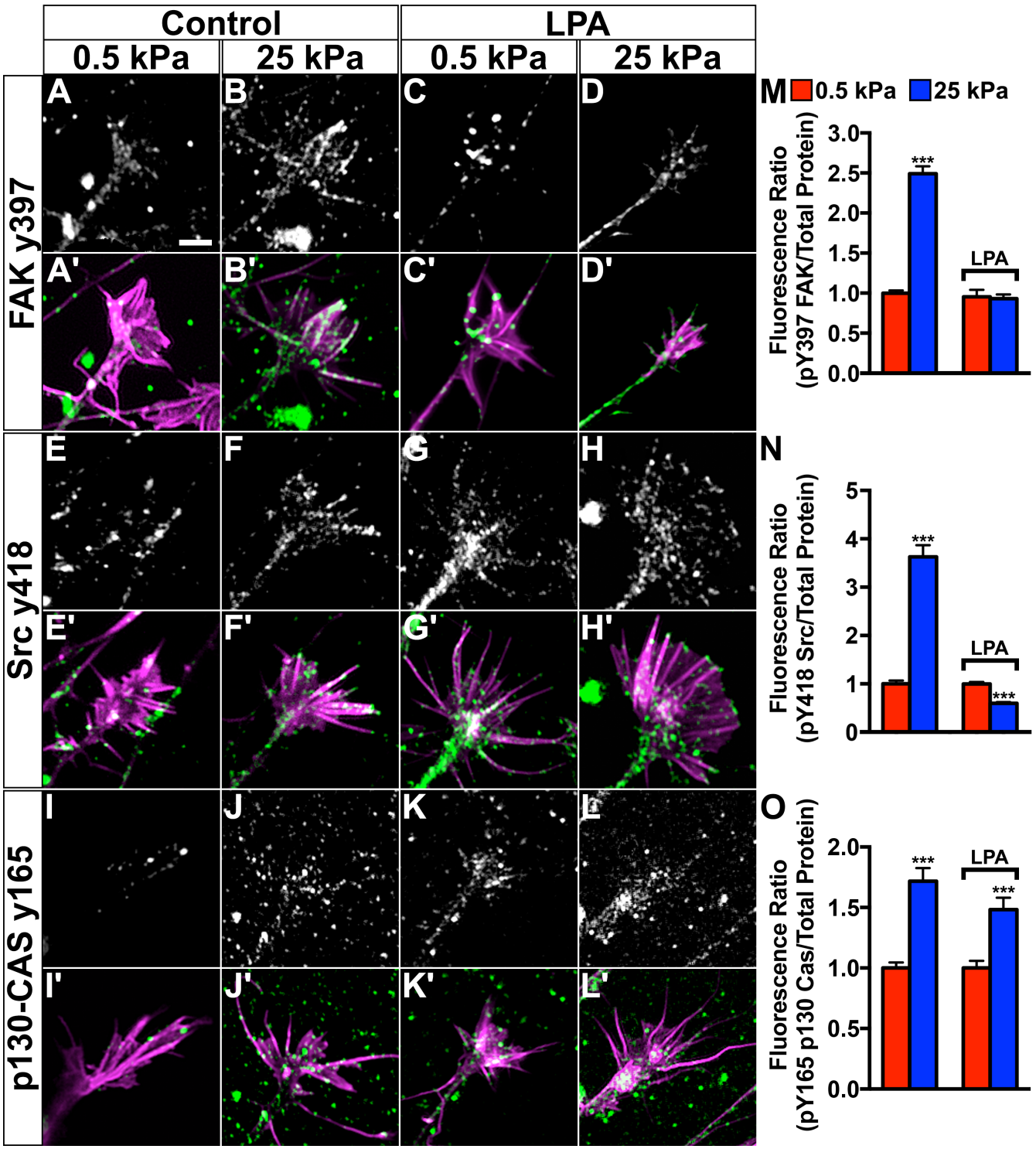
Control
LPA
0.5 kPa
25 kPa
0.5 kPa
25 kPa
FAK y397
Src y418
p130-CAS y165
A
B
C
D
A'
B'
C'
D'
E
F
G
H
E'
F'
G'
H'
I
J
K
L
I'
J'
K'
L'
M
0.5 kPa
25 kPa
Fluorescence Ratio
(pY397 FAK/Total Protein)
3.0
2.5
2.0
1.5
1.0
0.5
0.0
***
LPA
N
Fluorescence Ratio
(pY418 Src/Total Protein)
5
4
3
2
1
0
***
LPA
***
O
Fluorescence Ratio
(pY165 p130 Cas/Total Protein)
2.0
1.5
1.0
0.5
0.0
***
LPA
***

Supplemental Figure S1. Lack of differential neurite length trend on fibronectin coated polyacrylamide gels of varying rigidities (A-D) Immunofluorescent low magnification confocal images of hMN neurospheres labeled for βIII-tubulin (magenta) and F-actin (phalloidin, green). Neurospheres were cultured on polyacrylamide gels of varying elasticity, coated with fibronectin (FN), for 2 DIV. Scale bar, 100 μm. **(E)** Quantification of hFB neurite lengths on different elasticities. Due to the density of neurites, the ten longest neurites were measured for analysis and comparison between experimental groups. Note the absence of a differential growth trend dependent on substrata rigidity. All data sets are mean±s.e.m.

Supplemental Figure S1.

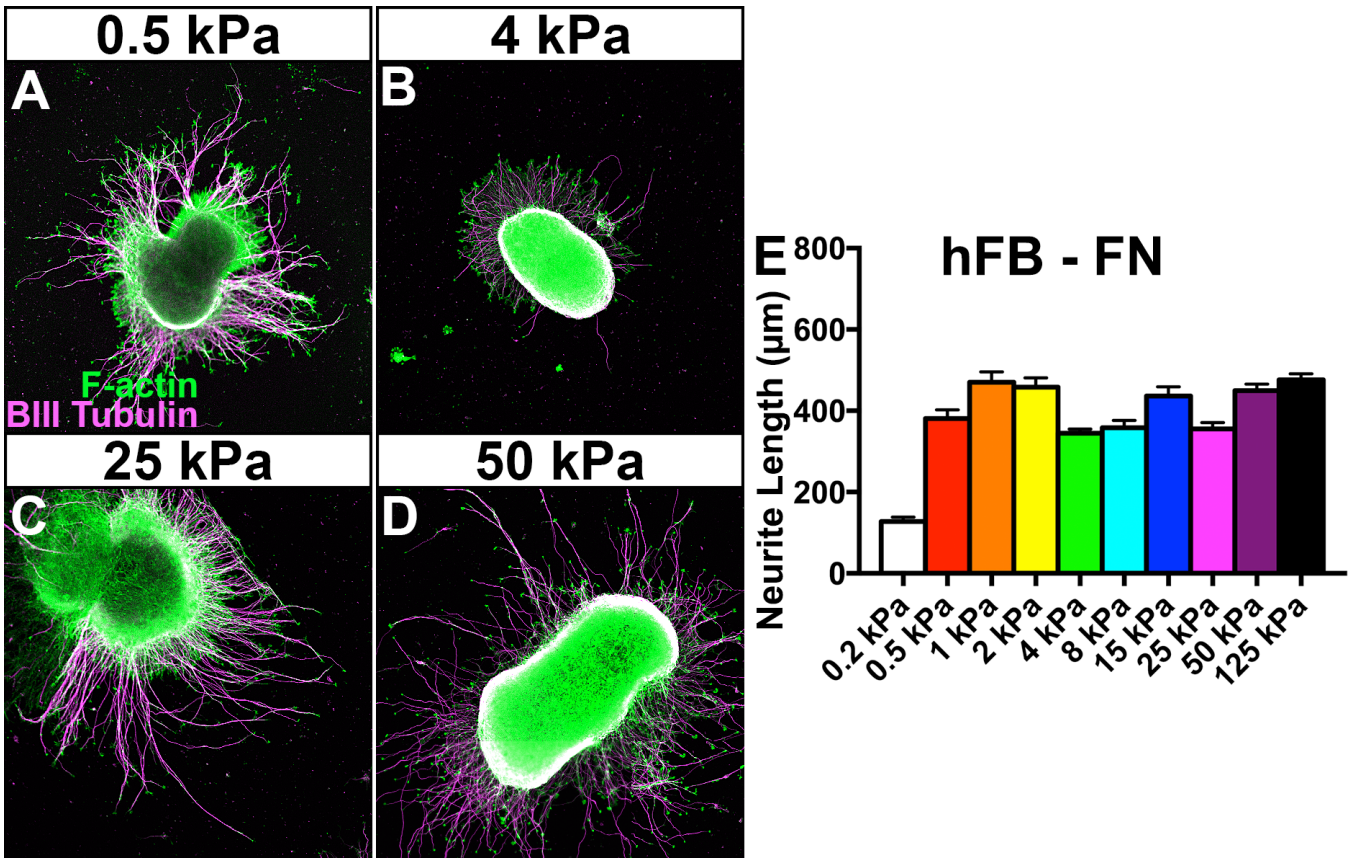

Supplemental Figure S2. RhoA activity is up-regulated on rigid substrata in hMN. (A) Schematic showing G-Lisa assay to probe for RhoA activity on rigid and soft substrata. Cells are lysed and incubated on a RhoA-GTP affinity plate, followed by detection with RhoA-GTP antibody and HRP, and reading absorption at 490 nm. **(B)** Quantification of RhoA G-Lisa activation signal described in **(A)** to assay for RhoA activation for hMN on soft versus rigid substrata. Significance determined by Student's t test. All data sets are mean±s.e.m. ***p<0.001.

Supplemental Figure S2

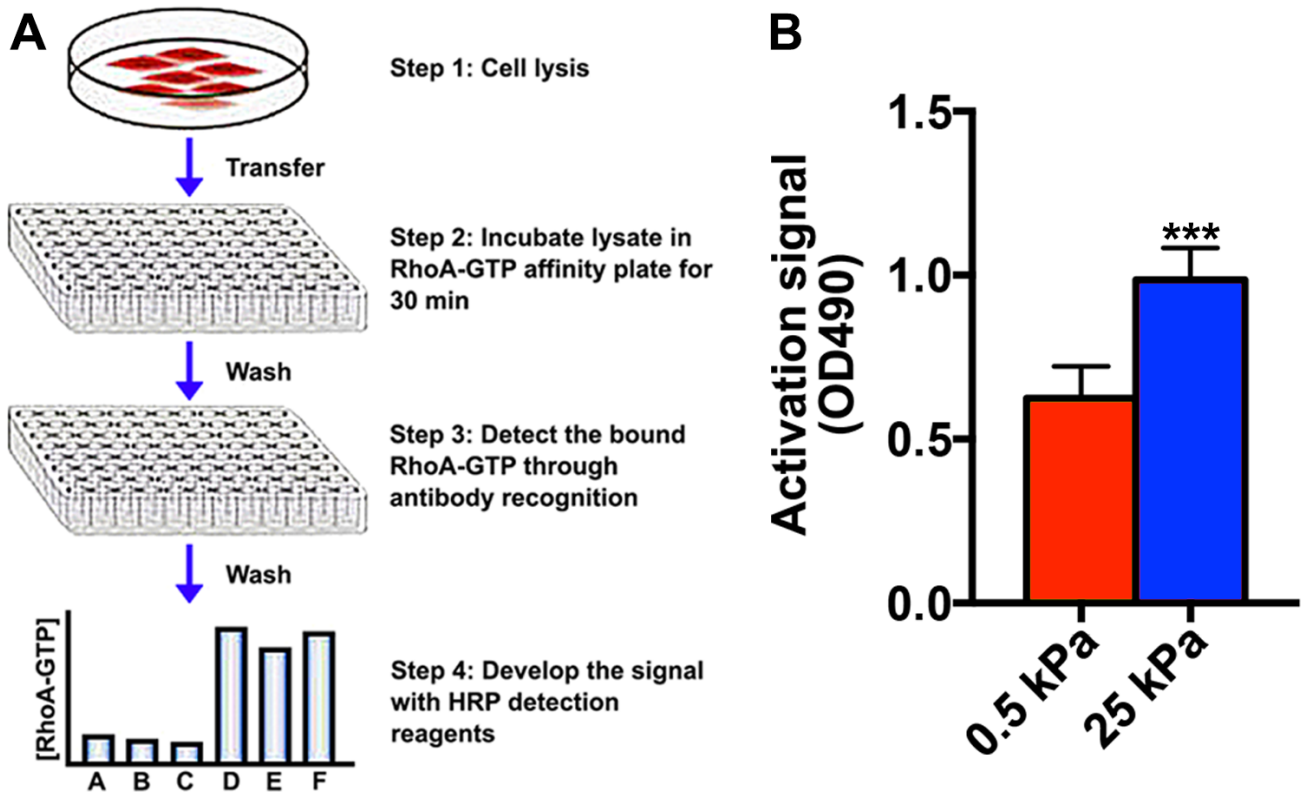

Supplemental Figure S3. Dose dependent effects of LPA induced neurite growth modulation on elastic substrata (A-H) Immunofluorescent low magnification confocal images of hMN neurospheres labeled for βIII-tubulin (magenta) and F-actin (phalloidin, green). Neurospheres were cultured on laminin coated polyacrylamide gels of two elasticities, soft (0.5 kPa) and rigid (25 kPa). hMN cultures were treated with control media (A, E) and 10 nM (B, F), 100 nM (C, G), and 1 μM LPA (D, H) LPA after 24 hours in culture and fixed 24 hours later. Scale bar, 100 μm. **(E)** Quantification of LPA dose dependent effects on hFB neurite lengths on soft and rigid substrata. Due to the density of neurites, the ten longest neurites were measured for analysis and comparison between experimental groups. Note the dose dependent increase of neurite length on soft substrata, and decrease on rigid substrata. All data sets are mean ±s.e.m.

Supplemental Figure S3.

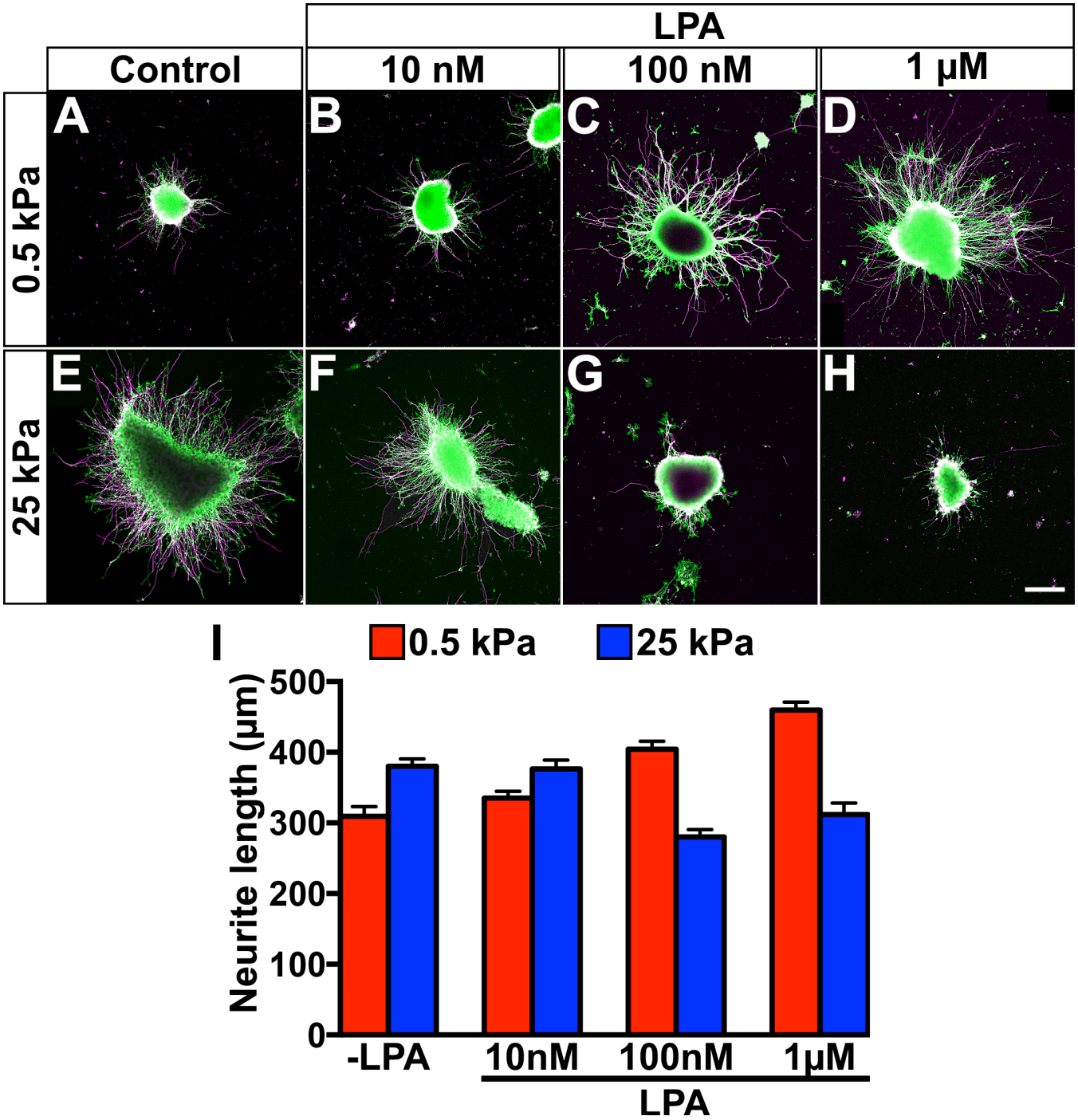

Artym VV, Swatkoski S, Matsumoto K, Campbell CB, Petrie RJ, Dimitriadis EK, Li X, Mueller SC, Bugge TH, Gucek M and Yamada KM (2015) Dense fibrillar collagen is a potent inducer of invadopodia via a specific signaling network. J Cell Biol 208(3): 331-350.

Bae YH, Mui KL, Hsu BY, Liu SL, Cretu A, Razinia Z, Xu T, Pure E and Assoian RK (2014) A FAK-Cas-Rac-lamellipodin signaling module transduces extracellular matrix stiffness into mechanosensitive cell cycling. Sci Signal 7(330): ra57.

Barros CS, Franco SJ and Muller U (2011) Extracellular matrix: functions in the nervous system. Cold Spring Harb Perspect Biol 3(1): a005108.

Beningo KA, Dembo M, Kaverina I, Small JV and Wang YL (2001) Nascent focal adhesions are responsible for the generation of strong propulsive forces in migrating fibroblasts. J Cell Biol 153(4): 881-888.

Bonanomi D and Pfaff SL (2010) Motor axon pathfinding. Cold Spring Harb Perspect Biol 2(3): a001735.

Bozkurt A, Brook GA, Moellers S, Lassner F, Sellhaus B, Weis J, Woeltje M, Tank J, Beckmann C, Fuchs P, Damink LO, Schugner F, Heschel I and Pallua N (2007) In vitro assessment of axonal growth using dorsal root ganglia explants in a novel three-dimensional collagen matrix. Tissue Eng 13(12): 2971-2979.

Chal J, Oginuma M, Al Tanoury Z, Gobert B, Sumara O, Hick A, Bousson F, Zidouni Y, Mursch C, Moncuquet P, Tassy O, Vincent S, Miyanari A, Bera A, Garnier JM, Guevara G, Hestin M, Kennedy L, Hayashi S, Drayton B, Cherrier T, Gayraud-Morel B, Gussoni E, Relaix F, Tajbakhsh S and Pourquie O (2015) Differentiation of pluripotent stem cells to muscle fiber to model Duchenne muscular dystrophy. Nat Biotechnol 33(9): 962-969.

Cheng CM, LeDuc PR and Lin YW (2011) Localized bimodal response of neurite extensions and structural proteins in dorsal-root ganglion neurons with controlled polydimethylsiloxane substrate stiffness. J Biomech 44(5): 856-862.

Choi CK, Vicente-Manzanares M, Zareno J, Whitmore LA, Mogilner A and Horwitz AR (2008) Actin and alpha-actinin orchestrate the assembly and maturation of nascent adhesions in a myosin II motor-independent manner. Nat Cell Biol 10(9): 1039-1050.

Chrzanowska-Wodnicka M and Burridge K (1996) Rho-stimulated contractility drives the formation of stress fibers and focal adhesions. J Cell Biol 133(6): 1403-1415.

Clark K, Langeslag M, Figdor CG and van Leeuwen FN (2007) Myosin II and mechanotransduction: a balancing act. Trends Cell Biol 17(4): 178-186.

Cohen-Hillel E, Mintz R, Meshel T, Garty BZ and Ben-Baruch A (2009) Cell migration to the chemokine CXCL8: Paxillin is activated and regulates adhesion and cell motility. Cellular and Molecular Life Sciences 66(5): 884-899.

Collinsworth AM, Zhang S, Kraus WE and Truskey GA (2002) Apparent elastic modulus and hysteresis of skeletal muscle cells throughout differentiation. Am J Physiol Cell Physiol 283(4): C1219-1227.

Cox EA and Huttenlocher A (1998) Regulation of integrin-mediated adhesion during cell migration. Microsc Res Tech 43(5): 412-419.

Cox EA, Sastry SK and Huttenlocher A (2001) Integrin-mediated adhesion regulates cell polarity and membrane protrusion through the Rho family of GTPases. Mol Biol Cell 12(2): 265-277.

da Silva JS and Dotti CG (2002) Breaking the neuronal sphere: regulation of the actin cytoskeleton in neuritogenesis. Nat Rev Neurosci 3(9): 694-704.

del Rio A, Perez-Jimenez R, Liu R, Roca-Cusachs P, Fernandez JM and Sheetz MP (2009) Stretching single talin rod molecules activates vinculin binding. Science 323(5914): 638-641.

Dent EW, Gupton SL and Gertler FB (2011) The growth cone cytoskeleton in axon outgrowth and guidance. Cold Spring Harb Perspect Biol 3(3).

Doyle A, Marganski W and Lee J (2004) Calcium transients induce spatially coordinated increases in traction force during the movement of fish keratocytes. J Cell Sci 117(Pt 11): 2203-2214.

Doyle AD, Carvajal N, Jin A, Matsumoto K and Yamada KM (2015) Local 3D matrix microenvironment regulates cell migration through spatiotemporal dynamics of contractility-dependent adhesions. Nat Commun 6: 8720.

Engler AJ, Sen S, Sweeney HL and Discher DE (2006) Matrix elasticity directs stem cell lineage specification. Cell 126(4): 677-689.

Flanagan LA, Ju YE, Marg B, Osterfield M and Janmey PA (2002) Neurite branching on deformable substrates. Neuroreport 13(18): 2411-2415.

Fox MA (2008) Novel roles for collagens in wiring the vertebrate nervous system. Curr Opin Cell Biol 20(5): 508-513.

Franze K (2013) The mechanical control of nervous system development. Development 140(15): 3069-3077.

Franze K, Gerdelmann J, Weick M, Betz T, Pawlizak S, Lakadamyali M, Bayer J, Rillich K, Gogler M, Lu YB, Reichenbach A, Janmey P and Kas J (2009) Neurite branch retraction is caused by a threshold-dependent mechanical impact. Biophys J 97(7): 1883-1890.

Geiger B, Spatz JP and Bershadsky AD (2009) Environmental sensing through focal adhesions. Nat Rev Mol Cell Biol 10(1): 21-33.

Gil V and del Rio JA (2012) Analysis of axonal growth and cell migration in 3D hydrogel cultures of embryonic mouse CNS tissue. Nat Protoc 7(2): 268-280.

Gomez TM, Harrigan D, Henley J and Robles E (2003) Working with Xenopus spinal neurons in live cell culture. Methods Cell Biol 71: 129-156.

Gomez TM, Robles E, Poo M and Spitzer NC (2001) Filopodial calcium transients promote substrate-dependent growth cone turning. Science 291(5510): 1983-1987.

Greenburg G and Hay ED (1982) Epithelia suspended in collagen gels can lose polarity and express characteristics of migrating mesenchymal cells. J Cell Biol 95(1): 333-339.

Guthrie S (2007) Patterning and axon guidance of cranial motor neurons. Nat Rev Neurosci 8(11): 859-871.

Haage A and Schneider IC (2014) Cellular contractility and extracellular matrix stiffness regulate matrix metalloproteinase activity in pancreatic cancer cells. FASEB J 28(8): 3589-3599.

Hayakawa K, Tatsumi H and Sokabe M (2008) Actin stress fibers transmit and focus force to activate mechanosensitive channels. J Cell Sci 121(Pt 4): 496-503.

Humphries JD, Wang P, Streuli C, Geiger B, Humphries MJ and Ballestrem C (2007) Vinculin controls focal adhesion formation by direct interactions with talin and actin. J Cell Biol 179(5): 1043-1057.

Hunter DD, Llinas R, Ard M, Merlie JP and Sanes JR (1992) Expression of s-laminin and laminin in the developing rat central nervous system. J Comp Neurol 323(2): 238-251.

Huttenlocher A, Ginsberg MH and Horwitz AF (1996) Modulation of cell migration by integrin-mediated cytoskeletal linkages and ligand-binding affinity. J Cell Biol 134(6): 1551-1562.

Hynes RO (2002) Integrins: bidirectional, allosteric signaling machines. Cell 110(6): 673-687.

Hynes RO (2009) The extracellular matrix: not just pretty fibrils. Science 326(5957): 1216-1219.

Jacques-Fricke BT, Seow Y, Gottlieb PA, Sachs F and Gomez TM (2006) Ca2+ influx through mechanosensitive channels inhibits neurite outgrowth in opposition to other influx pathways and release from intracellular stores. J Neurosci 26(21): 5656-5664.

Jiang FX, Yurke B, Firestein BL and Langrana NA (2008) Neurite outgrowth on a DNA crosslinked hydrogel with tunable stiffnesses. Ann Biomed Eng 36(9): 1565-1579.

Kerstein PC, Jacques-Fricke BT, Rengifo J, Mogen BJ, Williams JC, Gottlieb PA, Sachs F and Gomez TM (2013) Mechanosensitive TRPC1 channels promote calpain proteolysis of talin to regulate spinal axon outgrowth. J Neurosci 33(1): 273-285.

Kerstein PC, Nichol Iv RH and Gomez TM (2015) Mechanochemical regulation of growth cone motility. Front Cell Neurosci 9: 244.

Keynes RJ and Stern CD (1984) Segmentation in the vertebrate nervous system. Nature 310(5980): 786-789.

Kiyokawa E, Hashimoto Y, Kobayashi S, Sugimura H, Kurata T and Matsuda M (1998) Activation of Rac1 by a Crk SH3-binding protein, DOCK180. Genes Dev 12(21): 3331-3336.

Koch D, Rosoff WJ, Jiang J, Geller HM and Urbach JS (2012) Strength in the periphery: growth cone biomechanics and substrate rigidity response in peripheral and central nervous system neurons. Biophys J 102(3): 452-460.

Koser DE, Thompson AJ, Foster SK, Dwivedy A, Pillai EK, Sheridan GK, Svoboda H, Viana M, Costa LD, Guck J, Holt CE and Franze K (2016) Mechanosensing is critical for axon growth in the developing brain. Nat Neurosci 19(12): 1592-1598.

Kostic A, Sap J and Sheetz MP (2007) RPTPalpha is required for rigidity-dependent inhibition of extension and differentiation of hippocampal neurons. J Cell Sci 120(Pt 21): 3895-3904.

Kranenburg O, Poland M, van Horck FP, Drechsel D, Hall A and Moolenaar WH (1999) Activation of RhoA by lysophosphatidic acid and Galpha12/13 subunits in neuronal cells: induction of neurite retraction. Mol Biol Cell 10(6): 1851-1857.

Kruse SA, Rose GH, Glaser KJ, Manduca A, Felmlee JP, Jack CR, Jr. and Ehman RL (2008) Magnetic resonance elastography of the brain. Neuroimage 39(1): 231-237.

Landmesser LT (2001) The acquisition of motoneuron subtype identity and motor circuit formation. Int J Dev Neurosci 19(2): 175-182.

Lawson CD and Burridge K (2014) The on-off relationship of Rho and Rac during integrin-mediated adhesion and cell migration. Small GTPases 5: e27958.

Leung KM, van Horck FP, Lin AC, Allison R, Standart N and Holt CE (2006) Asymmetrical beta-actin mRNA translation in growth cones mediates attractive turning to netrin-1. Nat Neurosci 9(10): 1247-1256.

Li C, Rezania S, Kammerer S, Sokolowski A, Devaney T, Gorischek A, Jahn S, Hackl H, Groschner K, Windpassinger C, Malle E, Bauernhofer T and Schreibmayer W (2015) Piezo1 forms mechanosensitive ion channels in the human MCF-7 breast cancer cell line. Sci Rep 5: 8364.

Lieberam I, Agalliu D, Nagasawa T, Ericson J and Jessell TM (2005) A Cxcl12-CXCR4 chemokine signaling pathway defines the initial trajectory of mammalian motor axons. Neuron 47(5): 667-679.

Liu G, Li W, Gao X, Li X, Jurgensen C, Park HT, Shin NY, Yu J, He ML, Hanks SK, Wu JY, Guan KL and Rao Y (2007) p130CAS is required for netrin signaling and commissural axon guidance. J Neurosci 27(4): 957-968.

Lowery LA and Van Vactor D (2009) The trip of the tip: understanding the growth cone machinery. Nat Rev Mol Cell Biol 10(5): 332-343.

Machacek M, Hodgson L, Welch C, Elliott H, Pertz O, Nalbant P, Abell A, Johnson GL, Hahn KM and Danuser G (2009) Coordination of Rho GTPase activities during cell protrusion. Nature 461(7260): 99-103.

Mathur AB, Collinsworth AM, Reichert WM, Kraus WE and Truskey GA (2001) Endothelial, cardiac muscle and skeletal muscle exhibit different viscous and elastic properties as determined by atomic force microscopy. J Biomech 34(12): 1545-1553.

McCracken PJ, Manduca A, Felmlee J and Ehman RL (2005) Mechanical transient-based magnetic resonance elastography. Magn Reson Med 53(3): 628-639.

McMillen P, Chatti V, Julich D and Holley SA (2016) A Sawtooth Pattern of Cadherin 2 Stability Mechanically Regulates Somite Morphogenesis. Curr Biol 26(4): 542-549.

Medley QG, Buchbinder EG, Tachibana K, Ngo H, Serra-Pages C and Streuli M (2003) Signaling between focal adhesion kinase and trio. J Biol Chem 278(15): 13265-13270.

Moore SW, Roca-Cusachs P and Sheetz MP (2010) Stretchy proteins on stretchy substrates: the important elements of integrin-mediated rigidity sensing. Dev Cell 19(2): 194-206.

Moore SW, Zhang X, Lynch CD and Sheetz MP (2012) Netrin-1 attracts axons through FAK-dependent mechanotransduction. J Neurosci 32(34): 11574-11585.

Musah S, Wrighton PJ, Zaltsman Y, Zhong X, Zorn S, Parlato MB, Hsiao C, Palecek SP, Chang Q, Murphy WL and Kiessling LL (2014) Substratum-induced differentiation of human pluripotent stem cells reveals the coactivator YAP is a potent regulator of neuronal specification. Proc Natl Acad Sci U S A 111(38): 13805-13810.

Myers JP and Gomez TM (2011) Focal adhesion kinase promotes integrin adhesion dynamics necessary for chemotropic turning of nerve growth cones. J Neurosci 31(38): 13585-13595.

Myers JP, Santiago-Medina M and Gomez TM (2011) Regulation of axonal outgrowth and pathfinding by integrin-ECM interactions. Dev Neurobiol 71(11): 901-923.

Nichol IV RH, Hagen KM, Lumbard DC, Dent EW and Gomez TM (2016) Guidance of Axons by Local Coupling of Retrograde Flow to Point Contact Adhesions. J Neurosci 36(7): 2267-2282.

O'Connor KL, Chen M and Towers LN (2012) Integrin alpha6beta4 cooperates with LPA signaling to stimulate Rac through AKAP-Lbc-mediated RhoA activation. Am J Physiol Cell Physiol 302(3): C605-614.

Park I and Lee HS (2015) EphB/ephrinB signaling in cell adhesion and migration. Mol Cells 38(1): 14-19.

Pfaff D, Heroult M, Riedel M, Reiss Y, Kirmse R, Ludwig T, Korff T, Hecker M and Augustin HG (2008) Involvement of endothelial ephrin-B2 in adhesion and transmigration of EphB-receptor-expressing monocytes. J Cell Sci 121(Pt 22): 3842-3850.

Rahman S, Patel Y, Murray J, Patel KV, Sumathipala R, Sobel M and Wijelath ES (2005) Novel hepatocyte growth factor (HGF) binding domains on fibronectin and vitronectin coordinate a distinct and amplified Met-integrin induced signalling pathway in endothelial cells. BMC Cell Biol 6(1): 8.

Ridley AJ (2015) Rho GTPase signalling in cell migration. Curr Opin Cell Biol 36: 103-112.

Robles E, Huttenlocher A and Gomez TM (2003) Filopodial calcium transients regulate growth cone motility and guidance through local activation of calpain. Neuron 38(4): 597-609.

Robles E, Woo S and Gomez TM (2005) Src-dependent tyrosine phosphorylation at the tips of growth cone filopodia promotes extension. J Neurosci 25(33): 7669-7681.

Roeder BA, Kokini K, Sturgis JE, Robinson JP and Voytik-Harbin SL (2002) Tensile mechanical properties of three-dimensional type I collagen extracellular matrices with varied microstructure. J Biomech Eng 124(2): 214-222.

Santiago-Medina M, Gregus KA, Nichol RH, O'Toole SM and Gomez TM (2015) Regulation of ECM degradation and axon guidance by growth cone invadosomes. Development 142(3): 486-496.

Sawada Y, Tamada M, Dubin-Thaler BJ, Cherniavskaya O, Sakai R, Tanaka S and Sheetz MP (2006) Force sensing by mechanical extension of the Src family kinase substrate p130Cas. Cell 127(5): 1015-1026.

Schiller HB and Fassler R (2013) Mechanosensitivity and compositional dynamics of cell-matrix adhesions. EMBO Rep 14(6): 509-519.

Schmid RS and Anton ES (2003) Role of integrins in the development of the cerebral cortex. Cereb Cortex 13(3): 219-224.

Sheppard AM, Brunstrom JE, Thornton TN, Gerfen RW, Broekelmann TJ, McDonald JA and Pearlman AL (1995) Neuronal production of fibronectin in the cerebral cortex during migration and layer formation is unique to specific cortical domains. Dev Biol 172(2): 504-518.

Sholl A and Uttley AM (1953) Pattern discrimination and the visual cortex. Nature 171(4348): 387-388.

Siechen S, Yang S, Chiba A and Saif T (2009) Mechanical tension contributes to clustering of neurotransmitter vesicles at presynaptic terminals. Proc Natl Acad Sci U S A 106(31): 12611-12616.

Sun Z, Guo SS and Fassler R (2016) Integrin-mediated mechanotransduction. J Cell Biol 215(4): 445-456.

Sundararaghavan HG, Monteiro GA, Firestein BL and Shreiber DI (2009) Neurite growth in 3D collagen gels with gradients of mechanical properties. Biotechnol Bioeng 102(2): 632-643.

Sundararaghavan HG, Monteiro GA, Lapin NA, Chabal YJ, Miksan JR and Shreiber DI (2008) Genipin-induced changes in collagen gels: correlation of mechanical properties to fluorescence. J Biomed Mater Res A 87(2): 308-320.

Tan JL, Tien J, Pirone DM, Gray DS, Bhadriraju K and Chen CS (2003) Cells lying on a bed of microneedles: an approach to isolate mechanical force. Proc Natl Acad Sci U S A 100(4): 1484-1489.

ten Klooster JP, Jaffer ZM, Chernoff J and Hordijk PL (2006) Targeting and activation of Rac1 are mediated by the exchange factor beta-Pix. J Cell Biol 172(5): 759-769.

Tessier-Lavigne M and Goodman CS (1996) The molecular biology of axon guidance. Science 274(5290): 1123-1133.

Tojima T, Itofusa R and Kamiguchi H (2010) Asymmetric clathrin-mediated endocytosis drives repulsive growth cone guidance. Neuron 66(3): 370-377.

Totsukawa G, Yamakita Y, Yamashiro S, Hartshorne DJ, Sasaki Y and Matsumura F (2000) Distinct roles of ROCK (Rho-kinase) and MLCK in spatial regulation of MLC phosphorylation for assembly of stress fibers and focal adhesions in 3T3 fibroblasts. J Cell Biol 150(4): 797-806.

Toutant M, Costa A, Studler JM, Kadare G, Carnaud M and Girault JA (2002) Alternative splicing controls the mechanisms of FAK autophosphorylation. Mol Cell Biol 22(22): 7731-7743.

Tyler WJ (2012) The mechanobiology of brain function. Nat Rev Neurosci 13(12): 867-878.

Vicente-Manzanares M, Ma X, Adelstein RS and Horwitz AR (2009) Non-muscle myosin II takes centre stage in cell adhesion and migration. Nat Rev Mol Cell Biol 10(11): 778-790.

Wang Y, Botvinick EL, Zhao Y, Berns MW, Usami S, Tsien RY and Chien S (2005) Visualizing the mechanical activation of Src. Nature 434(7036): 1040-1045.

Wei C, Wang X, Chen M, Ouyang K, Song LS and Cheng H (2009) Calcium flickers steer cell migration. Nature 457(7231): 901-905.

Wilkinson GA, Schittny JC, Reinhardt DP and Klein R (2008) Role for ephrinB2 in postnatal lung alveolar development and elastic matrix integrity. Dev Dyn 237(8): 2220-2234.

Willits RK and Skornia SL (2004) Effect of collagen gel stiffness on neurite extension. J Biomater Sci Polym Ed 15(12): 1521-1531.

Woo S and Gomez TM (2006) Rac1 and RhoA promote neurite outgrowth through formation and stabilization of growth cone point contacts. J Neurosci 26(5): 1418-1428.

Woo S, Rowan DJ and Gomez TM (2009) Retinotopic mapping requires focal adhesion kinase-mediated regulation of growth cone adhesion. J Neurosci 29(44): 13981-13991.

Yamahashi Y, Cavnar PJ, Hind LE, Berthier E, Bennin DA, Beebe D and Huttenlocher A (2015) Integrin associated proteins differentially regulate neutrophil polarity and directed migration in 2D and 3D. Biomed Microdevices 17(5): 100.

Zhang X, Moore SW, Iskratsch T and Sheetz MP (2014) N-WASP-directed actin polymerization activates Cas phosphorylation and lamellipodium spreading. J Cell Sci 127(Pt 7): 1394-1405.

Chapter 4

Conclusions and future directions

This chapter was published in part as the following journal article:

Kerstein, P. C., Nichol IV R. H., and Gomez, T. M. (2015) Mechanochemical regulation of growth cone motility. *Front. Cell. Neurosci.* 9, 244.

Summary

Investigations into the mechanisms governing growth cone motility and axon guidance over the past several decades have almost exclusively focused on identifying chemical guidance cues, receptors, and intracellular signaling mechanisms that control neuronal morphogenesis (Tessier-Lavigne et al., 1996). However, the idea that the mechanical cues in the environment can regulate morphogenic responses is gaining traction. In this dissertation, I have described the effects of substrata rigidity on growth cone motility and the intracellular forces required to sense and respond to fluctuations in mechanical stimuli. Previous work has shown adhesion complexes act as a hub for mechanical force transduction (Schiller et al., 2013, Sun et al., 2016). In Chapter 2, I show intracellular forces such as myosin-II induced retrograde flow (RF) is regulated at growth cone adhesion sites, termed point contacts (Nichol IV et al., 2016). Point contact adhesions transmit forces between the ECM and the actin cytoskeleton. In non-neuronal migrating cells, focal adhesions are critical to “clutch” myosin-II-based F-actin retrograde flow (RF) to promote leading edge membrane protrusion. However, in growth cones it is unclear whether similar F-actin clutching forces affect axon outgrowth and guidance. In this work, I showed RF is reduced in rapidly migrating growth cones on laminin compared to non-integrin binding poly-d-lysine (PDL) in Xenopus spinal neurons. I showed a temporal correlation between point contact formation and reduced RF, and subsequently accelerated axon outgrowth, with acute stimulation with laminin. Inhibiting immobilized laminin substrata formation blocked this effect, further illustrating extracellular mechanical forces are linked to intracellular force through integrins. Moreover, with two channel imaging of RF and paxillin, I directly linked point contact formation and fluctuations in RF. I found RF is restricted at point contact adhesion sites. To further illustrate the role of RF during guidance responses I used micro-patterns of PDL and laminin and found that individual growth cones have differential RF rates while interacting with two distinct substrata. Our laboratory had previously

found chemoattractive and chemorepulsive axon guidance cues influence point contact adhesions. In agreement with this, I observed an attractive, BDNF and repulsive, Semaphorin3A, cue were found to have opposing effects on RF rates. Finally, I showed RF is significantly attenuated in vivo, suggesting RF is being restrained by molecular clutching forces within the spinal cord.

The developing human body consists of tissue of different elasticities from very soft, such as the brain and spinal cord, to very rigid, such as muscle and bone. In Chapter 3, I examined the role of mechanical forces on neurite development of human forebrain (hFB, model for cortical neurons) neurons and human motor neurons (hMN) derived from induced pluripotent stem cells (iPSCs). We hypothesized these two populations of neurons would respond differently in varying elastic environments. *In vivo*, cortical neurons and motor neurons innervate very distinct elastic tissue (Tyler, 2012). Motor axons, upon exiting the spinal cord, must navigate into more rigid peripheral tissues. Conversely, cortical neurons remain within the elastic central nervous system (CNS). Additionally, previous work from the Urbach laboratory found central and peripheral projecting neurons respond to substrata rigidity differently (Koch et al., 2012). Using polyacrylamide hydrogels I found hFB neurites exhibited little differential outgrowth, while hMN neuritogenesis was strongly promoted on more rigid substrata, reaching maximal growth on on 25 kPa, which is within the range of muscle (10-100 kPa) (Tyler, 2012). Interestingly, hFB had differential growth when cultured in three-dimensional collagen hydrogels as they grew longer neurites on soft substrata, similar to CNS tissue. This could be due to effects of the three-dimensional environment on neuronal differentiation, neurite formation, or neurite extension. Adhesion is a central regulator of mechanosensitive responses to mechanical stimuli in motile non-neuronal and cancer cells. I sought to investigate adhesion dynamics on different substrata in hMN and hFB. The observed differential growth rates were in part due to greater adhesion of the growth cone leading edge to rigid substrata, implying

hMN growth cones have higher adhesivity resulting in greater motility. Further implicating adhesion in hMN growth cone mechanotransduction, I discovered RhoA, an important adhesion regulating GTPase, had greater activity on rigid substrata. In fact, RhoA GTP/GDP levels appeared to act as as switch for mechanosensitivity. Overactivation of RhoA yielded more stable leading edge protrusions which resulted in increased hMN neurite outgrowth on soft substrata, while decreasing adhesivity and outgrowth on more rigid substrata. We hypothesize RhoA is downstream of an initial mechanosensor on elastic substrata and is needed balance intracellular contractile and adhesive forces. Using immunocytochemistry in hMN, I showed increased phosphorylation of mechanosensitive adhesion proteins FAK, Src, and p130-CAS on more rigid substrata in hMN. Finally, RhoA overactivation was found to reverse these results with phosphorylation of FAK and Src, but not p130-CAS, higher on soft substrata. This observation indicates myosin-II induced crosslinking of actin filaments, downstream of RhoA, could play a more important role than myosin-II induced contraction.

Taken together, my thesis work furthered understanding of how intracellular and extracellular forces are balanced by growth cone adhesions. Integrin based adhesion complexes act in parallel with mechanically sensitive ion channels to sense and respond to mechanical stimuli. I showed this leads to increased activity of adhesion signaling proteins such as FAK and Src. Upon adhesion formation RF is clutched and leading edge actin polymerization drives forward growth cone translocation. These adhesion complexes can also be regulated downstream of axon guidance cues such as BDNF and Semaphorin. In this chapter, I will discuss how my findings relate to current understanding in the field and future studies needed to further elucidate mechanisms of mechanosensitivity in growth cones.

Intrinsic forces that guide growth cone motility

How the mechanical regulation of intracellular forces during growth cone and ECM interactions directs pioneering axon growth could be crucial to understanding defects in diseases of axonal misrouting (Antar et al., 2006, Nie et al., 2010). While evidence from focal adhesions has proven to be very informative to understanding growth cone adhesions there are still differences that must be elucidated. In motile growth cones, intracellular forces are due to actin treadmilling driven largely by both pulling forces from myosin-II motor-mediated F-actin sliding and pushing forces at the membrane from barbed-end actin polymerization at the leading edge (Forscher et al., 1988, Lin et al., 1995, Brown et al., 2003). This appears to correlate strongly with migrating, non-neuronal cells. However, in non-neuronal cells myosin II-mediated contractile forces appear to be more dispensable as RF is largely powered by leading edge actin polymerization (Ponti et al., 2004, Vicente-Manzanares et al., 2009). The localization of myosin-II is proximal to the lamellipodium within the lamellum region where it organizes actin and contributes to RF. Additionally, the crosslinking of F-actin by myosin-II in response to mechanical stimuli appears to be more critical to adhesion maturation and migration (Choi et al., 2008). In nerve growth cones it is likely actomyosin filaments are less specifically organized structures and are much more dynamic, allowing nerve growth cones to respond rapidly to extracellular cues.

The unique morphology and dynamics of growth cones suggest they possess distinct localization of myosin-II and differential mechanisms governing traction forces at the leading edge. Indeed, immunocytochemical studies have localized myosin-II in the growth cone central domain, transition zone, and to a lesser extent along F-actin bundles in the peripheral domain (Bridgman et al., 2001, Medeiros et al., 2006, Burnette et al., 2008). However, this has been somewhat limiting, as there is no differentiation between unipolar versus bipolar myosin-II filaments. Whether the myosin-II in peripheral domain is involved in actin cytoskeleton

contraction or trafficking to the periphery has not been investigated. An extensive investigation into active RhoA, ROCK, and myosin-II localization in the growth cone lamellipodia and filopodia in response to mechanical cues can better differentiate the multiple functions of myosin-II. In addition, very little is known about F-actin microstructures within filopodia. An open question in the field is whether anti-parallel actin filaments exist in filopodia. The current hypothesis is that myosin-II is mainly active in the central domain to contract the branched actin network on a whole network scale (Rochlin et al., 1995, Lin et al., 1996, Brown et al., 2003). If myosin-II does crosslink anti-parallel F-actin within filopodia, this could allow for more local regulation of actin RF forces needed for rapid morphological responses. Additionally, as stated previously, myosin-II is important for adhesion maturation (Vicente-Manzanares et al., 2009). As growth cone adhesions initiate in lamellipodia and filopodia at the leading edge, myosin-II regulation could add another layer of local regulation in these areas.

Myosin-II induced actin crosslinking functions yields maturation of focal adhesion (Chrzanowska-Wodnicka et al., 1996, Lawson et al., 2014). However, whether myosin-II crosslinking activity or actomyosin contractile forces is more important for growth cone motility is not clear. In growth cones, adhesions initiate in lamellipodia and filopodia and stabilize into the central domain during forward translocation, and subsequently disassemble (Nichol IV et al., 2016). Our laboratory has identified key regulators of assembly and disassembly within the adhesion complex (Robles et al., 2006, Myers et al., 2011, Kerstein et al., 2013, Santiago-Medina et al., 2013). However, the requirement for myosin-II mediated forces in regulating adhesion formation, maturation, and disassembly in a spatial and temporal manner has not been examined. Whether myosin-II is needed for maturation but not initiation, similar to focal adhesions, is not known either. My data from Chapters 2 and 3 indicate both myosin-II contractile force and crosslinking functions modulate adhesions. In Chapter 2, we found inhibiting myosin-II reduced RF on laminin but not to the extent as we observed on PDL. This

indicates RF attenuation resulted in a compensatory reduction in adhesion stabilization, suggesting a requirement for contractile force to stabilize adhesions. Conversely, in Chapter 3, I showed increased myosin-II contractile force via RhoA overactivation did not cause increased activity of stretch-gated protein p130-CAS. However, this treatment did yield activation of FAK and Src, indicating crosslinking, but not contractile force, via myosin-II is critical for morphological responses. Future studies can utilize motor subunit defective myosin-II, which can still crosslink actin filaments, to differentiate the two roles of myosin-II (Choi et al., 2008). Understanding RhoA-ROCK-myosin-II contractile forces during neurite outgrowth are crucial to defining the intracellular forces that guide growth cone motility.

Extrinsic forces that guide growth cone motility

Intrinsic mechanical forces generated within motile growth cones are modulated by extracellular factors to guide axon extension (Tyler, 2012, Kerstein et al., 2015). Leading edge actin polymerization has been proposed to largely govern protrusive forces during translocation, however, in Chapter 2 I provide strong evidence modulating RF clutching forces plays a crucial role during axon outgrowth and guidance. Furthermore, I found RF at integrin based adhesion sites guide axons on ECM substrata, which could be important for pioneering axons innervating peripheral tissue. The majority of previous studies examining the clutch hypothesis have observed these forces with clutching to cell adhesion molecules, such as data from the Forscher laboratory in *Aplysia* growth cones (Lin et al., 1995). These studies have been critical for identifying the important molecules involved in adhesion and actin dynamics during RF clutching (Suter et al., 1998). However, because *Aplysia* growth cones migrate very slowly, studying the effect of clutching on overall outgrowth or local guidance is limited. Similarly, clutching on the cell adhesion molecule L1 reduces RF through the adapter protein shootin to promote axonal outgrowth downstream of Netrin-1 (Shimada et al., 2008, Toriyama

et al., 2013). While this data is illuminating in identifying molecular modulators of clutching RF, L1 is commonly expressed on established axons and may act as a permissive substrata for trailing axons, but not an instructive cue for pioneering axons (Bartsch et al., 1989, Hankin and Lagenaur, 1994). Another cell adhesion molecule, N-cadherin promotes clutching of actin RF through the adaptor protein α-catenin to control axon extension (Bard et al., 2008, Garcia et al., 2015). Therefore, as cell adhesion molecule clutching of RF plays a role in axon tract formation, my data from Chapter 2 supports the theory that pioneering growth cones use clutching to aid in navigating through a complex ECM early in development (Myers et al., 2011, Nichol IV et al., 2016). It is important for future studies to differentiate the effects of ECM versus cell-cell adhesion for guidance of different neuronal subtypes at different stages of development.

There are still many open questions in elucidating how the mechanisms of growth cone mechanotransduction may differ among neuronal subtypes. In Chapter 3 I provide strong evidence that in human neurons, peripheral projecting motor neurons, but not CNS neurons, reliably respond to mechanical stimuli through modulation of adhesion. However, while my data from Chapter 3 indicates human motor neurons prefer to grow on rigid substrata using polyacrylamide and collagen matrices, deducing the effects of mechanosensing on human neurites is somewhat limited in this context, as neurons were cultured on homogenous substrata of rigidity. Typically, neurite guidance is defined by presenting motile growth cones with a choice. Developing axons reach choice points during extension and must respond to the environment with directed growth (Tessier-Lavigne et al., 1996). These choice points have been mostly studied using soluble cues, such as BDNF, netrin, slits, ephrins and semaphorins, deposited in the environment as a gradient (Song et al., 1997, Hong et al., 2000, Campbell and Holt, 2001, Weinl et al., 2003, Hansen et al., 2004). Whether ECM passively acts as a permissive scaffold for growth, or if the substrata engages to guide axons is starting to be

described. Netrin, which has been previously described as a chemoattractant, using local gradients and border assays, has recently been redefined as an adhesive ligand both *in vitro* (Moore et al., 2009, Moore et al., 2012) and *in vivo* (Koser et al., 2016). Netrin induced traction forces are critical to chemoattractive responses (Moore et al., 2009). Recent studies have inquired whether ECM proteins may act similarly to guide growth cones at choice points, e.g. borders, and toward or away from gradients. Gradients and micropatterns of laminin and fibronectin can induce growth cone turning and neurite extension, similar to chemoattractant cues (Adams et al., 2005, Evans et al., 2007, Chelli et al., 2014). Using micropatterns in Chapter 2, I tested local RF fluctuations in single growth cones at laminin and PDL borders. RF was reduced locally in growth cone regions on laminin substrata relative to PDL. This provides excellent evidence to further investigate differences in traction forces at borders or on gradients to reveal mechanical dependent guidance mechanism.

In addition to modulating which ECM proteins can be examined for guidance effects, current research has been using gradients or borders of elasticity to explore how the biophysical properties of the environment can influence guidance of neurites. There are a number of techniques to alter substrata rigidity as gradients or borders. Gradients of rigidity on polydimethylsiloxane, polyacrylamide, and collagen have been generated via ultraviolet light induced crosslinking using silicone masks (Sunyer et al., 2012, Caliari and Burdick, 2016, Yu et al., 2016). Another way to create elastic gradients in collagen is by inducing crosslinking via genipin. A recent study used a microfluidics system to create a gradient of elasticity in 3D collagen gels using genipin. The authors observed increased number and length of neurites away from the source of genipin (Sundararaghavan et al., 2009). Our laboratory has developed the ability to similarly create an elastic gradient in three-dimensional collagen matrices. Future studies in our laboratory will test human forebrain and motor neuron

morphogenic development on elastic gradients to characterize the instructive versus permissive role of rigidity during neuritogenesis.

In Chapter 3 I described a number of different steps during motor axon development that the mechanical environment could be an important regulator. A developmental step where ECM and growth cone mechanical interactions could be most influenced by extracellular force is during motor axon exiting through the basal lamina. Both the motor axon receptor (Cxcr4) and ligand (Cxcl12) needed for attraction to exit points have been defined (Lieberam et al., 2005). Disruption of this interaction inhibits motor neuron axons from exiting the spinal cord, and they project dorsal and exit at inappropriate regions (Lieberam et al., 2005). However, how the basal lamina, which consists of laminin, fibronectin, collagen, proteoglycans, elastin, and tenascin, must be remodeled to produce interstitial spaces for motor axon exiting is beginning to be understood. One mechanism of ECM remodeling is through release of MMPs from motor neuron growth cone invadosomes. Growth cone invadosomes are apical and basal protrusions, with independent functions of filopodia, which we hypothesize are required for three-dimensional neurite guidance (Santiago-Medina et al., 2015). These structures are required for motor neuron axon exiting of the spinal cord. Growth cone invadosomes are similar to cancer cell invadopodia, with the ability break down ECM, which could function *in vivo* to alter substrata elasticity. In metastatic cancer cells and migrating fibroblasts these ECM remodeling events are regulated by the biophysical environment (Artym et al., 2015, Doyle et al., 2015, Li et al., 2015). MMP release is also directly regulated by elasticity (Haage et al., 2014), providing further evidence that *in vivo*, substrata rigidity may play an instructive role for motor neuron axon exiting from the spinal cord. My results Chapter 3 in collagen matrices illustrate how environmental mechanics affect neurite development in three-dimensional environments. Therefore, future studies should investigate the link between growth cone mechanotransduction and modulation of invadopodia or MMP release.

Future Prospectives and Challenges to the Field

There are many outstanding questions regarding the roles of mechanical forces in the regulation of growth cone motility and axon guidance. Within cells and growth cones, it is unclear which proteins function as mechanosensors and how molecular forces are transferred onto target proteins. In particular, it is not clear how MS ion channels are gated at the plasma membrane and the molecular targets of calcium signals. Ion channel gating may occur at point contact adhesions, where myosin II contractile forces are focused at integrin-ECM contacts (Gomez et al., 2001, Hayakawa et al., 2008, Matthews et al., 2010). Importantly, it is likely that specific calcium influx and release pathways control distinct downstream targets that can have opposing effects on motility (Gomez and Zheng, 2006). However, since many MS ion channels are activated by multiple stimuli, manipulating mechanically activated currents specifically is challenging. For example, TRPC1 subunits are known to assemble into channels that are activated by both mechanical and chemical signals (Wu et al., 2010). Another major challenge to our understanding of mechanical signaling, is the composition and regulation of ECM adhesions. This is particularly difficult in growth cones, as point contact adhesions are smaller and more dynamic than focal adhesions found in non-neuronal cells. Proteomic based approaches are being attempted for focal adhesions, but are hampered by sample heterogeneity (Kuo et al., 2012, Humphries et al., 2015). Point contact adhesions will certainly also be highly heterogenous within growth cones and their composition is regulated by cross talk from guidance cue receptors to control mechanical forces (Myers et al., 2011, Gomez and Letourneau, 2014). In addition, point contact adhesions have not been observed in vivo, where they will clearly differ depending on substratum association. During axon pathfinding to distal targets, growth cones will bind many different adhesive substrata, ranging from ECM proteins to cell adhesion molecules on neighboring neurons and glia. It is important to both visualize and manipulate point contact adhesions in vivo to test their roles in axon guidance.

Determining the roles of tissue elasticity and mechanical signaling is particularly difficult in vivo. While it is clear that growth cones must migrate across widely varying elastic microenvironments en route to their proper synaptic targets, it is not known whether changes in tissue elasticity influences growth cone morphology or motility. For example, motoneuron axons begin in the soft CNS, but exit by penetrating the surrounding basal lamina (Santiago-Medina et al., 2015) to enter the sclerotome, which they preferentially cross within the rostral half (Keynes et al., 1984). After entering the periphery, motor axons are sorted toward targets in the body wall and limb muscles (Bonanomi et al., 2010), which are significantly more rigid tissues (Discher et al., 2009). Distinguishing specific effects of the mechanical environment vs. chemical signals is difficult in vivo. However, progress has been made by examining the effects of mutations in ECM cross linking enzymes that regulate the mechanical, but not the chemical composition of the environment (Kim et al., 2014). Additional functional studies should test the effects on axon guidance of manipulations that both increase and decrease tissue elasticity. Moreover, these functional studies can be coupled with direction measurements of elastic modulus within tissues in vivo using AFM (Franze, 2011).

Future applications

In Chapter 3, I examined neurite development in different environments using iPSCs derived forebrain and motor neurons. Previous studies utilizing iPSCs have mainly focused on methodological and therapeutic applications of iPSCs from patients with varying disorders. However, the use of iPSCs, and embryonic stem cells (ESCs) for understanding basic human neuronal development and function will be crucial to elucidating differences in human cognition relative to other animals. The prospective applications of using iPSCs for basic scientific applications are limitless. This new technology can also help to replace cell culture animal models and reduce the use of animals in scientific research. Moreover, using ESCs and iPSCs

researchers have created functional cerebral organoids, which include cortex, midbrain, and brain stem (Mason and Price, 2016). Futures studies should investigate the ability of these organoids to create and remodel local ECM components. This could provide an *in vivo* model of human neurons to investigate the role of matrix rigidity during neuritogenesis.

I provided evidence that substrata elasticity can regulate neuritogenesis on ECM components such as collagen. The fluidity of collagen fibril structure is seen in development as well as during pathological conditions. Collagen can vary in density, crosslinking, and alignment. In fact, during cancer metastasis collagen alignment and rigidity can play a key role in invasion into other tissue (Schedin et al., 2011, Riching et al., 2014). In breast cancer, which includes an increase in matrix rigidity, the availability of more aligned collagen provides tracks for cancerous cells to migrate out of the tumor (Schedin et al., 2011, Riching et al., 2014). This increased collagen alignment is correlated with decreased patient survival (Schedin et al., 2011, Riching et al., 2014). Whether collagen alignment and rigidity also affect neurite growth during development and in pathological conditions is less well known. Importantly, the cleavage of collagen by matrix metalloproteases has been shown to be an important factor that is dysregulated in Fragile X Syndrome. In short, matrix metalloprotease 9 (MMP9) is upregulated in Fragile X Syndrome and this induces increased collagen breakdown causing myriad behavioral phenotypes (Lovelace et al., 2016). Loss of MMP9 can ameliorate some of these phenotypes (Lovelace et al., 2016). However, the effects of increased MMP9 during neuritogenesis has not been studied. As there are axon tract defects in Fragile X Syndrome, this disorder provides an excellent path to study the relationship between collagen matrix structure and neurite development. In addition to further identifying the role of matrix structure and rigidity in neurodevelopmental disorders, future studies should investigate the ability of axons to regenerate after injury in varying elastic conditions. After injury the environment is inhibitory for neuronal cell growth via the activation of multiple inhibitory mechanisms that block

regeneration (Pires and Pego, 2015). However, recent advances in biological engineering methods have provided biomaterial-based scaffolds which can provide the needed biophysical support for regenerating axons. Rigidity tunable materials, such as fibrin, are promising matrix components to be used in promoting nerve repair given their natural occurrence in peripheral nerve injuries (Man et al., 2011). My data provides evidence that human motor neurons can be guided by these biophysical properties. Future studies should investigate the ability of different biomaterials in regenerating human axonal growth via elastic properties.

Bibliography

Adams DN, Kao EY, Hypolite CL, Distefano MD, Hu WS and Letourneau PC (2005) Growth cones turn and migrate up an immobilized gradient of the laminin IKVAV peptide. J Neurobiol 62(1): 134-147.

Antar LN, Li C, Zhang H, Carroll RC and Bassell GJ (2006) Local functions for FMRP in axon growth cone motility and activity-dependent regulation of filopodia and spine synapses. Mol Cell Neurosci 32(1-2): 37-48.

Artym VV, Swatkoski S, Matsumoto K, Campbell CB, Petrie RJ, Dimitriadis EK, Li X, Mueller SC, Bugge TH, Gucek M and Yamada KM (2015) Dense fibrillar collagen is a potent inducer of invadopodia via a specific signaling network. J Cell Biol 208(3): 331-350.

Bard L, Boscher C, Lambert M, Mege RM, Choquet D and Thoumine O (2008) A molecular clutch between the actin flow and N-cadherin adhesions drives growth cone migration. J Neurosci 28(23): 5879-5890.

Bartsch U, Kirchhoff F and Schachner M (1989) Immunohistological localization of the adhesion molecules L1, N-CAM, and MAG in the developing and adult optic nerve of mice. J Comp Neurol 284(3): 451-462.

Bonanomi D and Pfaff SL (2010) Motor axon pathfinding. Cold Spring Harb Perspect Biol 2(3): a001735.

Bridgman PC, Dave S, Asnes CF, Tullio AN and Adelstein RS (2001) Myosin IIB is required for growth cone motility. J Neurosci 21(16): 6159-6169.

Brown ME and Bridgman PC (2003) Retrograde flow rate is increased in growth cones from myosin IIB knockout mice. J Cell Sci 116(Pt 6): 1087-1094.

Burnette DT, Ji L, Schaefer AW, Medeiros NA, Danuser G and Forscher P (2008) Myosin II activity facilitates microtubule bundling in the neuronal growth cone neck. Dev Cell 15(1): 163-169.

Caliari SR and Burdick JA (2016) A practical guide to hydrogels for cell culture. Nat Methods 13(5): 405-414.

Campbell DS and Holt CE (2001) Chemotropic responses of retinal growth cones mediated by rapid local protein synthesis and degradation. Neuron 32(6): 1013-1026.

Chelli B, Barbalinardo M, Valle F, Greco P, Bystrenova E, Bianchi M and Biscarini F (2014) Neural cell alignment by patterning gradients of the extracellular matrix protein laminin. Interface Focus 4(1): 20130041.

Choi CK, Vicente-Manzanares M, Zareno J, Whitmore LA, Mogilner A and Horwitz AR (2008) Actin and alpha-actinin orchestrate the assembly and maturation of nascent adhesions in a myosin II motor-independent manner. Nat Cell Biol 10(9): 1039-1050.

Chrzanowska-Wodnicka M and Burridge K (1996) Rho-stimulated contractility drives the formation of stress fibers and focal adhesions. J Cell Biol 133(6): 1403-1415.

Discher DE, Mooney DJ and Zandstra PW (2009) Growth factors, matrices, and forces combine and control stem cells. Science 324(5935): 1673-1677.

Doyle AD, Carvajal N, Jin A, Matsumoto K and Yamada KM (2015) Local 3D matrix microenvironment regulates cell migration through spatiotemporal dynamics of contractility-dependent adhesions. Nat Commun 6: 8720.

Evans AR, Euteneuer S, Chavez E, Mullen LM, Hui EE, Bhatia SN and Ryan AF (2007) Laminin and fibronectin modulate inner ear spiral ganglion neurite outgrowth in an in vitro alternate choice assay. Dev Neurobiol 67(13): 1721-1730.

Franze K (2011) Atomic force microscopy and its contribution to understanding the development of the nervous system. Curr Opin Genet Dev 21(5): 530-537.

Gomez TM and Letourneau PC (2014) Actin dynamics in growth cone motility and navigation. J Neurochem 129(2): 221-234.

Gomez TM, Robles E, Poo M and Spitzer NC (2001) Filopodial calcium transients promote substrate-dependent growth cone turning. Science 291(5510): 1983-1987.

Gomez TM and Zheng JQ (2006) The molecular basis for calcium-dependent axon pathfinding. Nat Rev Neurosci 7(2): 115-125.

Haage A and Schneider IC (2014) Cellular contractility and extracellular matrix stiffness regulate matrix metalloproteinase activity in pancreatic cancer cells. FASEB J 28(8): 3589-3599.

Hankin MH and Lagenaur CF (1994) Cell adhesion molecules in the early developing mouse retina: retinal neurons show preferential outgrowth in vitro on L1 but not N-CAM. J Neurobiol 25(5): 472-487.

Hansen MJ, Dallal GE and Flanagan JG (2004) Retinal axon response to ephrin-as shows a graded, concentration-dependent transition from growth promotion to inhibition. Neuron 42(5): 717-730.

Hayakawa K, Tatsumi H and Sokabe M (2008) Actin stress fibers transmit and focus force to activate mechanosensitive channels. J Cell Sci 121(Pt 4): 496-503.

Hong K, Nishiyama M, Henley J, Tessier-Lavigne M and Poo M (2000) Calcium signalling in the guidance of nerve growth by netrin-1. Nature 403(6765): 93-98.

Humphries JD, Paul NR, Humphries MJ and Morgan MR (2015) Emerging properties of adhesion complexes: what are they and what do they do? Trends Cell Biol 25(7): 388-397.

Kerstein PC, Jacques-Fricke BT, Rengifo J, Mogen BJ, Williams JC, Gottlieb PA, Sachs F and Gomez TM (2013) Mechanosensitive TRPC1 channels promote calpain proteolysis of talin to regulate spinal axon outgrowth. J Neurosci 33(1): 273-285.

Kerstein PC, Nichol RHt and Gomez TM (2015) Mechanochemical regulation of growth cone motility. Front Cell Neurosci 9: 244.

Keynes RJ and Stern CD (1984) Segmentation in the vertebrate nervous system. Nature 310(5980): 786-789.

Kim SN, Jeibmann A, Halama K, Witte HT, Walte M, Matzat T, Schillers H, Faber C, Senner V, Paulus W and Klambt C (2014) ECM stiffness regulates glial migration in Drosophila and mammalian glioma models. Development 141(16): 3233-3242.

Koch D, Rosoff WJ, Jiang J, Geller HM and Urbach JS (2012) Strength in the periphery: growth cone biomechanics and substrate rigidity response in peripheral and central nervous system neurons. Biophys J 102(3): 452-460.

Koser DE, Thompson AJ, Foster SK, Dwivedy A, Pillai EK, Sheridan GK, Svoboda H, Viana M, Costa LD, Guck J, Holt CE and Franze K (2016) Mechanosensing is critical for axon growth in the developing brain. Nat Neurosci 19(12): 1592-1598.

Kuo JC, Han X, Yates JR, 3rd and Waterman CM (2012) Isolation of focal adhesion proteins for biochemical and proteomic analysis. Methods Mol Biol 757: 297-323.

Lawson CD and Burridge K (2014) The on-off relationship of Rho and Rac during integrin-mediated adhesion and cell migration. Small GTPases 5: e27958.

Li C, Rezania S, Kammerer S, Sokolowski A, Devaney T, Gorischek A, Jahn S, Hackl H, Groschner K, Windpassinger C, Malle E, Bauernhofer T and Schreibmayer W (2015) Piezo1 forms mechanosensitive ion channels in the human MCF-7 breast cancer cell line. Sci Rep 5: 8364.

Lieberam I, Agalliu D, Nagasawa T, Ericson J and Jessell TM (2005) A Cxcl12-CXCR4 chemokine signaling pathway defines the initial trajectory of mammalian motor axons. Neuron 47(5): 667-679.

Lin CH, Espreafico EM, Mooseker MS and Forscher P (1996) Myosin drives retrograde F-actin flow in neuronal growth cones. Neuron 16(4): 769-782.

Lin CH and Forscher P (1995) Growth cone advance is inversely proportional to retrograde F-actin flow. Neuron 14(4): 763-771.

Matthews BD, Thodeti CK, Tytell JD, Mammoto A, Overby DR and Ingber DE (2010) Ultra-rapid activation of TRPV4 ion channels by mechanical forces applied to cell surface beta1 integrins. Integr Biol (Camb) 2(9): 435-442.

Medeiros NA, Burnette DT and Forscher P (2006) Myosin II functions in actin-bundle turnover in neuronal growth cones. Nat Cell Biol 8(3): 215-226.

Moore SW, Biais N and Sheetz MP (2009) Traction on immobilized netrin-1 is sufficient to reorient axons. Science 325(5937): 166.

Moore SW, Zhang X, Lynch CD and Sheetz MP (2012) Netrin-1 attracts axons through FAK-dependent mechanotransduction. J Neurosci 32(34): 11574-11585.

Myers JP and Gomez TM (2011) Focal adhesion kinase promotes integrin adhesion dynamics necessary for chemotropic turning of nerve growth cones. J Neurosci 31(38): 13585-13595.

Myers JP, Santiago-Medina M and Gomez TM (2011) Regulation of axonal outgrowth and pathfinding by integrin-ECM interactions. Dev Neurobiol 71(11): 901-923.

Nichol IV RH, Hagen KM, Lumbard DC, Dent EW and Gomez TM (2016) Guidance of Axons by Local Coupling of Retrograde Flow to Point Contact Adhesions. J Neurosci 36(7): 2267-2282.

Nie D, Di Nardo A, Han JM, Baharanyi H, Kramvis I, Huynh T, Dabora S, Codeluppi S, Pandolfi PP, Pasquale EB and Sahin M (2010) Tsc2-Rheb signaling regulates EphA-mediated axon guidance. Nat Neurosci 13(2): 163-172.

Ponti A, Machacek M, Gupton SL, Waterman-Storer CM and Danuser G (2004) Two distinct actin networks drive the protrusion of migrating cells. Science 305(5691): 1782-1786.

Robles E and Gomez TM (2006) Focal adhesion kinase signaling at sites of integrin-mediated adhesion controls axon pathfinding. Nat Neurosci 9(10): 1274-1283.

Rochlin MW, Itoh K, Adelstein RS and Bridgman PC (1995) Localization of myosin II A and B isoforms in cultured neurons. J Cell Sci 108 (Pt 12): 3661-3670.

Santiago-Medina M, Gregus KA and Gomez TM (2013) PAK-PIX interactions regulate adhesion dynamics and membrane protrusion to control neurite outgrowth. J Cell Sci 126(Pt 5): 1122-1133.

Santiago-Medina M, Gregus KA, Nichol RH, O'Toole SM and Gomez TM (2015) Regulation of ECM degradation and axon guidance by growth cone invadosomes. Development 142(3): 486-496.

Schiller HB and Fassler R (2013) Mechanosensitivity and compositional dynamics of cell-matrix adhesions. EMBO Rep 14(6): 509-519.

Shimada T, Toriyama M, Uemura K, Kamiguchi H, Sugiura T, Watanabe N and Inagaki N (2008) Shootin1 interacts with actin retrograde flow and L1-CAM to promote axon outgrowth. J Cell Biol 181(5): 817-829.

Song HJ, Ming GL and Poo MM (1997) cAMP-induced switching in turning direction of nerve growth cones. Nature 388(6639): 275-279.

Sun Z, Guo SS and Fassler R (2016) Integrin-mediated mechanotransduction. J Cell Biol 215(4): 445-456.

Sundararaghavan HG, Monteiro GA, Firestein BL and Shreiber DI (2009) Neurite growth in 3D collagen gels with gradients of mechanical properties. Biotechnol Bioeng 102(2): 632-643.

Sunyer R, Jin AJ, Nossal R and Sackett DL (2012) Fabrication of hydrogels with steep stiffness gradients for studying cell mechanical response. PLoS One 7(10): e46107.

Suter DM, Errante LD, Belotserkovsky V and Forscher P (1998) The Ig superfamily cell adhesion molecule, apCAM, mediates growth cone steering by substrate-cytoskeletal coupling. J Cell Biol 141(1): 227-240.

Tessier-Lavigne M and Goodman CS (1996) The molecular biology of axon guidance. Science 274(5290): 1123-1133.

Tyler WJ (2012) The mechanobiology of brain function. Nat Rev Neurosci 13(12): 867-878.

Vicente-Manzanares M, Ma X, Adelstein RS and Horwitz AR (2009) Non-muscle myosin II takes centre stage in cell adhesion and migration. Nat Rev Mol Cell Biol 10(11): 778-790.

Weinl C, Drescher U, Lang S, Bonhoeffer F and Loschinger J (2003) On the turning of Xenopus retinal axons induced by ephrin-A5. Development 130(8): 1635-1643.

Wu LJ, Sweet TB and Clapham DE (2010) International Union of Basic and Clinical Pharmacology. LXXVI. Current progress in the mammalian TRP ion channel family. Pharmacol Rev 62(3): 381-404.

Yu S, Sun Y, Ni Y, Zhang X and Zhou H (2016) Controlled Formation of Surface Patterns in Metal Films Deposited on Elasticity-Gradient PDMS Substrates. ACS Appl Mater Interfaces 8(8): 5706-5714.